

MODELING THE EFFECT OF LAND COVER/LAND USE CHANGE ON
ESTUARINE ENVIRONMENTAL FLOWS

A Dissertation

by

DEBABRATA SAHOO

Submitted to the Office of Graduate Studies of
Texas A&M University
in partial fulfillment of the requirements for the degree of

DOCTOR OF PHILOSOPHY

May 2008

Major Subject: Biological and Agricultural Engineering

MODELING THE EFFECT OF LAND COVER/LAND USE CHANGE ON
ESTUARINE ENVIRONMENTAL FLOWS

A Dissertation

by

DEBABRATA SAHOO

Submitted to the Office of Graduate Studies of
Texas A&M University
in partial fulfillment of the requirements for the degree of

DOCTOR OF PHILOSOPHY

Approved by:

Chair of Committee,
Committee Members,

Patricia Smith
Raghavan Srinivasan
Raghupathy Karthikeyan
Fuqing Zhang
Sorin Popescu
Gerald Riskowski

Head of Department,

May 2008

Major Subject: Biological and Agricultural Engineering

ABSTRACT

Modeling the Effect of Land Cover/Land Use Change on Estuarine Environmental
Flows.

(May 2008)

Debabrata Sahoo, B.S., College of Agriculture and Technology;

M.S, University of Arkansas

Chair of Advisory Committee: Dr. Patricia Smith

Environmental flows are important to maintain the ecological integrity of the estuary. In a watershed, it is influenced by land use land cover (LULC) change, climate variability, and water regulations. San Antonio, Texas, the 8th largest city in the US, is likely to affect environmental flows to the San Antonio Bay/Guadalupe Estuary, due to rapid urbanization.

Time series analysis was conducted at several stream gauging stations to assess trends in hydrologic variables. A bootstrapping method was employed to estimate the critical value for global significance. Results suggested a greater number of trends are observed than are expected to occur by chance. Stream gauging stations present in lower half of the watershed experienced increasing trend, whereas upper half experienced decreasing trends. A similar spatial pattern was not observed for rainfall. Winter season observed maximum number of trends.

Wavelet analysis on hydrologic variables, suggested presence of multi-scale temporal variability; dominant frequencies in 10 to 15 year scale was observed in some of the hydrologic variables, with a decadal cycle. Dominant frequencies were also observed in 17 to 23 year scale with repeatability in 20 to 30 years. It is therefore important to understand various ecological processes that are dominant in this scale and quantify possible linkages among them.

Genetic algorithm (GA) was used for calibration of the Hydrologic Simulation Program in FORTRAN (HSPF) model. Although, GA is computationally demanding, it is better than manual calibration. Parameter values obtained for the calibrated model had physical representation and were well within the ranges suggested in the literature.

Information from LANDSAT images for the years 1987, 1999, and 2003 were introduced to HSPF to quantify the impact of LULC change on environmental flows. Modeling studies indicated, with increase in impervious surface, peak flows increased over the years. Wavelet analysis pointed, that urbanization also impacted storage. Modeling studies quantified, on average about 50% of variability in freshwater inflows could be attributed to variation in precipitation, and approximately 10% of variation in freshwater inflows could be attributed to LULC change.

This study will help ecologist, engineers, scientist, and politicians in policy making pertinent to water resources management.

DEDICATION

I would dedicate my research to my loving parents, family and the scientific community, involved in protecting the “PLANET EARTH”.

ACKNOWLEDGEMENTS

All these years of journey in my Ph.D. studies, beyond my B.S. and M.S., have made me realize: “This degree is a solitary effort”. I completely understand, although this is a solitary effort, there are numerous visible and invisible sacrifices that have helped me to reach this point. I realize investigation of science and engineering for betterment of society needs this sacrifice.

First of all, I would like to thank my major professor, Dr. Patricia Smith, for giving me this wonderful opportunity and support in the last four years. During these years we have discussed numerous interesting topics: science, engineering, politics, books, etc. She has never doubted my ability to accomplish this research. Her ability to make one think and execute my work independently has been excellent. It is my honor to be her student.

My special thanks is given to my loving parents, siblings, in-laws and relatives in this endeavor. My parents have always stood like a pillar of strength. My special thanks also goes out to my elder sister and her family for making my life easy. I would like to extend my deep gratitude to my late father-in-law for his ever invisible support.

I thank my advisors Dr. Raghavan Srinivasan, Dr. Sorin Popescu, Dr. Fuqing Zhang, and Dr. Raghupathy Karthikeyan for their guidance, support, and encouragement during the research process. I would also like to thank Dr. Sabu Paul and Dr. Sen Bai for their help.

In this effort, my special thanks to Dr. Indrajeet Chaubey for his constant encouragement.

Dr. Binayak Mohanty has always been a source of inspiration to me. We have discussed several research opportunities that we thought are important for the scientific community. I thank him for his time. I would also like to thank Dr. Amor Ines for discussing several research ideas. He has wholeheartedly welcomed me all the time. Thanks to him. My special regards to Sushant Dhal as well.

Friends like Biswajit, Naren, Feri, Bikram, Raghu, Sujit, Sumit, Anurag, Asish, Amith, and Himanshu have always helped me, both personally and professionally. It has been fun all these years staying in tuned with them.

I would also like to thank Texas Water Resources Research Institute, Mills Scholarships, NASA, and US Geological Survey for providing me grants and scholarships during my research. I am very thankful to USGS stream flow database, and the National Climatic Data Center (NCDC) climate database. Many thanks to San Antonio River Authority (SARA), San Antonio Water Systems (SAWS), and <http://www.edwardsaquifer.net/> for providing me with information relevant to this research.

Last but not the least, I would like to thank my wonderful wife who has been a constant source of happiness for all these years. She made my work really fun. Without her

sacrifice, this research would not have been possible. I thank her for nights out in the department, and plugging numbers. She is truly my best friend and better half. God bless her.

TABLE OF CONTENTS

	Page
ABSTRACT	iii
DEDICATION	v
ACKNOWLEDGEMENTS	vi
TABLE OF CONTENTS	ix
LIST OF FIGURES.....	xii
LIST OF TABLES	xvii
CHAPTER	
I GENERAL INTRODUCTION	1
1.1 Overview	1
1.2 Background	6
1.2.1 Trend Analysis of Streamflow	7
1.2.2 Wavelet Analysis of Streamflow Variations	7
1.2.3 Monitoring Urban Land Use/Land Cover Change by Remote Sensing on a Regional Scale	9
1.2.4 Effect of Land Use and Land Surface Hydrologic Processes on a Basin Scale	10
1.2.5 Modeling Environmental Flows to an Estuary.....	11
1.2.6 Parameter Estimation in Model Calibration.....	12
1.3 Study Objectives	14
II HYDROLOGIC TREND DETECTION IN A RAPIDLY URBANIZING SEMI-ARID COASTAL RIVER BASIN	15
2.1 Overview	15
2.2 Introduction	16
2.3 Study Area.....	21
2.4 Methodology	24
2.4.1 Selection of Hydrologic Variables	25
2.4.2 Selection of Gauging Stations	27
2.4.3 Trend Analysis	28

CHAPTER	Page
2.4.4 Significance of Trend	29
2.4.5 Freshwater Inflow Analysis	31
2.4.6 Rainfall Characterization.....	32
2.5 Results and Discussion.....	32
2.6 Conclusions	54
III CHARACTERIZATION OF ENVIRONMENTAL FLOWS IN A RAPIDLY URBANIZING SEMI-ARID WATERSHED USING WAVELET ANALYSIS.....	56
3.1 Overview	56
3.2 Introduction	57
3.3 Study Site Description.....	61
3.3.1 Physiography.....	61
3.3.2 Land Use Change	64
3.4 Data	65
3.4.1 Hydrological Data and Rainfall Data.....	65
3.5 Methodology	66
3.6 Results and Discussions	67
3.6.1 Total Seasonal Flow.....	67
3.6.2 Total Seasonal Baseflow	70
3.6.3 Minimum Seasonal Total Flow	78
3.6.4 Minimum Seasonal Baseflow.....	79
3.6.5 Maximum Seasonal Total Flow	83
3.6.6 Maximum Seasonal Baseflow.....	84
3.7 Conclusion.....	92
IV PARAMETER ESTIMATION FOR CALIBRATION AND VALIDATION OF HSPF USING AN EVOLUTIONARY ALGORITHM AND INVERSE MODELING.....	93
4.1 Overview	93
4.2 Introduction	95
4.3 Methodology	104
4.3.1 Study Area.....	104
4.3.2 Model Description.....	106
4.3.3 Data Description.....	109
4.3.4 Operation of Genetic Algorithms.....	112
4.3.5 Model Calibration Using GA	112
4.3.6 Model Validation.....	115
4.4 Results and Discussions	116
4.5 Conclusion.....	126

CHAPTER		Page
V	MODELING THE EFFECTS OF LAND COVER/LAND USE CHANGE AND PRECIPITATION VARIABILITY ON FRESHWATER INFLOWS	130
	5.1 Overview	130
	5.2 Introduction	131
	5.3 Methodology	136
	5.3.1 Study Area.....	137
	5.3.2 Land Cover Land Use Assessment.....	138
	5.3.3 Model Description.....	142
	5.3.4 Data Description.....	143
	5.3.5 Calibration and Validation	144
	5.3.6 Scenario Analysis	145
	5.4 Results and Discussion.....	146
	5.5 Conclusions	164
VI	CONCLUSIONS AND FUTURE WORK	165
	REFERENCES	169
	VITA	180

LIST OF FIGURES

FIGURE		Page
II-1	San Antonio River Watershed with USGS gauging stations, NCDC weather stations and WWTP	23
II-2	Population trend since 1940 for the City of San Antonio and Bexar County, in which San Antonio is located (Texas State Data Center, 2005).....	24
II-3	Cumulative frequency distribution showing number of significant trends	35
II-4	Spatial distribution of USGS gauging stations showing increasing, decreasing, and no trend for minimum stream flow for fall season	39
II-5	Spatial distribution of USGS gauging stations showing increasing, decreasing, and no trend for minimum base flow for fall season.....	40
II-6	Total seasonal flow, baseflow, and runoff for Winter Season at the most downstream USGS gauging station 08188500, 1940 to 2003	43
II-7	Maximum seasonal flow, baseflow, and runoff for Winter Season at the most downstream USGS gauging station 08188500, 1940 to 2003.....	44
II-8	Minimum seasonal flow, baseflow, and runoff for Winter Season at the most downstream USGS gauging station 08188500, 1940 to 2003.....	45
II-9	Trend in total rainfall at NCDC gauge 413618 for winter, spring/summer and fall seasons.....	49
II-10	Trend in maximum rainfall at NCDC gauge 413618 for winter, spring/summer and fall seasons.....	50
III-1	San Antonio River watershed with gauging stations, weather stations, and various counties in the watershed.....	62
III-2	Total seasonal environmental flow, total baseflow, total runoff, and total rainfall magnitudes from 1940-2003 as monitored in USGS gauging station 08188500 and NCDC 413618 station	69

FIGURE	Page
III-3 Scale and period of total seasonal flow for (from top to bottom) Dec-Mar, Apr-Jul, and Aug-Nov obtained from USGS 08186000 gauging data	72
III-4 Scale and period of total seasonal flow for (from top to bottom) Dec-Mar, Apr-Jul, and Aug-Nov obtained from USGS 08183500 gauging data	73
III-5 Scale and period of total seasonal flow for (from top to bottom) Dec-Mar, Apr-Jul, and Aug-Nov obtained from USGS 08188500 gauging data	74
III-6 Scale and period of total seasonal base flow for (from top to bottom) Dec-Mar, Apr-Jul, and Aug-Nov obtained from USGS 08186000 gauging data	75
III-7 Scale and period of total seasonal base flow for (from top to bottom) Dec-Mar, Apr-Jul, and Aug-Nov obtained from USGS 08183500 gauging data	76
III-8 Scale and period of total seasonal base flow for (from top to bottom) Dec-Mar, Apr-Jul, and Aug-Nov obtained from USGS 08188500 gauging data	77
III-9 Scale and period of minimum seasonal total flow for (from top to bottom) Dec-Mar, Apr-Jul, and Aug-Nov obtained from USGS 08186000 gauging data	80
III-10 Scale and period of minimum seasonal total flow for (from top to bottom) Dec-Mar, Apr-Jul, and Aug-Nov obtained from USGS 08183500 gauging data	81
III-11 Scale and period of minimum seasonal total flow for (from top to bottom) Dec-Mar, Apr-Jul, and Aug-Nov obtained from USGS 08188500 gauging data	82
III-12 Scale and period of maximum seasonal total flow for (from top to bottom) Dec-Mar, Apr-Jul, and Aug-Nov obtained from USGS 08186000 gauging data	85

FIGURE	Page
III-13 Scale and period of maximum seasonal total flow for (from top to bottom) Dec-Mar, Apr-Jul, and Aug-Nov obtained from USGS 08183500 gauging data	86
III-14 Scale and period of maximum seasonal total flow for (from top to bottom) Dec-Mar, Apr-Jul, and Aug-Nov obtained from USGS 08188500 gauging data	87
III-15 Scale and period of maximum seasonal baseflow for (from top to bottom) Dec-Mar, Apr-Jul, and Aug-Nov obtained from USGS 08186000 gauging data	89
III-16 Scale and period of maximum seasonal baseflow for (from top to bottom) Dec-Mar, Apr-Jul, and Aug-Nov obtained from USGS 08183500 gauging data	90
III-17 Scale and period of maximum seasonal baseflow for (from top to bottom) Dec-Mar, Apr-Jul, and Aug-Nov obtained from USGS 08188500 gauging data	91
IV-1 A binary representation of chromosome in GA for optimal parameter estimation in hydrologic calibration.....	102
IV-2 San Antonio River watershed with 2003 land use, gauging stations, weather stations, and various counties in the watershed.....	105
IV-3 San Antonio River watershed with weather stations and the sub-basins associated with the weather stations.....	111
IV-4 A figure showing GA linked with HSPF (Modified from Ines and Droogers, 2002).....	113
IV-5 Graph showing generations versus best fitness that suggest model improvement over time	117
IV-6 From top to bottom: Average observed daily and average simulated daily flow ; Average observed monthly and average simulated monthly flow; average observed seasonal and average simulated seasonal flow; average observed yearly and average simulated year	120
IV-7 From top to bottom: Observed daily flow and simulated daily flow (2002-2004) in wavelet domain	122

FIGURE	Page
IV-8 From top to bottom: Average observed daily and average simulated daily flow; average observed monthly and average simulated monthly flow for the validation year 2001, at the watershed outlet.....	124
IV-9 From top to bottom: Average observed daily and average simulated daily flow; average observed monthly and average simulated monthly flow for the validation year 2005, at the watershed outlet.....	125
IV-10 From top to bottom: Observed daily flow and simulated daily flow (2001) in wavelet domain.....	127
IV-11 From top to bottom: Observed daily flow and simulated daily flow (2005) in wavelet domain.....	128
V-1 San Antonio River watershed indicating USGS gauging station and NCDC weather stations used in the analysis.....	140
V-2 San Antonio River watershed with 1987 land use land cover dataset, focusing Bexar County.....	148
V-3 San Antonio River watershed with 1999 land use land cover dataset, focusing Bexar County.....	149
V-4 San Antonio River watershed with 2003 land use land cover dataset, focusing Bexar County.....	150
V-5 Percentage change in land use from 1987 to 2003, in watershed scale (top), and in Bexar County (bottom), obtained from remote sensing and GIS analysis.....	151
V-6 Daily total rainfall for the watershed, estimated by thiessen polygon method for the year 1999, and 2003.....	153
V-7 Estimated daily total potential evapotranspiration for the watershed for the year 1999, and 2003	154
V-8 Average daily flow (top) and average monthly flow (below) after changing the land use for 1999, and 1987.....	155
V-9 Morlet wavelet analysis for various land use change; (from top to bottom) simulations results for LULC 1987, 1999, and 2003	159

FIGURE	Page
V-10 Simulation results with a common 2003 rainfall dataset and respective LULC datasets of the years. Average daily flow (top) and average monthly flow (bottom) for both the years	160
V-11 Simulation results with a common 1999 rainfall dataset and respective LULC datasets of the years. Average daily flow (top) and average monthly flow (bottom) for both the years	161
V-12 Simulation results with a common 2003 LULC dataset and original hydroclimatic data for the year 1999 and 2003. Average daily flow (top) and average monthly flow (bottom) for both the years	162
V-13 Simulation results with a common 1999 LULC dataset and original hydroclimatic data for the year 1999 and 2003. Average daily flow (top) and average monthly flow (bottom) for both the years	163

LIST OF TABLES

TABLE	Page
II-1 Duration of flow used in analysis for San Antonio River watershed USGS gauging stations.....	27
II-2 Duration of rainfall used in analysis for San Antonio River watershed NCDC weather stations	33
II-3 Serial correlation of all hydrologic variables for all the stations and all the seasons.....	34
II-4 Trend test results for 9 USGS gauging stations in the San Antonio River watershed for the 1940-2003 period.....	36
II-5 Mann-Kendall test statistics by station for trends in seasonal hydrologic variables that were significant at both local and global significance levels ($\alpha_l = \alpha_g = 0.2$).....	38
II-6 Summary statistics for the hydrologic variables analyzed from the flow at USGS gauging station 08188500.....	42
II-7 Serial correlation of rainfall data for all the stations and all the seasons.....	48
II-8 Trend test results for 5 NCDC weather stations in the San Antonio River watershed.....	48
II-9 Mann-Kendall test statistics by station for trends in seasonal hydrologic variables that were significant at both the local and global significance levels ($\alpha_l = \alpha_g = 0.2$).....	48
II-10 Comparison of total stream flow, base flow, and runoff obtained from similar rainfall events in 1950s and 1990s, at USGS gauging station 08188500 and NCDC weather station 413618.....	52
II-11 Comparison of total stream flow, base flow, and runoff obtained from similar rainfall events in 1950s and 1990s, at USGS gauging station 08178800 and NCDC weather station 417945	53

TABLE		Page
IV-1	Various model parameter that control water quantity in HSPF, their length in the chromosome, and accuracy	108
IV-2	Various parameters values obtained from GA-HSPF, and their comparison with literature.....	119
V-1	LANDSAT series imageries used for the LULC change analysis in the San Antonio watershed.....	141
V-2	Scenarios used for various simulation to separate precipitation variability from LULC change effect on freshwater inflows	147

CHAPTER I

GENERAL INTRODUCTION

1.1 Overview

The study of environmental inflows is a developing science that encompasses the interactions of hydrology, biology, biogeochemistry, economics, physical processes, hydraulics, geomorphology, water quality, and water quantity (NRC, 2005). Evaluating environmental flow needs focuses on balancing ecosystem flow requirements with human use. This science attempts to answer the very eco-political question, “How much water should be available in a lotic/lentic ecosystem to meet both the ecosystem and human demand?”. Instream flow programs rely on science, and take the legal, social, and political processes into account. It is challenging to combine science and policy of environmental flows into a lucid program (NRC, 2005).

The world and the U.S, in particular, are struggling with the issues of providing adequate environmental flows in times of high demand (both human and ecosystem) and low supply. The State of Texas is no exception. The differences in hydrologic regimes

This dissertation follows the style of *Journal of Hydrology*.

across the state of Texas have important implications on instream flow science (NRC, 2000). With a variety of streams, rivers and ecosystems, a growing urban population, placing substantial pressure on water supplies, and periodic water shortage, Texas faces environmental flow challenges. Texas Senate Bill 2 (2001) has instructed three state agencies, the Texas Water Development Board (TWDB), the Texas Parks and Wildlife Department (TPWD), and the Texas Commission on Environmental Quality (TCEQ), to develop a state program for instream flows and freshwater inflows to support a “sound ecological environment” in rivers and estuaries by 2010. Freshwater inflow study in Texas can provide a framework to evaluate flow allocation in similar aquatic systems.

Estuaries are the connecting link between terrestrial and marine ecosystems, and provide a critical coastal habitat that is essential ecologically and economically to the world economy (Alongi, 1998; Kennish, 2001). Important species such as finfish and shellfish depend on estuaries for their survival and contribute more than 90% of the total fisheries activity in the Gulf of Mexico (Kennish, 2000). Estuarine and coastal marine fisheries return more than \$23.0 billion annually to the US economy (Kennish, 2000). In addition, estuaries support multi-billion dollar commercial and recreational activities such as tourism, shipping, marine biotechnology, mineral exploration, and employment to millions of people world wide. The State of Texas has approximately 367 miles of coastline and in recent years, coastal industries (tourism, fisheries, etc.) contributed \$5.4 billion to the state economy (<http://www.window.state.tx.us>). Therefore, it is important to maintain the productivity and ecological integrity of estuarine ecosystems.

The productivity of estuarine systems depends on the timing and magnitude of freshwater inflow along with the associated nutrients such as nitrogen (N) and phosphorus (P), metals, and organic matter from the terrestrial environment (TWDB, 1994). Freshwater inflows are essential to ecological processes including dilution of salt water creating a unique environment and habitats for several species, regulation of bay water temperature, and for marine bio-geochemical cycles. Variations in freshwater inflows can alter the ecology of the estuarine environment and potentially hamper productivity. The San Antonio Bay estuarine system is located on the Texas Gulf Coast. This bay provides opportunity for tourism; particularly tourism related to the Whooping Crane. The Whooping Crane, a bird listed on the Endangered Species List (TPWD, 1998) migrates to this estuary during the winter (October to April) because it provides a unique habitat. In recent years there has been a decrease in number of Whooping Crane coming to this area, which has been attributed to reduction in number of blue crabs (TPWD, 1998). Reduction in blue crab population has been attributed to reduction in freshwater inflows (TPWD, 1998).

Hydrology is potentially the most critical element of instream flow studies. It is considered the "master variable" because the biology, physical processes, water quantity and quality components directly relate to it (Poff et al., 1997). Hydrology is used to assess hydraulic functions, water quality factors, channel maintenance, riparian forming processes, and physical habitat for target aquatic species. The Hydrologic flow regime takes into account seasonality and periodicity of various types of flows (e.g., subsistence flows, base flows, high flow pulses, and overbank flows). Hydrologic assessment helps

to understand and quantify the magnitude, frequency, timing, and duration of various types of flows. It also helps to understand the degree to which the natural flow regime has been altered due to reasons such as water management, land use change, and climate variability.

Freshwater inflows along with their associated nutrient and metal delivery are influenced by the land use/land cover (LULC) and water management practices in the contributing watershed, particularly in watersheds that are experiencing rapid human induced disturbances such as urbanization. The San Antonio River Watershed is a semi-arid to subtropical region experiencing rapid human population growth. Urbanization is significantly impacting various ecological services through land fragmentation and changes in land cover. While scientific studies have clearly stated that once dominant savanna grasses are disappearing and being replaced by woody plants in this region (Archer et al., 2001), the consequences of those changes on the regional water budget have not been studied explicitly (Asner et al., 2003).

Previous studies (TWDB, 1998; TPWD, 1998) have determined methods for quantifying coastal freshwater inflows in Texas using computer optimization and hydrodynamic modeling. The modeling quantifies theoretical estimates of minimum and maximum freshwater inflows, MinQ and MaxQ respectively, and maximum fisheries harvest inflow MaxH, for each estuary on the Texas Gulf Coast. TPWD (1998) empirically evaluated fisheries survey data from the TPWD Coastal Fisheries Resource Monitoring Database. The agency has made recommendations for the flow requirements

for the entire Guadalupe Estuary, which receives flows from both the San Antonio and Guadalupe River Watersheds. The MinQ flow recommended was 1271 million m³/year and the MaxQ flow was 1591 million m³/year (TPWD, 1998). Optimal flow that produced MaxH within the range of inflows between MinQ and MaxQ was estimated to be 1418 million m³/year. Past study (particularly historical flow analysis) on freshwater inflows to Texas bays and estuaries (Longley, 1994) suggested that the largest fraction of freshwater inflows to the Guadalupe Estuary comes from gaged portions of the Guadalupe River Basin. The gauged area of Guadalupe River Basin contributed approximately 58% (1653 million m³/year) of the total freshwater inflows to the estuary. Gauged portions of the San Antonio River contributed about 23% (656 million m³/year) of total freshwater inflows. None of the studies modeled the effect of land use change on the environmental flow availability. Past studies have not assessed seasonal flows which may be more important than yearly/monthly flows (Longley, 1994). Seasonal flows are important because many ecological processes depend on seasonal signatures. Seasonal flows are also important because most of the water resources demand depend on seasons; for example, human water consumption increases during summer.

Although, the San Antonio River contributes only 20-30 % of freshwater inflows to the Guadalupe Estuary (Longley, 1994), it is hypothesized that urban development will significantly alter the flow (both timing and magnitude) regime by effecting processes such as reservoir operations, return flows, ground water usage, base flow, and peak flows. Urban development refers primarily to an increase in population and impermeable surfaces.

The **primary purpose** of this research was to quantify the regional hydrologic budget response (freshwater inflow and urban water demands) to change in LULC in the rangeland ecosystem of the San Antonio River Watershed.

1.2 Background

The present study area, San Antonio River Basin, covers approximately 10, 826 km². The river runs approximately 405 river km through four different counties. Major tributaries to this river are Leon Creek, Salado Creek, Cibolo Creek, and Medina Creek. About 60% of the area in this watershed is dominated by pasture/rangeland, followed by forest, and urban impervious surfaces. Population in this river basin has increased in the last 30 years, primarily due to the growth of the City of San Antonio. The city of San Antonio, is the 8th largest city in the U.S. San Antonio is currently experiencing rapid urbanization as a result of increasing population. Population in this area has grown at an average of 1.8 % per year (U.S. Census Bureau, 2005). It is predicted that population in the San Antonio Metropolitan Area would be approximately 2.2 million people by 2020 (Texas State Data Center, 2005; Nivin and Perez, 2006). This urbanization is mainly concentrated in Bexar, and Medina Counties (Peschel, 2004). Historically, the City of San Antonio has primarily depended on the Edwards Aquifer as its sole source to meet its growing water needs (McCarl et al., 1999; San Antonio Water Systems, 2006). With the increasing demand of water for domestic and industrial purposes for this city, the watershed is struggling to provide enough water to the Guadalupe Estuary systems. Previous study (Longley, 1994) suggested a need of about 656 million m³/year of total

freshwater inflow from this watershed to the Guadalupe Estuary. The amount of impervious surface has also increased. An increase in impervious surface could possibly have altered the timing and magnitude of freshwater inflows to the estuary.

1.2.1 Trend Analysis of Streamflow

Statistical analysis of environmental flow can help to evaluate changes due to climate and/or LULC (urbanization in this case) in the watershed. Studying the detection of trends in hydroclimatic variables in a river basin is important because it provides information regarding any changes in basin management. Detection of past trends, changes, and variability in environmental flows and precipitation pattern is important for understanding of potential future changes resulting from anthropogenic activities or climate variability on environmental flows.

1.2.2 Wavelet Analysis of Streamflow Variations

Researchers seeking to quantify the amount and timing of freshwater inflows typically use computer models to simulate the system of interest and/or statistical analysis of daily, seasonal and annual flow patterns. Statistical tests based on time intervals are used to characterize cyclic phenomena by calculating the means, and variances. Spectral analysis, particularly wavelet analysis (Daubechies, 1992; Farge 1992; Liu, 1994; White et al., 2005; Kumar and Foufoula-Georgiou, 1997), provides an alternative methodology to traditional time series analysis, where variations in environmental flow can be

analyzed without pre-assigning time frames. Wavelets can be used to localize simultaneous modulations in the scale (inverse of frequency and analogous to period) and amplitude of freshwater flow, an approach that is not possible with traditional analysis. Wavelet analysis requires no *a priori* assumption about the timing and length of important processes and provides an easily interpreted image of the amplitude of cycles at all scales and at all times.

Wavelet analysis provides a unique methodology to evaluate cyclic changes in the time series. It helps in establishing the relationship between these cyclic changes and ecological characteristics of the system in question. For example, if six month cycles were required for a particular river ecological restoration goal that depends on water availability, wavelets would be an ideal assessment tool to evaluate how water resources should be planned to allocate water that will meet the ecological need during the six month period. Therefore, wavelet techniques can be utilized to understand the cyclic nature of the events that are important for sound ecological management.

Wavelets have been used in several hydrologic studies, including detection of changes in streamflow variance (Cahill, 2002), simulation of streamflow (Bayazit and Aksoy, 2001), identification of climate impact on stream flow (Bradshaw and McIntosh, 1994), and differentiating between natural and anthropogenic influences on streamflow (Nakken, 1999). Studies have not yet been conducted to characterize the effect of urbanization on freshwater inflows using a wavelet technique.

1.2.3 Monitoring Urban Land Use/Land Cover Change by Remote Sensing on a Regional Scale

Remotely sensed data from satellites is a reliable source for land use classification and land cover change analysis. It is a useful tool for ecological analysis as well. Availability of satellite data at less cost and increasing computational power has made the application more practical for studying larger areas. Also, availability of remotely sensed data with high temporal and spatial resolution, has allowed analysis methods to become more suitable for application over large areas (Tanaka and Sugimura, 2001). The LANDSAT program is one of the longest running satellite data acquisition programs in the United States. Remotely sensed data has been used to obtain information about vegetation, ice and snow, soils, and geomorphology (Allen et al., 1997). Various studies have demonstrated the potential of remote sensing technology application for analysis of urban/suburban environment with focus on land cover/land use, socioeconomic information, and transportation infrastructure (Acevedo et al., 1996; White, 1998; Donnay et al., 2001). Studies related to urban mapping have used urban impervious surfaces as one of the indicators to quantify the extent of urbanization. Various techniques used to quantify impervious surfaces are multiple regression, spectral unmixing (Flanagan and Civco, 2001), artificial neural networks (Flanagan and Civco, 2001), classification trees (Smith et al., 2003), and integration of remotely sensed data with GIS (Brivio et al., 2002). In general, mapping of urban areas by remote sensing is rather a complex process due to the heterogeneity in the urban environment. Complexity increases due to the presence of built up structures (such as buildings,

transportation nets etc.), several types of vegetation cover (such as parks, gardens, agricultural areas), bare soil zones, and water bodies.

1.2.4 Effects of Land Use on Land Surface Hydrologic Processes on a Basin Scale

LULC change can significantly alter hydrology on the local, regional, continental and global scales. Although, the human impacts and disturbances on the global hydrologic cycle, and the potential consequences of this on climate are still in debate (Sala and Paruelo, 1997), studies suggest that land use can bring atmospheric changes (Stohlgren et al., 1998), streamflow variability (Waylen and Poveda, 2002) and modification in the dynamics of tree populations (Stohlgren et al., 1998). With increasing urban growth, ongoing LULC change can alter the amount of flow through changes in storm flow, evapotranspiration, and groundwater storage (Bhaduri et al., 2001). One of the most important land cover type characteristics of urban environments is impervious surface developed through anthropogenic activities. Impenetrable surfaces, such as rooftops, roads, and parking lots, have been identified as key environmental indicators of urban land use, water quality and water quantity. Impervious surfaces also increase the frequency and intensity of downstream runoff and decrease water quality. While there have been studies assessing the effects of climate change and landuse change on streamflow (Legesse et al., 2003; Waylen and Poveda, 2002), previous studies did not explicitly examine the hydrologic influence of land use conversion due to urbanization and its effect on freshwater inflow. The role of land surface hydrologic processes (including soil moisture and groundwater) on nutrient and metal distribution and

transport is one of the least understood aspects at local, regional, continental, and global scales. Variation in hydrology resulting from LULC change can cause variability in freshwater inflows along with the instream nutrients and metals that determine the productivity of an estuary. Spatial and temporal variability in catchment characteristics makes it difficult, at best, to generalize nutrient flux by hydrologic systems at the regional scale. Therefore, better methods are needed for making accurate estimates of freshwater inflows over regional, local, catchment, and continental scales.

1.2.5 Modeling Environmental Flows to an Estuary

Several countries have taken different approaches to model environmental flows to their respective estuaries (Pierson et al., 2002; Adams et al., 2002; TWDB 1994; TPWD 1998). Past studies have used historical stream flow data (e.g., the 7-day 10 year minimum flow, or 7Q10) to set the lower bounds for estuarine inflow (Alber and Flory, 2002). Studies in Australia, in some cases have used flow-duration based recommendation (Pierson et al., 2002). In the State of Texas, agencies such as TWDB, and TPWD have used optimization techniques and hydrodynamic modeling to quantify coastal freshwater inflows requirement.

Several agencies such as USGS, San Antonio Water Systems (SAWS), and San Antonio River Authority (SARA) working in San Antonio River Watershed are involved in modeling this watershed, especially the upper portion of the river basin, and streams in Bexar County. These agencies are using Hydrologic Simulation Program in Fortran

(HSPF) (Bicknell et al., 1997) as the hydrologic model (personal communication, with Steven Raabe, SARA, and Dr. Y. C. Su, PBS&J). HSPF is preferred by these agencies (SARA, 2003) to other hydrologic models because it simulates hydrology more accurately in these urban dominated systems (SARA, 2003). HSPF is a comprehensive, conceptual, continuous watershed simulation model designed to simulate all the water quantity and water quality processes that occur in a watershed, including sediment transport and movement of contaminants. Although it is usually classified as a lumped model, it can reproduce spatial variability by dividing the basin in hydrologically homogeneous land segments and simulating runoff for each land segment independently, using different meteorologic input data and watershed parameters. The model includes fitted parameters as well as parameters that can be measured in the watershed (www.usgs.gov).

1.2.6 Parameter Estimation in Model Calibration

Parameter estimation is an important stage of model calibration (Sorooshian and Gupta, 1995). Parameter estimation follows the decision of which parameters of the simulation model to calibrate. Manual calibration and automatic calibration are two types of parameter estimation approaches. Although manual calibration is widely used, often it is time consuming, and the success of model calibration depends on the experience of the modeler and his/her knowledge of the study watershed, along with model assumptions and its algorithms. Automatic calibration is fast, less subjective, and it makes an extensive search of the existing parameter possibilities. It is highly likely that results

would be better than that which could be manually obtained. Senarath et al. (2000) and Eckhardt and Arnold (2001) have implemented automatic calibration for distributed models. Both studies have used Shuffled Complex Evolution search algorithms (Duan et al., 1992). None of these studies has used automatic calibration for HSPF using a genetic algorithm (GA).

Genetic algorithm (GA) is a kind of search method widely used by researchers for optimization problems (Ines and Droogers, 2002; Srivastava et al., 2002; Liong et al., 1996), including those in hydrologic models. GA is a search algorithm and also an evolutionary algorithm mathematically represented, that mimic the processes of natural selection and evolution (Goldberg, 1989; Carrol, 1997; Reeves, 1993).

In GA, the parameters that control the outcome of the optimization are mathematically termed as decision variables. Combinations of decision variables form a population. Each individual in the population is a “chromosome”. Chromosomes are composed of bits termed as “genes”, which are the decision variables. Therefore, each chromosome contains all possible information of the decision variables pertinent to the problem domain, i.e. a single chromosome is one possible combination of values for all the parameters used in the calibration.

Most of the earlier studies, on use of GA in optimization, has addressed land use planning (Stewart et al., 2004), water management practices (Ines and Honda, 2005), best management practices (Srivastava et al., 2002) and automatic calibration of

distributed watershed models (Muleta and Nicklow, 2005). Past studies have not addressed parameter optimization in HSPF for surface water quantity.

1.3 Study Objectives

The objectives of the research were:

1. Examine increasing/or decreasing trends on hydrologic variables in a rapidly urbanizing semi-arid coastal river basin.
2. Characterize freshwater inflows to estuary and environmental flows at various stream gauging stations in a rapidly urbanizing semi-arid watershed using wavelet analysis.
3. Implement a GA based parameter estimation on calibration of HSPF.
4. Study the effect of land use and land cover change in San Antonio River Basin on freshwater inflows to the gulf coast estuary.

CHAPTER II

HYDROLOGIC TREND DETECTION IN A RAPIDLY URBANIZING SEMI-ARID COASTAL RIVER BASIN

2.1 Overview

The productivity of estuarine systems depends on the quantity and quality of freshwater inflow which in turn depends on landuse/land cover and water management in the contributing watershed. This study examines the presence of trends in seasonal environmental flows in the San Antonio River Basin. Trend analysis can provide important information on short or long term changes to the hydrologic variable in question. This study used daily streamflow obtained from nine USGS gauging stations that had at least 15 years continuous data. Baseflow was separated from stormflow using a baseflow separation filter program on total streamflow. Pre-whitening was used to remove serial correlation from the hydrologic variables' time series. A bootstrapping method was used to determine the critical value for the percentage of stations expected to show a trend by chance. In addition, streamflow data, obtained from the most downstream USGS gauging station having the longest continuous record on the San Antonio River was used to examine trends in freshwater inflows contributed by the entire watershed to the Guadalupe Estuary. Analysis was also conducted on seasonal precipitation data, obtained from various weather stations spread across the watershed, using similar technique described above. Bootstrapping results suggested, 2 stations as critical value for global significant for most hydrologic variables. Whereas,

bootstrapping on rainfall data suggested, 1 station as critical value for global significant. Overall results suggested winter season observed increasing trends in most of the hydrologic and rainfall variables. While a distinct spatial pattern was observed in seasonal flow, no similar pattern was observed in rainfall. Flow gauging stations in upper portion of the watershed experienced decreasing trend, whereas stations in the lower portion experienced increasing trend. Presence of decreasing trend in baseflow in upper portion of the watershed (close to the urban area) could be attributed to increase in impervious surface over the years. Analysis also suggested increase in runoff in the river basin, which could be pointed to increase in impervious surface.

2.2 Introduction

Water in aquatic systems supports a variety of requirements, including ecosystem and anthropogenic needs. Present water rights and projected demands have sometimes resulted in a conflict between the use of rivers as water and energy sources, and their conservation as integrated ecosystems (Tharme, 2003; Caissie and El-Jabi, 2003). The amount of water needed to maintain stream habitat on a year round basis is termed in-stream flow need (Cooperrider et al., 1986), and the amount of water needed to maintain a healthy estuarine ecosystem is termed freshwater inflow (NRC, 2000). Both terms fall broadly under “environmental flows”. Evaluating environmental inflow needs focuses on balancing ecosystem flow requirements with human use. The world and the U.S, in particular, are struggling with issues of providing adequate environmental flows in times of high demand (both human and ecosystem) and low supply. The State of Texas is no

exception (Longley, 1994). With a combination of a variety of aquatic ecosystems, a growing urban population and periodic water shortages, Texas faces environmental flow challenges. In 2001, Texas Senate Bill 2, instructed three state agencies, the Texas Water Development Board (TWDB), the Texas Parks and Wildlife Department (TPWD), and the Texas Commission on Environmental Quality (TCEQ), to develop a state program of environmental flows to support a “sound ecological environment” on rivers and estuaries by 2010.

Estuaries are the connecting link between terrestrial and marine ecosystems, and provide a critical coastal habitat that is essential ecologically and economically to the world economy (Kennish, 2001); therefore, it is important to maintain their productivity and ecological integrity. The productivity of these systems depends on the timing and magnitude of freshwater inflow along with the associated delivery of nutrients such as nitrogen (N) and phosphorous (P), metals, and organic matter from the terrestrial environment. Variations in freshwater inflows can alter the ecology of the estuarine environment, potentially hampering productivity. Freshwater inflow, nutrient, and metal delivery are influenced by the land use/land cover and water management practices in the contributing watershed, particularly in watersheds that are experiencing rapid human induced disturbances. Changes in long-term environmental flows can be caused by climate variability, such as changes in precipitation pattern, land cover/land use change (LCLUC), and water management strategies. In large basins, prominent factors such as LCLUC and precipitation pattern change most likely alter the timing and volume of long term discharge (Costa et al., 2003).

Streamflow is composed of storm flow and baseflow. Storm flow is intermittent flow supported by surface runoff from discrete rainfall events. Baseflow is continuously sustained flow supported by either groundwater discharge to the stream or spring flows or return flows from the WWTPs. Baseflow is the major source of streamflow during dry periods; whereas storm flow is the major portion of streamflow immediately following rainfall (depending on the soil moisture content). Trends in stream flow in several river basins have been studied extensively to study the effects of climate change, vegetation cover and green house warming (Lins and Slack, 1999; Peterson et al., 2002; Costa et al., 2003). Lins and Slack (1999) while evaluating trends for 395 stream gauging stations in the Conterminous United States suggested that the U. S is getting wetter but less extreme. Peterson et al, (2002) suggested that average annual discharge from the largest Eurasian rivers to the Arctic Ocean increased by 7% from 1936 to 1999. The discharge had a correlation with changes in North Atlantic Oscillation (NAO), and global mean surface air temperature. Costa et al, (2003) while investigating 50 years long time series of discharge and precipitation data for Tocantins River concluded that changes in vegetation cover had altered the hydrologic response of the study region. Little study has been conducted to assess the impact of human activities such as urbanization on environmental flows (Copeland et al., 1996).

Land development in the U.S is proceeding at a rate greater than population growth (Heimlich and Anderson, 2001). From an ecological perspective, land development is one of the most disturbing processes, dramatically altering the natural energy and

material cycles (Pielke et al., 1999). In a study of the effect of urbanization on ecological services in the City of San Antonio Kreuter et al. (2001) found the net effect of urbanization on local ecosystems to be neutral. However, Cummins (2000) illustrated a clear impact of urbanization on the riparian areas around local streams, which play a vital role in nutrient cycling, maintaining water quality of streamflows and influence the timing and magnitude of nutrient transport (Chaubey et al., 2007).

Previous studies have investigated the presence of trends in annual or monthly streamflow (Coulibaly and Burn, 2005; Zhang et al., 2001; Douglas et al., 2000; Yue et al., 2001; Burn and Elnur, 2002) but did not assess seasonal flows which may be more important to estuary ecosystem needs (Longley, 1994). For example, the Whooping Crane, a bird listed on the Endangered Species List (TPWD, 1998) migrates to the Guadalupe Estuary during the winter (October to April) because it provides a unique habitat for nesting and for the blue crab, a major component of the bird's diet. In recent years there has been a decrease in the blue crab population, which has been attributed in part to reduced freshwater inflows (TPWD, 1998) which in turn has led to a decreased number of Whooping Crane.

Statistical analysis of environmental flow can help to evaluate changes resulting from climate variability and/or LCLUC in the watershed. Detection of past trends, changes, and variability in hydroclimatic variables is important for understanding the potential impact future change resulting from anthropogenic activities such as urbanization and agriculture, can have on environmental flows (Hurrell, 1995; Leggese et al., 2003; Lins

and Michaels, 1994; Lettenmair et al., 1994; Lins and Slack, 1999; Zhang et al., 2001; Zhang and Schilling, 2006). Lins and Michaels (1994), analyzed streamflow in the U.S and suggested increased stream flow had a correlation with greenhouse gas. Lettenmair et al, (1994) analyzed spatial pattern of trends in average temperature, precipitation, streamflow and average daily temperature in the continental U. S. Their study indicated strong spatial and seasonal pattern in trend results. Increasing trend in annual temperature was observed in many stations in North and West. Whereas decreasing trend was observed for same variable in South and East. Lins and Slack (1999) evaluated trends in 395 stream gauging stations in the Conterminous United States and suggested that the U. S is getting wetter but less extreme. Zhang et al, (2001) presented a study that analyzed trends from the past 30-50 years for 11 hydroclimatic variables obtained from Canadian Reference Hydrometric Basin Network database. In general, southern part of Canada experienced decreasing trend in mean stream flow during this period. Zhang and Schilling (2006) investigated flow in Mississippi River Basin using data from 1940-2000. Their study showed increasing baseflow in the river was due to land use change and associated agricultural activities. While study in agricultural dominated watershed has indicated change in agricultural practices influenced environmental flows, little information is available in urban dominated watershed.

The overall objectives of this research are:

- Investigate the presence of trends at several stream gauging stations in several seasonal flow variables in the rapidly urbanizing semi-arid San Antonio River Basin.

- Investigate the effect of spatial correlation of the significance of the trends found.
- Investigate the presence of trends in freshwater inflows contributed by the San Antonio River to the Guadalupe Estuary.
- Determine the role that variability in precipitation may play in watershed scale trends in streamflow.

2.3 Study Area

The 10, 826 km² San Antonio River Basin extends from the headwaters of the Medina River to the point at which the San Antonio River joins with the Guadalupe River before emptying into the Guadalupe Estuary (Figure II-1). The San Antonio River begins just below Olmos Dam and runs 405 river km through four counties. In addition, the watershed drains some portion of eight additional counties. Northwest of the City of San Antonio, the terrain slopes to the Edwards Plateau and to the southeast it slopes toward the Gulf Coastal Plains. Soils are blackland clay and silty loam on the plains and thin limestone soils on the Edwards Plateau. About 60% of the area in this watershed is dominated by pasture/rangeland (Figure II-1), 24% by forest, and 14% by urban

impervious surfaces. In a study of freshwater inflow needs of Texas bays and estuaries Longley (1994) estimated an annual volume of 656 million m³ of total freshwater was needed from the San Antonio River to maintain the health of the Guadalupe Estuary.

Population in this river basin has increased in the last 30 years primarily due to the growth of the City of San Antonio, the 8th largest city in the U.S. (Figure II-2). San Antonio is currently experiencing rapid urbanization as a result of a population that has grown at an average of 1.8 % per year (U.S. Census Bureau, 2005). It is predicted that the population in the San Antonio Metropolitan Area will be approximately 2.2 million people by 2020 (Texas State Data Center, 2005; Nivin and Perez, 2006). This growth is mainly concentrated in Bexar, and Medina Counties (Peschel, 2004). Historically, the city of San Antonio has primarily depended on the Edwards Aquifer as its sole source to meet its growing water needs (McCarl et al., 1999; San Antonio Water Systems, 2006). As demand has increased, treated wastewater in this river basin has either been recycled or discharged to streams for downstream environmental flows (San Antonio Water System, 2006; San Antonio River Authority, 2006). In recent years with the increase in population, a number of new WWTP have been brought on-line in this watershed (Figure II-1). However, data is limited on the quantity of water being discharged to the San Antonio River from these WWTP.

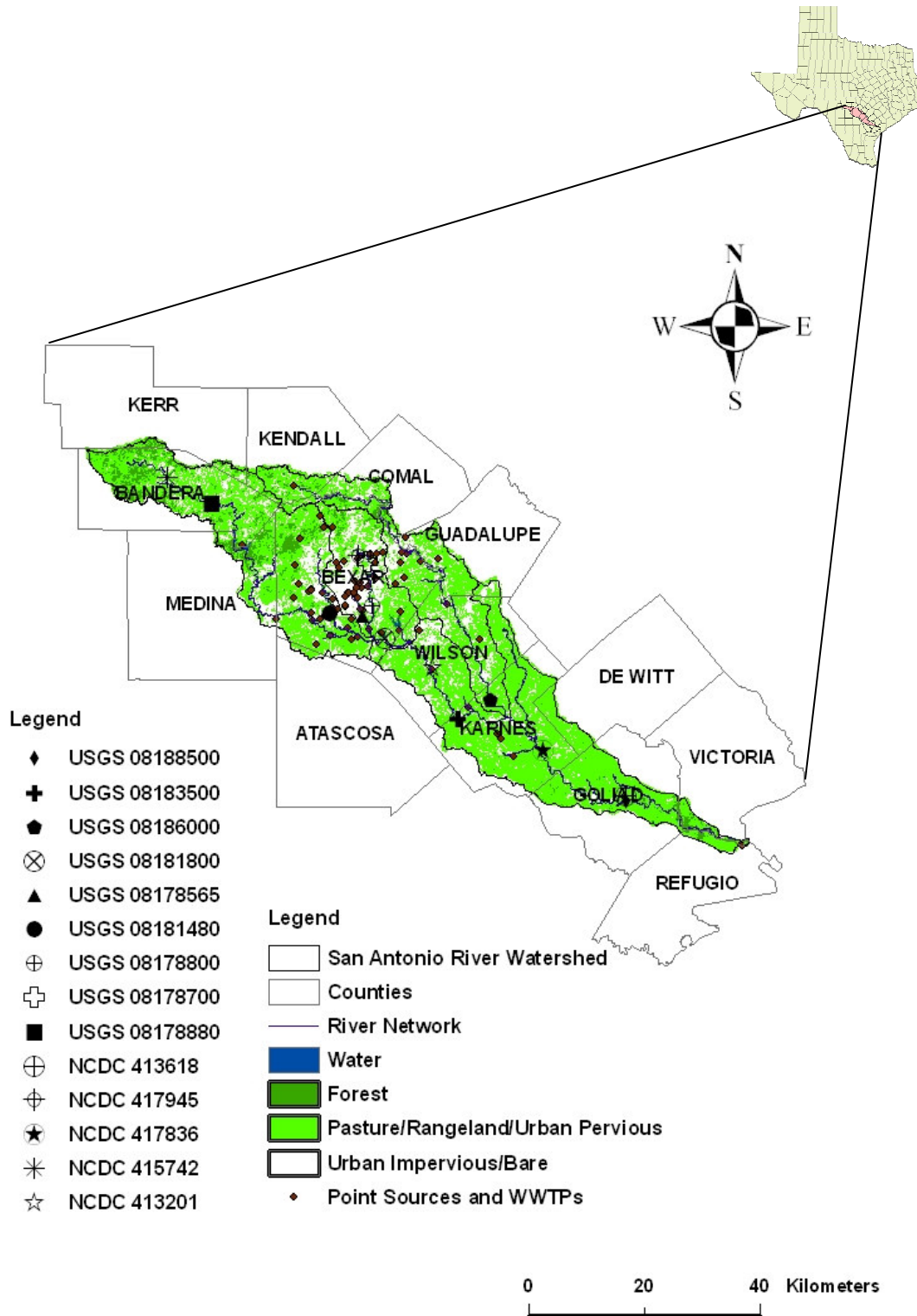


Figure II-1: San Antonio River Watershed with USGS gauging stations, NCDC weather stations, and WWTP.

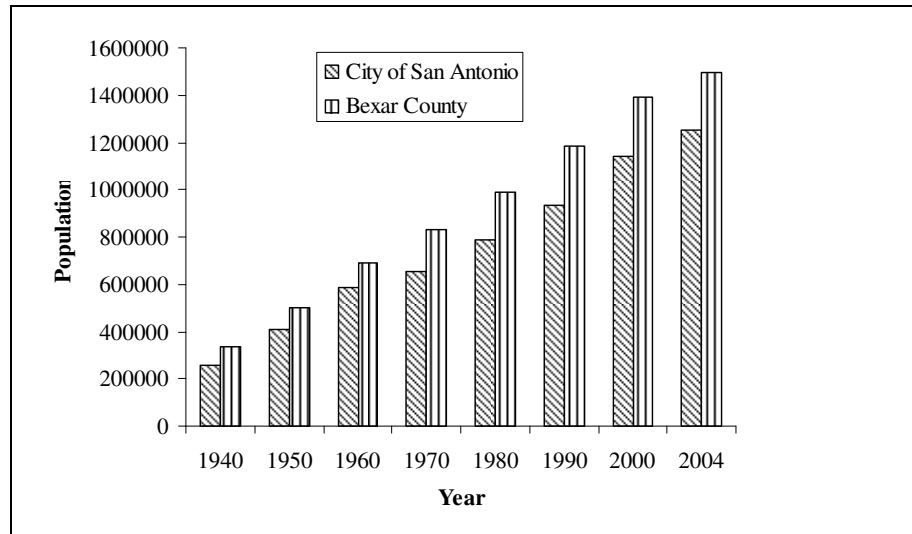


Figure II-2: Population trend since 1940 for the City of San Antonio and Bexar County, in which San Antonio is located (Texas State Data Center, 2005).

2.4 Methodology

A stepwise approach was used in the detection of trends in the time series representing several hydrologic variables on a seasonal time scale. Those steps can be summarized as:

1. Select hydrologic variables that adequately assess the state of environmental flows in the San Antonio River.
2. Select streamflow gauging stations in the San Antonio River Watershed to be investigated. The primary criterion for selection of representative gauging stations was the length of record of continuous streamflow data.
3. Determine the presence of trends in all hydrologic variables using the Mann-Kendall non-parametric test.
4. Determine the significance of detected trends employing a permutation method

following Burns and Elnur (2002).

5. Determine trends in seasonal hydrologic variables representing freshwater inflows from the San Antonio River Watershed to the Guadalupe Estuary. This was done using the most downstream gauging station that maintained the longest continuous record of streamflow in the San Antonio River.
6. Characterize the variability in precipitation across the watershed and determine precipitation effect on regional streamflow trends.

2.4.1 Selection of Hydrologic Variables

The selection of hydrologic variables was based on the ability of the variable to indicate either change due to climate variability and/or LCLUC. A large number of variables were chosen because it is believed that different hydrologic variables will be affected in different ways by both climate variability and LCLUC. Previous studies (Zhang et al., 2001; Zhang and Schilling, 2006; Coulibaly and Burn, 2005) analyzed primarily annual and monthly flow. Coulibaly and Burn (2005) looked at the distribution of the flows and separated them into seasonal flows. This study took a similar approach to Coulibaly and Burn (2005) to differentiate seasonal flows. Average daily data (total streamflow, baseflow, and storm flow) for all the investigated variables were aggregated into three seasons, winter (December 1 to March 31), spring/summer (April 1 to July 31) and fall (August 1 to November 30). A total of 24 hydrologic variables were analyzed; for each of the three seasons, total, maximum and minimum streamflow, total maximum and minimum baseflow and total and maximum storm flow were determined.

Streamflow was proportioned into baseflow and storm flow using a baseflow separation program (Arnold and Allen, 1999) that has been used successfully in several other studies (Arnold et al., 1995; Lim et al., 2005; Eckhardt, 2005). Baseflow and storm flow were considered separately because it is hypothesized baseflow and storm flow will be affected differently by changes in land use land cover and climate variability.

The baseflow separation program is a digital filter (Nathan and McMahon, 1990; Lyne and Hollick, 1979; Arnold and Allen, 1999; Mau and Winter, 1997) that separates baseflow from total stream flow based on high and low frequency. High frequency waves can be associated with the direct runoff and low frequency waves can be associated with the base flow (Arnold and Allen, 1999; Eckhardt, 2005). This technique is objective and reproducible (Arnold and Allen, 1999). The filtered surface runoff (quick response) at time t , q_t is calculated as:

$$q_t = \beta q_{t-1} + \frac{1}{2}[(1 + \beta) * (Q_t - Q_{t-1})] \quad (1)$$

where t is one day, Q is the original streamflow (m^3), and β is the filter parameter. β in this study was set at 0.925 as determined by Arnold et al., (1995), where the authors suggested this value of β gave realistic results when compared to manual separation. Baseflow (m^3), b_t , is calculated with the equation:

$$b_t = Q_t - q_t \quad (2)$$

2.4.2 Selection of Gauging Stations

Data for the initial trend analysis was obtained from USGS gauging stations (www.usgs.gov) throughout the San Antonio River Watershed. Locations of the gauging stations are shown in figure II-1. The primary criterion for including a gauging station in the analysis was the length of continuous record of daily streamflow available. A minimum continuous record of 15 years of daily streamflow was required for a gauge to be included in the analysis. The end result was nine gauging with 15 or more years of data (Table II-1).

Table II-1: Duration of flow used in analysis for San Antonio River watershed USGS gauging stations.

Station ID	Flow duration data	Symbols
08188500	1940-2003	◆
08183500	1941-2003	+
08186000	1941-2003	◆
08181800	1963-2003	⊗
08178565	1987-2003	▲
08181480	1985-2003	●
08178800	1961-2003	⊕
08178700	1961-2003	⊕
08178880	1983-2003	■

Symbols can be used to locate stations on Figure II-1.

2.4.3 Trend Analysis

The Mann-Kendall non-parametric test (Mann, 1945; Kendall, 1975; Haan, 2002) was used for trend analysis on all hydrologic time series. This test has been widely used to test trends in hydrology and climatology (Lettenmaier et al., 1994; Zhang et al., 2000; Burn and Elnur, 2002). The test computes the slope of the line formed by plotting the hydroclimatic variables per time, but only considers the sign not the magnitude of the slope. The Mann-Kendall test statistic is calculated from the sum of the signs of the slopes. Each value in the time series $X(t')$ for $t' = t + 1, t + 2, \dots, N$ (number of observations in the time series) is compared to $X(t)$ and assigned a score $z(k)$ given by:

$$\begin{aligned} z(k) &= 1 && \text{if } X(t) > X(t'); \\ z(k) &= 0 && \text{if } X(t) = X(t'); \\ z(k) &= -1 && \text{if } X(t) < X(t'); \end{aligned} \quad (3)$$

For k from 1 to $N(N-1)/2$ the sum of the slopes is given by:

$$S = \sum_{k=1}^{N(N-1)/2} z(k) \quad (4)$$

The Mann-Kendall test statistic, U_c , for $N \geq 10$ is calculated as:

$$U_c = (S + m) / \sqrt{V(S)} \quad (5)$$

where $m = 1$ if $S < 0$ and $m = -1$ if $S > 0$ and $V(S)$ is given by:

$$V(S) = (1/18) * [N(N-1)(2N+5)] \quad (6)$$

The hypothesis of no trend is rejected if $|U_c| > z_{1-\alpha/2}$ where z is from the standard normal distribution, and α is level of significance. In this study a significance level of $\alpha = 0.2$ was chosen based on past studies (Zhang et al., 2001; Yue and Wang, 2002). There might be some measurement uncertainty in the stream flow data. Therefore, the significance level was lowered to 0.2.

2.4.4 Significance of Trend

Determining the significance of the trend tests permits the calculation of the percentage of tests that are expected to show a trend at the given significance level by chance. The significance of trend results was determined by the method described by Burn and Elnur (2002). As a first step, the correlation structure of the data had to be considered including both serial correlation in the time series, and cross correlation between the stations.

Serial correlation in data structure could increase the number of false positive outcomes in the Mann-Kendall test (Burn and Elnur, 2002). It is therefore important to remove the serial correlation prior to calculating the significance of the trend. One method to remove serial correlation is pre-whitening. The method used here calculates the serial correlation in the time series and removes the correlation if the calculated serial correlation is significant at the 5% significance level (Burn and Elnur, 2002). This significance level was selected because it was necessary to have more confidence on the serial correlation in data series. The Box-Ljung statistic was used to determine if the

serial correlation is significantly different from zero (Yue and Wang, 2002; SPSS 14.0, 2007). If the serial correlation was significantly different from zero, then the serial correlation was removed from the time series by (Burn and Elnur, 2002):

$$yp_t = y_{t+1} - ry_t \quad (7)$$

where yp_t is the pre-whitened series value for time interval t , y_t the original time series value for time interval t , and r is the estimated serial correlation.

The effect of cross correlation in the data structure increases the expected number of trends detected under a hypothesis of no trend in the time series. A bootstrapping (or resampling) method was used to determine the critical value for the percentage of stations that are expected to show a trend by chance following Burn and Elnur (2002). Briefly, the bootstrapping method was:

1. A year was randomly selected from the period of analysis.
2. Data for each station that had a value for the selected year were added to a new or “resampled” data set.
3. Steps (1) and (2) are repeated until the number of station-station years in the resampled dataset was equal to the number of station-years in the original dataset.
4. The Mann-Kendall nonparametric test was applied to each station in the resampled dataset and the percentage of results that are significant to the $\alpha_1\%$ or local significance level was determined.

5. Steps 1 through 4 were repeated 500 times. The result was a distribution of the percentage of results that were significant at α_l % level. From this distribution, the value that exceeded the α_g % or global significance level was selected as the critical value, p_{crit} .

Results in the trend analysis where the percentage of stations having a significant trend were larger than p_{crit} were considered significant at the α_g % global significance level. In this study both α_l and α_g were set at 20%, in order to be consistent for local significant and global significant trend. There might be some measurement uncertainty in the stream flow data. Therefore, the significance level was considered at 20%.

2.4.5 Freshwater Inflow Analysis

The streamflow record from USGS gauge 08188500 was used in a separate trend analysis. This gauge is considered particularly important because it can be used as an indicator for the volume of freshwater flow contributed by the San Antonio River Watershed to the Guadalupe Estuary. This station also had the longest continuous flow record beginning in 1940.

Baseflow and storm flow were filtered and data were aggregated as previously described. The Mann-Kendall nonparametric trend test was conducted on the original data without removing serial correlation from the data set. Yue et al. (2001) compared the results of trend analyses using Mann-Kendall trend analysis with and without

removing serial correlation (using pre-whitening) in the time series (Yue et al., 2001). They found a significant difference between the trends in the original data and pre-whitened data suggesting a change in the data structure with pre-whitening. Therefore, trend tests on this gauging station were done without removing serial correlation in the data.

2.4.6 Rainfall Characterization

In addition to environmental flow variables, precipitation data was also analyzed for presence of possible trends. Precipitation data was obtained for various weather stations located in the watershed (Figure II-1). Data was obtained from www.ncdc.noaa.gov for these stations (Table II-2) (NCDC, 2006). Daily precipitation data was then aggregated to total seasonal rainfall, corresponding to seasonal environmental flows. Analysis of rainfall will help in investigating possible connection of precipitation variability and seasonal environmental flows. Similar statistical techniques for trend analysis and significance of trend as described above were also employed to seasonal rainfall data.

2.5 Results and Discussion

Table II-3 shows the serial correlations for all hydrologic variables and all seasons of analysis. Of the 216 time series analyzed, 213 had significant serial correlation which was removed prior to performing the Mann-Kendall test. As an example, Figure II-3 shows the cumulative distribution of the percentage of stations that showed a significant

trend for a local significance of $\alpha_l = 20\%$ level for total winter streamflow. The p_{crit} value was found for a global significance of $\alpha_g = 20\%$ level to be 2. Table II-4 shows the p_{crit} values for all hydrologic variables and all seasons of analysis. Trend results including the number of stations that had trends that were significant at the local significance level, the number of stations with an increasing trend, the number of stations with a decreasing trend, and the percentage of stations with a significant trend at the global significance level are also shown in Table II-4. The greatest percentages of significant trends at all stations were in minimum streamflow and minimum baseflow in all three seasons, with at least 55% of stations showing significant trends. Significant trends were observed in all hydrologic variables in the winter season. The number of increasing trends was nearly twice the number of decreasing trends, 37 and 19, respectively, across all hydrologic variables and seasons.

Table II-2: Duration of rainfall used in analysis for San Antonio River watershed NCDC weather stations.

NCDC Station ID	Rainfall duration data
413201	1947-2003
415742	1967-1999
417836	1947-2003
417945	1947-2003
413618	1940-2003

Table II-3: Serial correlation of all hydrologic variables for all the stations and all the seasons.

Total Seasonal Flow		08188500	08183500	08186000	08181800	08178565	08181480	08178800	08178700	08178880
	<i>Winter</i>	0.198	0.198	0.275	0.164	0.344	0.399	0.310	0.275	0.205
	<i>Spring/Summer</i>	-0.017	-0.043	0.014	-0.080	0.236	-0.187	0.121	-0.082	-0.162
	<i>Fall</i>	-0.008	-0.019	-0.038	0.000	0.029	-0.304	-0.080	-0.113	-0.121
Minimum Seasonal Flow										
	<i>Winter</i>	0.293	0.282	0.421	0.309	0.264	0.104	0.448	-0.080	-0.068
	<i>Spring/Summer</i>	0.184	0.197	0.164	0.166	0.155	0.037	0.304	0.052	-0.253
	<i>Fall</i>	0.322	0.336	0.290	0.302	0.047	0.017	0.484	0.000	0.030
Maximum Seasonal Flow										
	<i>Winter</i>	0.157	0.194	0.105	0.173	0.381	0.388	0.168	0.077	0.074
	<i>Spring/Summer</i>	-0.068	-0.146	0.044	-0.107	-0.135	-0.231	0.015	-0.107	-0.216
	<i>Fall</i>	-0.077	-0.111	-0.130	-0.135	-0.253	-0.221	-0.105	-0.085	-0.201
Total Seasonal Baseflow										
	<i>Winter</i>	0.182	0.322	0.252	0.136	0.322	0.331	0.379	0.392	0.087
	<i>Spring/Summer</i>	0.014	0.270	0.000	-0.042	0.270	-0.164	0.151	-0.115	-0.126
	<i>Fall</i>	0.132	0.031	0.074	0.093	0.031	-0.313	0.000	-0.119	-0.051
Minimum Seasonal Baseflow										
	<i>Winter</i>	0.286	0.272	0.411	0.285	0.250	0.128	0.381	-0.083	-0.057
	<i>Spring/Summer</i>	0.184	0.187	0.168	0.144	0.165	0.023	0.393	0.057	-0.246
	<i>Fall</i>	0.251	0.253	0.294	0.244	0.049	0.397	0.464	0.082	0.000
Maximum Seasonal Baseflow										
	<i>Winter</i>	0.104	0.091	-0.004	0.183	0.068	0.259	-0.033	-0.105	0.204
	<i>Spring/Summer</i>	-0.083	-0.135	-0.080	-0.137	-0.019	-0.210	-0.048	-0.132	-0.194
	<i>Fall</i>	-0.081	-0.129	-0.119	-0.151	-0.107	-0.224	-0.104	-0.101	-0.079
Total Seasonal Runoff										
	<i>Winter</i>	0.272	0.239	0.236	0.207	0.314	0.375	0.391	0.272	0.237
	<i>Spring/Summer</i>	-0.069	-0.112	0.010	-0.131	0.171	-0.199	0.092	-0.078	-0.195
	<i>Fall</i>	-0.092	-0.116	-0.080	-0.089	0.053	-0.294	-0.098	-0.105	-0.203
Maximum Seasonal Runoff										
	<i>Winter</i>	0.110	0.154	0.086	0.126	0.357	0.389	0.154	0.071	0.049
	<i>Spring/Summer</i>	-0.050	-0.148	0.054	-0.101	-0.137	-0.235	0.005	-0.104	-0.219
	<i>Fall</i>	-0.075	-0.108	-0.129	-0.134	-0.249	-0.221	-0.105	-0.085	-0.209

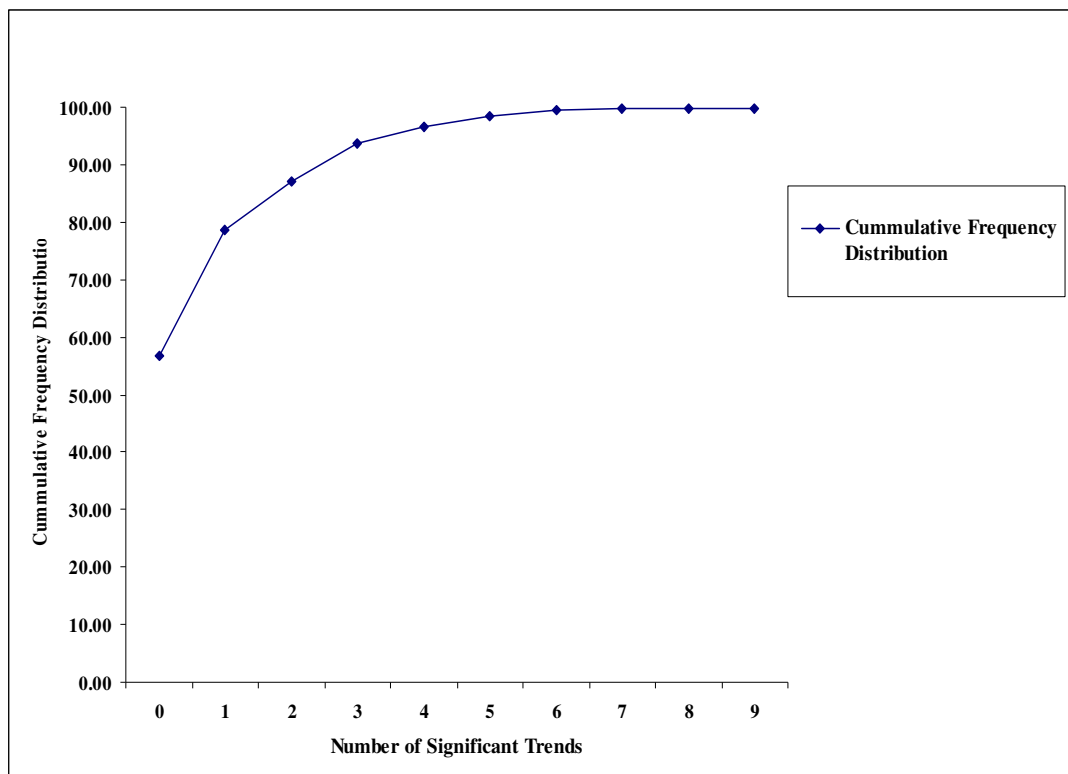


Figure II-3: Cumulative frequency distribution showing number of significant trends.

Table II-4: Trend test results for 9 USGS gauging stations in the San Antonio River watershed for the 1940-2003 period.

Variable	Season	No. of Stations	Global Critical Value P_{crit}	No. of Stations with Significant Trend (Local)	No. of Decreasing Trends	No. of Increasing Trends	% Significant Trend (Global)
Total	Winter	9	2	3	0	3	0.33
Streamflow	Spring/Summer	9	2	1	0	0	0.00
	Fall	9	2	2	0	0	0.00
	Minimum	Winter	9	2	5	1	4
Streamflow	Spring/Summer	9	2	5	2	3	0.55
	Fall	9	2	6	3	3	0.66
	Maximum	Winter	9	2	4	2	2
Streamflow	Spring/Summer	9	2	1	0	0	0.00
	Fall	9	2	0	0	0	0.00
	Total	Winter	9	2	4	0	4
Baseflow	Spring/Summer	9	2	2	0	0	0.00
	Fall	9	2	4	0	4	0.44
	Minimum	Winter	9	2	5	1	4
Baseflow	Spring/Summer	9	1	5	2	3	0.55
	Fall	9	2	5	2	3	0.55
	Maximum	Winter	9	2	3	2	1
Baseflow	Spring/Summer	9	2	1	0	0	0.00
	Fall	9	2	2	0	0	0.00
	Total	Winter	9	2	3	1	2
Runoff	Spring/Summer	9	2	1	0	0	0.00
	Fall	9	1	1	0	0	0.00
	Maximum	Winter	9	2	4	3	1
Runoff	Spring/Summer	9	2	1	0	0	0.00
	Fall	9	2	0	0	0	0.00

The Mann-Kendall test statistics for all hydrologic variables during each season is presented by station number in Table II-5. Stations are arranged from the most upstream gauging station (08178880) to the most downstream station (08188500). The number of hydrologic variables having a globally significant trend increases for all seasons as you progress from the top of the watershed to the outlet. In general stations in the upper half

of the watershed (i.e. above 08181800) show a decreasing trend in variables with significant trends. The upper half of the San Antonio Watershed has experienced the greatest urban growth in the watershed over the last 60 years. All stations in the lower half of the watershed have increasing trends over all seasons in the hydrologic variables with significant trends. USGS gauges 08183500, 08188500 and 08186000 have the greatest number of significant trends across all variables in all seasons at 12, 11 and 10 trends each. The strongest overall positive (increasing) trends were at station 08186000 for minimum streamflow and minimum baseflow for all three seasons. The strongest negative (decreasing) trends were at station 08178700 for total and minimum baseflow in the spring/summer and fall seasons only. Figures II-4 and II-5 depict the spatial distribution across the watershed in trends of minimum streamflow and minimum baseflow in the fall season. This same general pattern holds for winter and spring/summer for these two variables. Generally, increase in impervious surface increases runoff and reduces baseflow. Therefore, presence of decreasing trend in baseflow at some stations upstream of 08181800 could be attributed to increase in impervious surface in the area. On the contrary, station 08178565 which is upstream of station 08181800 observed an increasing trend for Fall total baseflow and Winter minimum baseflow. This station is very close to urban settlement in the City of San Antonio. One possible reason for increasing trend for these variables could be attributed to WWTP discharges.

Table II-5: Mann-Kendall test statistics by station for trends in seasonal hydrologic variables that were significant at both the local and global significance levels ($\alpha_l = \alpha_g = 0.2$).

Station Number	Hydrologic Variable	Winter	Spring/ Summer	Fall
08178880	Maximum Runoff	-2.25	NT*	NT
08178700	Minimum Streamflow	NT	-4.19	-3.03
	Minimum Baseflow	NT	-4.17	-2.66
08178800	Minimum Streamflow	-2.37	NT	-1.70
	Minimum Baseflow	-2.13	NT	-1.65
	Maximum Baseflow	-2.30	NT	NT
08178565	Minimum Streamflow	1.71	NT	NT
	Maximum Streamflow	-1.71	NT	NT
	Total Baseflow	NT	NT	1.98
	Minimum Baseflow	1.80	NT	NT
	Maximum Runoff	-2.25	NT	NT
08181480	Minimum Streamflow	NT	-2.99	-2.00
	Maximum Streamflow	-2.53	NT	NT
	Minimum Baseflow	NT	-2.91	NT
	Maximum Baseflow	-2.91	NT	NT
	Total Runoff	-2.46	NT	NT
	Maximum Runoff	-2.53	NT	NT
08181800	Total Baseflow	-2.13	NT	NT
08183500	Total Streamflow	4.34	NT	NT
	Minimum Streamflow	3.96	2.32	2.99
	Maximum Streamflow	2.86	NT	NT
	Total Baseflow	4.90	NT	3.46
	Minimum Baseflow	4.12	2.46	2.77
	Maximum Baseflow	1.60	NT	NT
	Maximum Runoff	1.88	NT	NT
08186000	Total Streamflow	2.41	NT	NT
	Minimum Streamflow	5.09	2.44	2.22
	Total Baseflow	4.12	NT	2.10
	Minimum Baseflow	5.10	2.60	2.37
	Total Runoff	2.16	NT	NT
08188500	Total Streamflow	3.55	NT	NT
	Minimum Streamflow	4.31	2.10	2.40
	Maximum Streamflow	1.74	NT	NT
	Total Baseflow	4.35	NT	2.88
	Minimum Baseflow	4.22	2.04	2.25
	Total Runoff	1.86	NT	NT

* Indicates no trend at the global significance level.

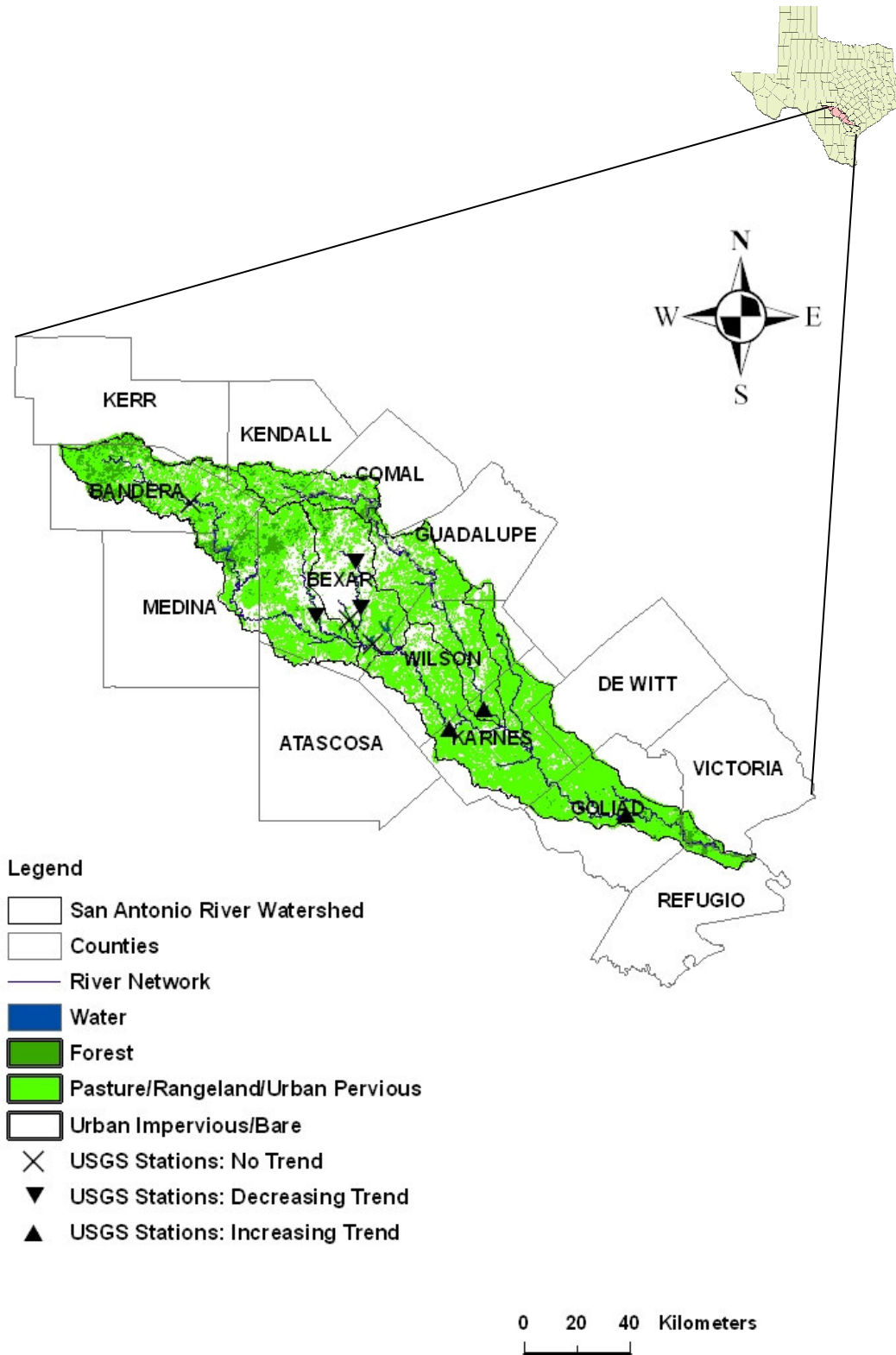


Figure II-4: Spatial distribution of USGS gauging stations showing increasing, decreasing and no trend for minimum stream flow for fall season.

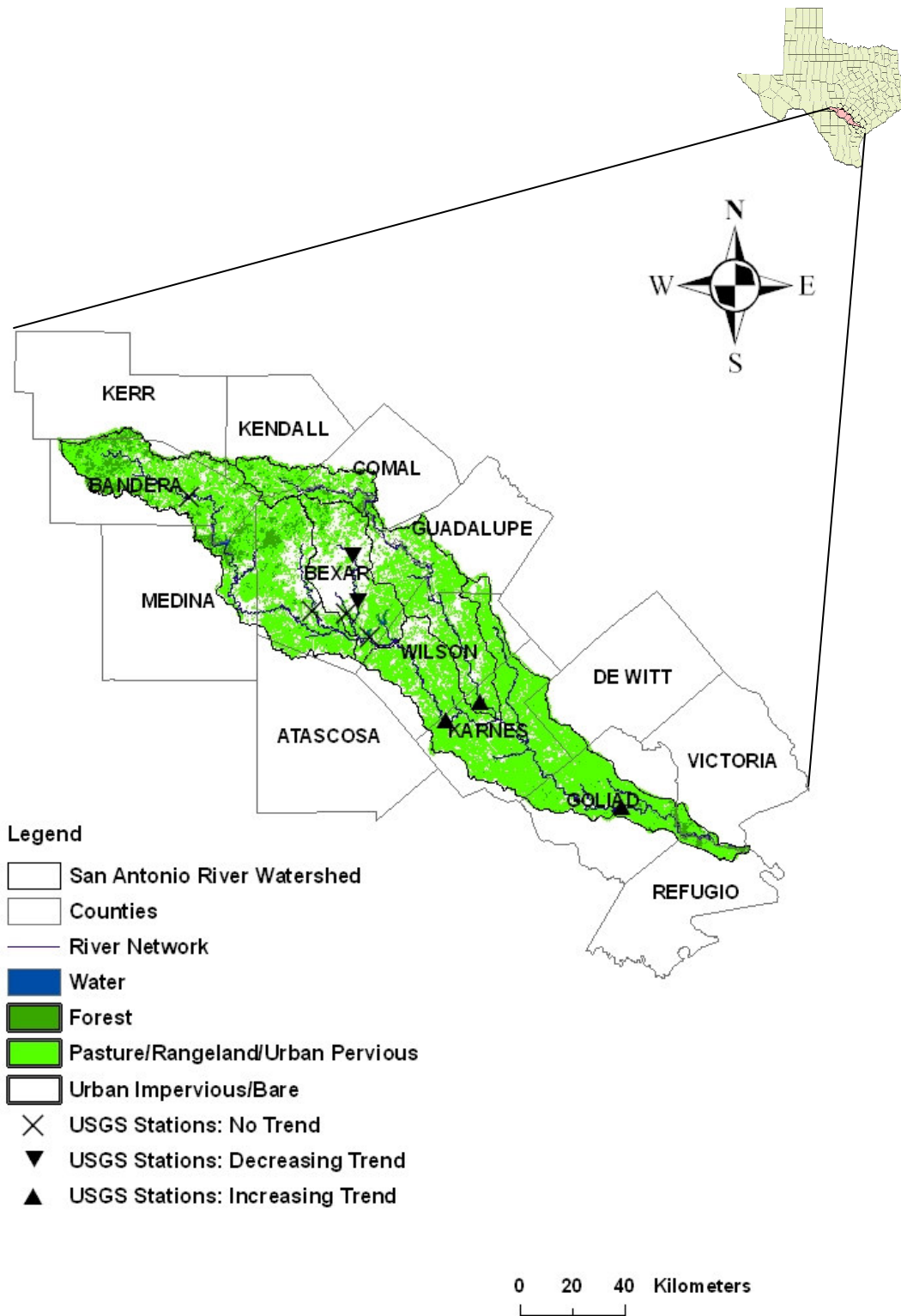


Figure II-5: Spatial distribution of USGS gauging stations showing increasing, decreasing and no trend for minimum base flow for fall season.

Table II-6 presents summary statistics over the length of record (1940-2003) for station (08188500). As stated earlier, a separate trend analysis was done at this station because it can be used as an indicator for the amount of freshwater inflow reaching the Guadalupe Estuary. Figures II-6 through II-8 graphically depict the time series for average seasonal values of winter total, maximum and minimum values of the hydrologic variable, respectively. The greatest average streamflow, baseflow and runoff all occur in the spring/summer season at this gauge. Not surprisingly, minimum average streamflow is equal to minimum average baseflow across all seasons. A significant linear relationship ($R^2 = 0.90$, $p < 0.05$) was observed between total streamflow and total baseflow for all the seasons. Baseflow is the largest part of streamflow in this river basin in all seasons; however, spring/summer runoff is a substantial portion of total streamflow at 40 %. It is evident from Figures II-6 through II-8 that the trends in streamflow are highly dependent on trends in baseflow.

Table II-6: Summary statistics for the hydrologic variables analyzed from the flow at USGS gauging station 08188500.

Variable	Mean (million m³)	Std. Deviation (million m³)	Maximum (million m³)	Minimum (million m³)
Total streamflow				
Winter	183.81	160.26	1148.32	34.51
Spring/Summer	288.84	296.15	1425.62	26.54
Fall	235.46	237.12	1053.08	27.56
Minimum streamflow				
Winter	0.62	0.32	1.89	0.12
Spring/Summer	0.51	0.43	2.54	0.005
Fall	0.47	0.34	1.78	0.03
Maximum streamflow				
Winter	62.41	12.19	62.41	0.41
Spring/Summer	149.99	22.76	149.99	1.63
Fall	292.72	40.90	292.72	1.44
Total baseflow				
Winter	139.54	103.23	743.58	32.56
Spring/Summer	174.02	175.45	920.69	14.09
Fall	138.78	116.72	604.15	20.57
Minimum baseflow				
Winter	0.62	0.32	1.89	0.12
Spring/Summer	0.51	0.43	2.54	0.005
Fall	0.46	0.34	1.78	0.03
Maximum baseflow				
Winter	4.99	5.83	30.83	0.07
Spring/Summer	6.50	8.26	46.23	0.49
Fall	5.23	7.73	47.60	0.35
Total runoff				
Winter	44.27	69.13	404.73	1.83
Spring/Summer	114.82	130.99	639.65	3.60
Fall	96.67	134.98	681.59	6.91
Maximum runoff				
Winter	7.96	10.37	51.44	0.28
Spring/Summer	15.52	18.86	127.01	0.47
Fall	18.19	37.68	273.99	0.83

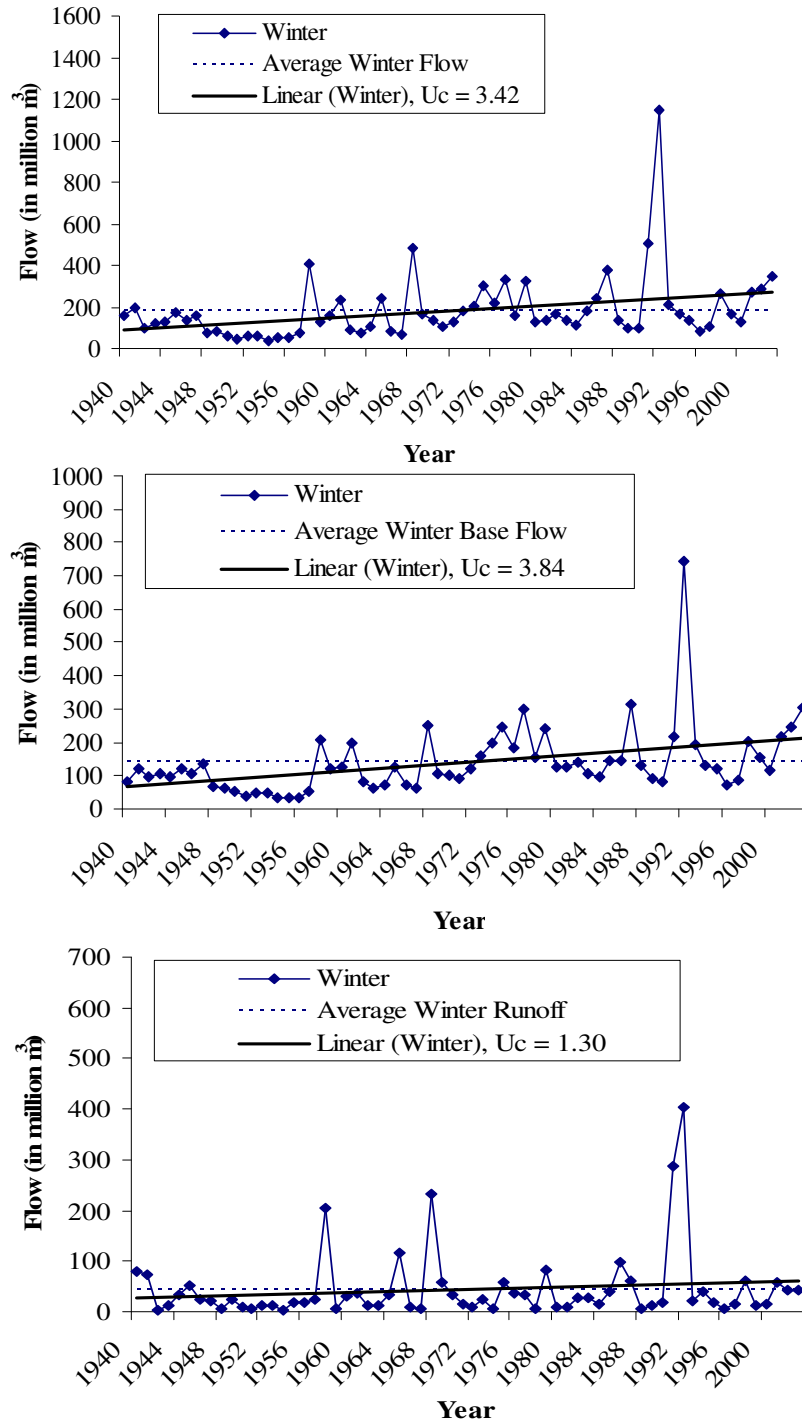


Figure II-6: Total seasonal flow, baseflow, and runoff for Winter Season at the most downstream USGS gauging station 08188500 1940 to 2003.

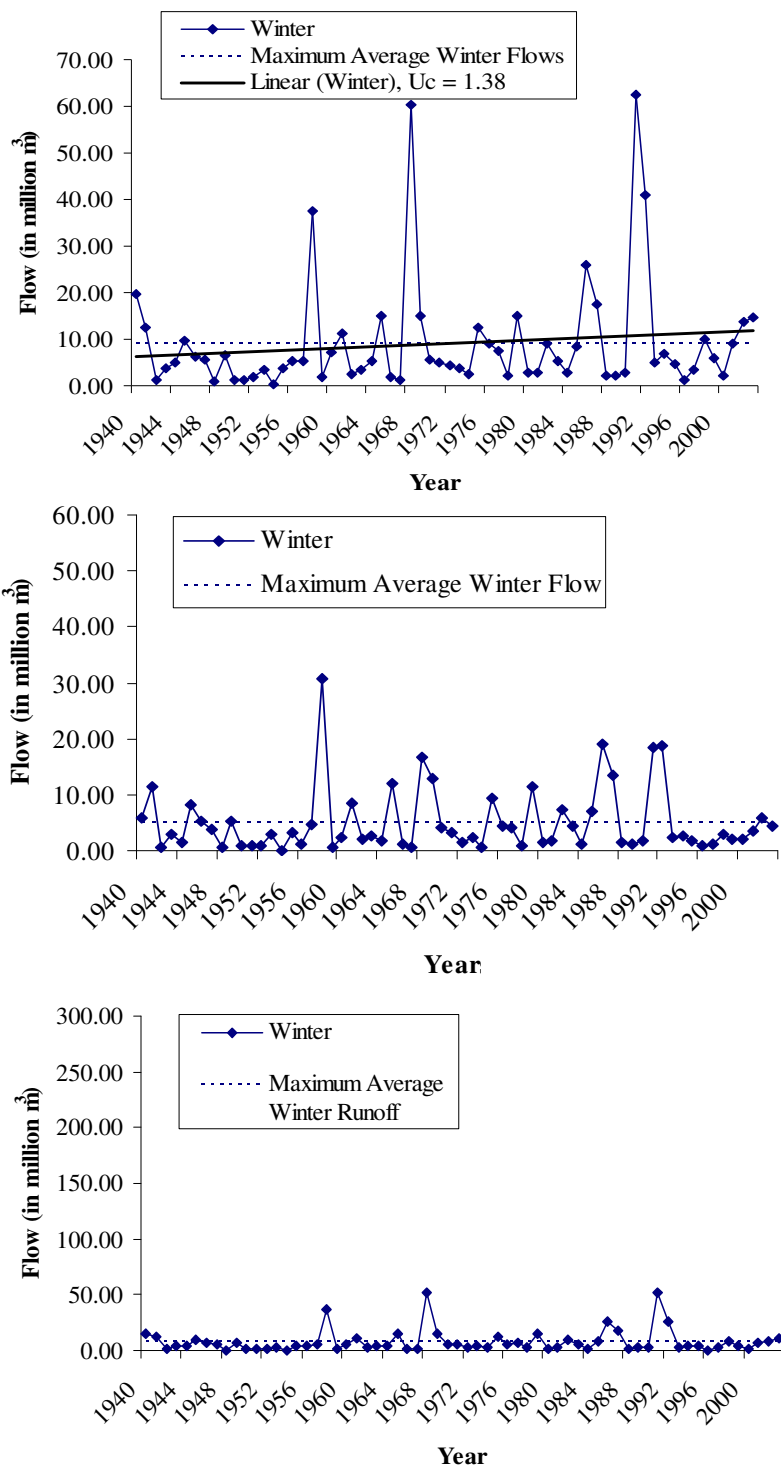


Figure II-7: Maximum seasonal flow, baseflow, and runoff for Winter Season at the most downstream USGS gauging station 08188500, 1940 to 2003.

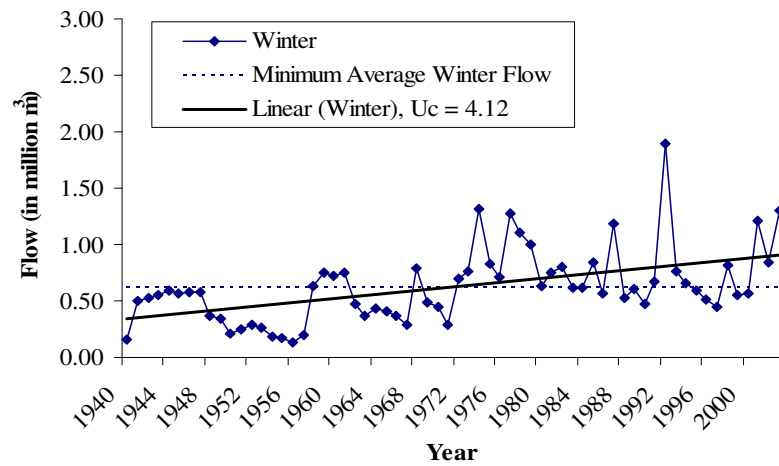
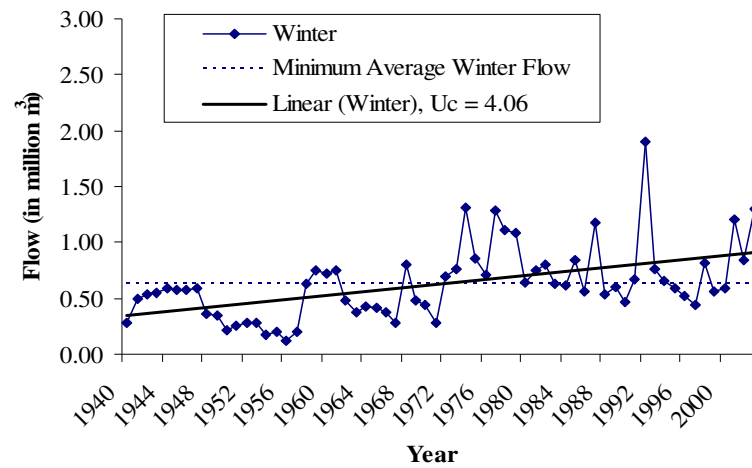


Figure II-8: Minimum seasonal flow, baseflow, and runoff for Winter Season at the most downstream USGS gauging station 08188500, 1940 to 2003.

Serial correlation of the rainfall data at all the stations in all the seasons is shown in Table II-7. Of the 15 rainfall time series analyzed, 12 had significant serial correlation. Serial correlation was removed from these variables prior to performing Mann-Kendall test. In this analysis, the p_{crit} value was found for a global significance of $\alpha_g = 20\%$ level to be 1 (Table II-8). The greatest percentages of significant trends at all stations were in total rainfall in winter season, with at least 33% of stations showing significant trend. No significant trend was observed in total rainfall for the spring/summer and fall seasons. Winter rainfall observed only increasing trend, and no decreasing trends.

The Mann-Kendall test statistics for all rainfall variables at each station during each season is shown in Table II-9. Stations are arranged from headwaters to downstream direction. No particular spatial pattern is observed in rainfall, as it is observed in other hydrologic variables.

Analysis of rainfall data from the last weather station NCDC COOPID 413618, that is close to the last USGS gauging station 08188500 suggested, out of the 64 year time series, not quite half of the years (29, 30 and 27 for winter, spring/summer and fall, respectively) experienced greater than average seasonal rainfall (Figure II-9).

Similarly, analysis of maximum seasonal rainfall showed no presence of either an increasing or decreasing trend (Figure II-10). Mann-Kendall test statistic values for winter, spring/summer, and fall were 1.27, 0.24, and 0.25 respectively. Average

maximum rainfall for winter, spring/summer, and fall were approximately 47, 76, and 80 mm, respectively. Again, less than half of the years in the 64 year time series (27, 22 and 24 for winter, spring/summer and fall, respectively) experienced greater than average maximum rainfall.

More numbers of increasing trends were found in winter flows as well as in winter rainfall. Therefore, it could be conclusively said that winter flows were influenced by rainfall.

A comparison between total streamflow, baseflow and stormflow at USGS gauge 08188500 that resulted from similar high, medium and low rainfall events recorded at NCDC gauge 413618 in the 1950s and 1990s was done for all three seasons (Table II-10). Analysis suggested total flow from 1990s rainfall events increased substantially from 1950s rainfall events. In general, storm flow as well as baseflow in 1990s events increased substantially in all the high, medium, and low category events over similar 1950s events. In all rainfall depth-season combinations except high rainfall-winter, there was an increase in the contribution of baseflow to total streamflow. Therefore, the increase in seasonal total flow was primarily due to increase in seasonal total baseflow at this portion of the watershed. Comparison of 64 years of averaged total streamflow, averaged baseflow, and averaged runoff suggested that baseflow contributed about 80% of total streamflow in winter flows; 64% in spring/summer flows and 66% in fall flows.

Table II-7: Serial correlation of rainfall data for all the stations and all the seasons.

Total Rainfall	413201	415742	417836	417945	413618
Winter	0.000	-0.213	0.118	0.215	0.000
Spring/Summer	0.109	0.072	-0.187	0.111	0.147
Fall	0.013	-0.230	0.000	-0.150	0.148

Table II-8: Trend test results for 5 NCDC weather stations in the San Antonio River watershed.

Variable	Season	No. of Stations	Global Critical Value P_{crit}	No. of Stations with Significant Trend (Local)	No. of Decreasing Trends	No. of Increasing Trends	% Significant Trend (Global)
Total	Winter	5	1	3	0	3	0.33
Rainfall	Spring/Summer	5	1	0	0	0	0.00
	Fall	5	1	0	0	0	0.00

Table II-9: Mann-Kendall test statistics by station for trends in seasonal hydrologic variables that were significant at both the local and global significance levels ($\alpha_l = \alpha_g = 0.2$).

Station Number	Winter	Spring/ Summer	Fall
415742	1.83	NT	NT
417945	1.67	NT	NT
413201	NT	NT	NT
417836	2.13	NT	NT
413618	NT	NT	NT

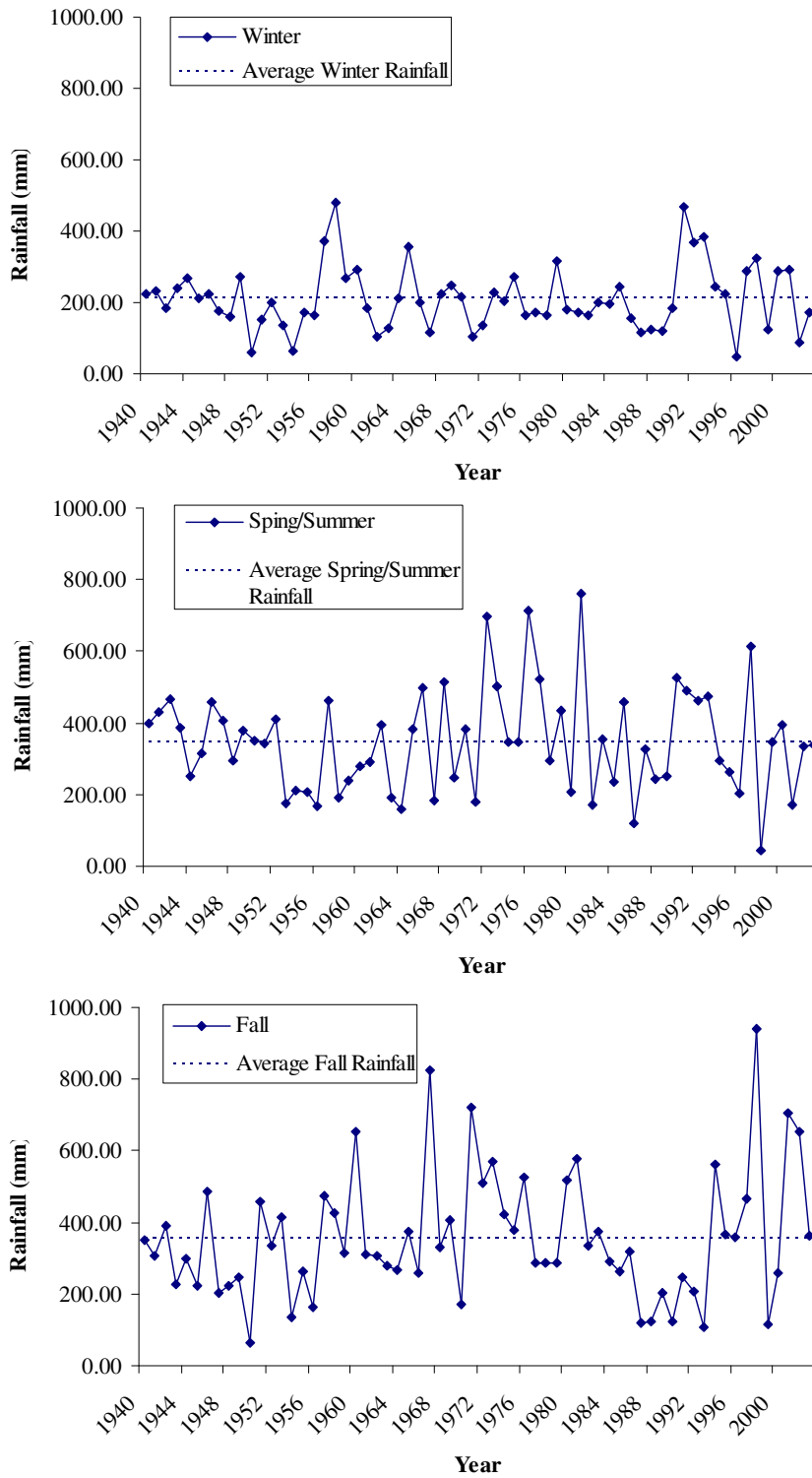


Figure II-9: Trend in total rainfall at NCDC gauge 413618 for winter, spring/summer and fall seasons.

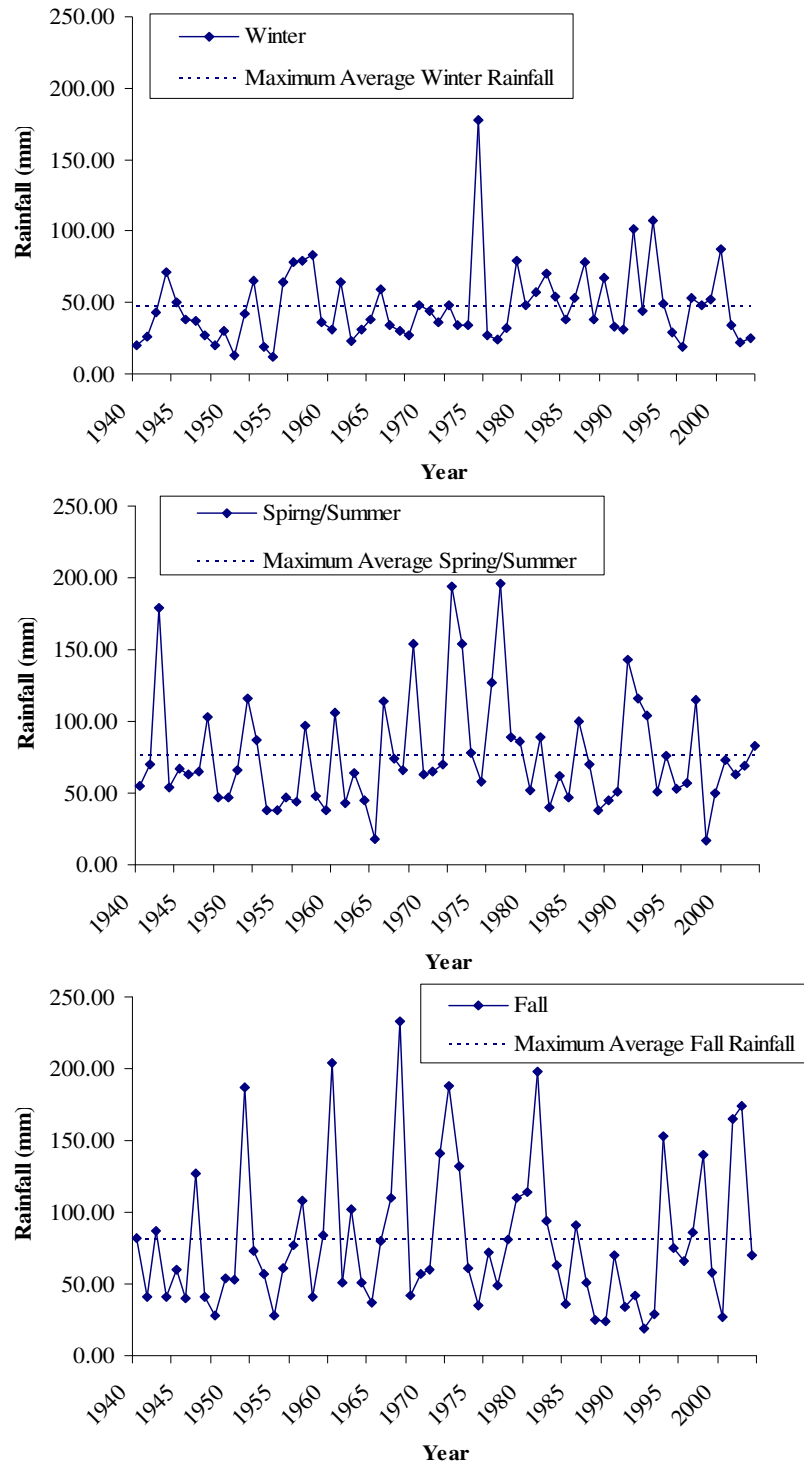


Figure II-10: Trend in maximum rainfall at NCDC gauge 413618 for winter, spring/summer and fall seasons.

Similar, analysis was also conducted at USGS gauge 08178800 with rainfall recorded at NCDC gauge 417945 (Table II-11). This USGS gauging station is very close to the urban area in the City of San Antonio. The NCDC weather station is also located very close to the gauging station. In this case analysis was performed from 1960s and 1990s event. Overall analysis suggested total flow increased substantially in 1990s than 1960s, particularly in high rainfall events category. In general, comparison of 42 years of averaged total streamflow, averaged baseflow, and averaged runoff suggested that baseflow contributed about 59% of total streamflow in winter flows, 45% in spring/summer flows and 44 % in fall flows. Therefore, runoff contributed more to average total flow during spring/summer and fall seasons. Overall, whereas runoff contribution to the total flow in the upper portion of the watershed is more, baseflow contribution to total flow is more in the lower portion of the watershed.

Table II-10: Comparison of total stream flow, base flow, and runoff obtained from similar rainfall events in 1950s and 1990s, at USGS gauging station 08188500 and NCDC weather station 413618.

	Rainfall (mm)	Total Flow (Million m ³)	Base Flow (Million m ³)	Runoff (Million m ³)	% Baseflow	% Runoff	Seasonal Required Total Flow (Million m ³)	
Dec-Mar								
High								
	1958	478	409	206	203	50.37	49.63	187
	1991	468	502	217	285	43.23	56.77	187
Medium								
	1952	200	57	46	11	80.70	19.30	187
	1995	223	136	118	18	86.76	13.24	187
Low								
	1950	58	62	54	8	87.10	12.90	187
	1996	47	80	75	5	93.75	6.25	187
Apr-Jul								
High								
	1957	461	581	276	305	47.50	52.50	250
	1992	464	1315	920	395	69.96	30.04	250
Medium								
	1952	408	85	49	36	57.65	42.35	250
	2000	395	141	100	41	70.92	29.08	250
Low								
	1956	168	26	14	12	53.85	46.15	250
	2001	171	184	139	45	75.54	24.46	250
Aug-Nov								
High								
	1957	474	291	125	166	42.96	57.04	217
	1997	464	113	92	21	81.42	18.58	217
Medium								
	1955	262	41	25	16	60.98	39.02	217
	2000	259	280	145	135	51.79	48.21	217
Low								
	1954	135	27	20	7	74.07	25.93	217
	1990	125	112	91	21	81.25	18.75	217

Table II-11: Comparison of total stream flow, base flow, and runoff obtained from similar rainfall events in 1950s and 1990s, at USGS gauging station 08178800 and NCDC weather station 417945.

	Rainfall (mm)	Total Flow (Million m ³)	Base Flow (Million m ³)	Runoff (Million m ³)	% Baseflow	% Runoff
Dec- Mar						
High						
1963	251	5	3	2	60	40
1998	249	15	7	8	47	53
Medi um						
1967	107	4	3	1	75	25
1999	102	6	3	3	50	50
Low						
1961	81	8	6	2	75	25
1995	77	4	3	1	75	25
Apr- Jul						
High						
1961	391	10	5	5	50	50
1991	373	19	8	11	42	58
Medi um						
1968	226	10	6	4	60	40
1999	225	8	3	5	37	63
Low						
1963	102	3	2	1	67	33
1996	65	2	1	1	50	50
Aug- Nov						
High						
1967	501	10	4	6	40	60
1994	489	17	5	12	30	70
Medi um						
1968	233	7	5	2	71	29
1996	245	5	2	3	40	60
Low						
1963	143	4	2	2	50	50
1991	142	3	2	1	67	33

2.6 Conclusions

Results from this study suggested, more number of increasing trends in hydrologic variables were observed in winter season. The number of hydrologic variables having global significant trend, increased from the headwaters to outlet of the watershed. Generally, gauging stations in upper half of the watershed showed a decreasing trend; whereas, stations in the lower half of the watershed showed an increasing trend. Presence of decreasing trend in baseflow at some upstream stations (upstream of 08181800) could be attributed to increase in impervious surface in the surrounding area. Increase in impervious surface could result in less infiltration, thereby decreasing amount of baseflow reaching the gauging station. One station USGS 08178565, which is also upstream of 08181800, observed increase in flow that could possibly be attributed to WWTP discharges. Separate analysis of the most downstream gauging station data suggested baseflow to be the largest part of stream flow in the river basin. One of the important things to note here was total flow increased substantially in 1990s than in 1950s and 1960s.

Where trend analysis of hydrologic variables observed a spatial pattern, trend analysis of rainfall observed no particular spatial pattern. No negative trends were observed in rainfall. Trends were only observed in winter rainfall. It is important to note that more number of increasing trends in stream flow variables was observed in winter season, as well.

Conclusion from this study is relevant for assessment of land use land cover change (urbanization in particular) impact on freshwater inflows to estuary, especially in semi-arid watershed that drains to the gulf coast of USA. This study will help water resources managers for obtaining appropriate water management strategies to maintain proper aquatic ecosystem health, along with meeting water demand of increasing population. Proper understanding of total seasonal flow, minimum seasonal total flow, total seasonal baseflow, and minimum seasonal baseflow will help understanding the delivery mechanism of sediment, nutrients and metal to downstream aquatic ecosystems, especially in urban dominated ecosystems. Adequate knowledge of such processes will help managers and policy makers to take appropriate land management strategies to meet estuarine ecosystem water demand across various seasons.

CHAPTER III

CHARACTERIZATION OF ENVIRONMENTAL FLOWS IN A RAPIDLY URBANIZING SEMI-ARID WATERSHED USING WAVELET ANALYSIS

3.1 Overview

Environmental flows to rivers and estuaries are important because several ecological processes depend on it. It is therefore important to maintain the productivity of such systems. The productivity of these systems depends on the quantity and quality of freshwater inflow. Characterization of such flows is needed to do basin scale river management. Continuous wavelet techniques are one of the ways to visualize scale and time in frequency domain of the observed signals. This technique can help in understanding the geophysical signals and help in linking to estuarine ecological processes. Stream flow data were obtained from three USGS gauging stations located in the San Antonio River Basin. Obtained daily average flow data were aggregated to seasonal data. Three seasons were considered for analysis; Dec-Mar (Winter), Apr-Jul (Spring-Summer), and Aug-Nov (Fall). Wavelet analysis suggested presence of multi-scale temporal variability in the data series. It also suggested presence of dominant frequencies in 10-15 years scale in the hydrologic variables such as total seasonal flow, and total seasonal baseflow, at all gauging stations, with the cycle occurring in every 10-15 years, as well. Dominant frequencies were also observed in 17-23 years period in most

of the hydrologic variables such as minimum seasonal total flow and minimum seasonal baseflow, and were bi-decadal (20-30 years cycle) in cycle. Higher frequencies, in couple of hydroclimatic variables did show a shift in scale; location of frequencies changed when 1940s flow data was compared with 1990s flow data. Especially, this was prominent in some seasonal base flows. Understanding of environmental flows in wavelet domain can help us understanding various estuarine ecological processes occurring in similar scale; further, helping us providing a better management of River Basin.

3.2 Introduction

Environmental flows in aquatic ecosystems are vital to all life (Tharme, 2003). In ecosystems such as estuaries, environmental flows serve not only ecological purposes such as proper salinity gradient, but economic purposes as well (e.g. maintaining fish habitats) (Kennish, 2001). Evaluating environmental flow needs focuses on balancing ecosystem flow requirements with human use. Water managers worldwide are struggling with the issue of providing adequate environmental flows in times of high demand and low supply. The State of Texas, with a variety of water sources (e.g., lakes, rivers, aquifers) and ecosystems (e.g., coastal, rangeland) a growing urban population placing substantial pressure on water supplies, and periodic water shortages, is no exception (Longley, 1994). In the year 2001, Texas Senate Bill 2 instructed three state agencies, the Texas Water Development Board, the Texas Parks and Wildlife Department and the

Texas Commission on Environmental Quality to develop a state program of instream flows to support a “sound ecological environment” on rivers by 2010.

The productivity of estuarine systems depends on the timing, magnitude, and frequency of freshwater inflow along with the flow associated sediments, nutrients, metals, and organic matter from the terrestrial environment. Changes in the long-term freshwater inflows can be caused by climate variability (e.g. change in precipitation pattern), changes in land use and land cover, and water management (e.g. return flows from waste water treatment plants, water diversion, and upstream lakes and reservoirs (Costa et al., 2003).

Analysis of freshwater flows in various river basins around the world has been extensively studied to assess various ecological processes such as climate change, snow melting processes, and global warming (Lins and Slack, 1999; Peterson et al., 2002). These studies have used wavelet techniques to characterize some of these above mentioned processes. Also, wavelet technique has been used to understand the effect of dam removal on ecological processes (White et al., 2005). However, fewer studies have been conducted to assess environmental flows in rivers and freshwater inflows to estuary using wavelet techniques in rapidly growing semi-arid urban river basin (Copeland et al., 1996; Nakken, 1999; Smith et al., 1998).

Historically, characterization of geophysical time series such as freshwater inflow has been conducted by classical statistical techniques such as by comparing mean, and variance. These methods assign a fixed time interval for the duration of analysis and observe the pattern such as cyclic events, within that time window. However, wavelet analysis (Daubechies, 1992; Farge 1992; Liu, 1994; Kumar and Foufoula-Georgiou, 1997; Torrence and Compo, 1998) provides a different perspective for analyzing time series. This method does not require fixing the time window. It allows the user to observe simultaneously the available frequencies and location of the frequencies in the time series i.e. it simultaneously shows the modulation in scale and amplitude of the signal (e.g. freshwater). Results obtained from wavelet analysis could possibly show the alteration in the time series of important processes due to factors such as urbanization, climate change, and dam construction. Therefore, wavelet analysis provides a unique method to evaluate cyclic changes of the ecological processes in question and allows the user to understand possible linkage with other ecological phenomena.

Wavelets have been used in several hydrologic and climatic studies. Researchers have used this technique to understand inter-annual and inter-decadal variability in hydroclimatic signals (Bradshaw and McIntosh, 1994; Daubechies, 1992; Farge 1992; Liu, 1994;). For example wavelet analysis of southern Quebec stream flow in Canada suggested presence of dominating features in 2-3 years time scale that had possible linkage to local climatic pattern (Anctil and Coulibaly, 2004). Wavelet analysis on hydrologic regime of Amazon during 1903-1998, suggested presence of inter-annual and

inter-decadal oscillations (Labat et al., 2004). Studies have also used wavelets in detecting changes in stream flow variance (Cahill, 2002), stream flow simulations (Bayazit and Aksoy, 2001), and detecting natural and anthropogenic influences on stream flow. Nakken 1999, in a study utilized wavelet techniques to analyze time series data of rainfall-runoff process that occurred during 1911-1996 in Began River basin, Australia. That study suggested, climate forcing dominated catchment response in short time scales, usually about 27-32 months. Wavelet techniques have also been employed to group various regions that are geographically separated but have similar wavelet signatures based on stream flow (Saco and Kumar, 2000). In Texas the high variability at the smaller scales arises from the flash-flood type of flows characteristic of semiarid regions. The rivers in Southern Plains (Nueces, San Antonio, Guadalupe, and Colorado) are characterized by the presence of high variability at the smaller scales (Lins, 1997). This small scale variability (6 days to 1 month time scale) is generated by the intense rainfall events that can occur at any time of the year with some prevalence in spring and summer.

Most of the earlier studies have investigated annual stream flow, and monthly flow (Saco and Kumar, 2000; Lins, 1997). Past studies did not assess scale and frequency of seasonal flows which may be more important for ecological management of the estuary and river management (Labat et al., 2004; Bayazit and Aksoy, 2001). Therefore, the overall objective of this study is to characterize various seasonal freshwater inflows variables (such as seasonal total flow, seasonal baseflow, maximum seasonal total flow, maximum seasonal baseflow, minimum seasonal total flow, minimum seasonal baseflow) at the

most downstream gauging station of San Antonio River, and stream flows at various segments of the River. The technique was used to evaluate if there was any similarities between these geophysical variables at all the stations. Further, this method investigated the changes in frequencies and scales at different stream gauging stations.

3.3 Study Site Description

3.3.1 Physiography

The San Antonio River Basin (Figure III-1) covers 10, 826 km² from the headwaters of the Medina River to the point at which the San Antonio River joins with the Guadalupe River before emptying into the Gulf of Mexico. The San Antonio River runs 390 river kilometers through four counties: Bexar, Wilson, Karnes, and Goliad Counties. However, the watershed drains through some portion of 8 counties: Kerr, Kendall, Comal, Guadalupe, Dewitt, Victoria, Refugio, and Medina Counties. Major tributaries to the San Antonio River are Leon Creek, Salado Creek, Cibolo Creek, and Medina Creek. This study area is located between latitude 29.91° N and 28.51° N and longitude 99.57° W and 97.01° W. Average elevation of the basin area is about 229 meters. Lowest elevation is 2 meters, and highest elevation in the study area is about 710 meters. Average slope of the basin is 1.38 degrees.

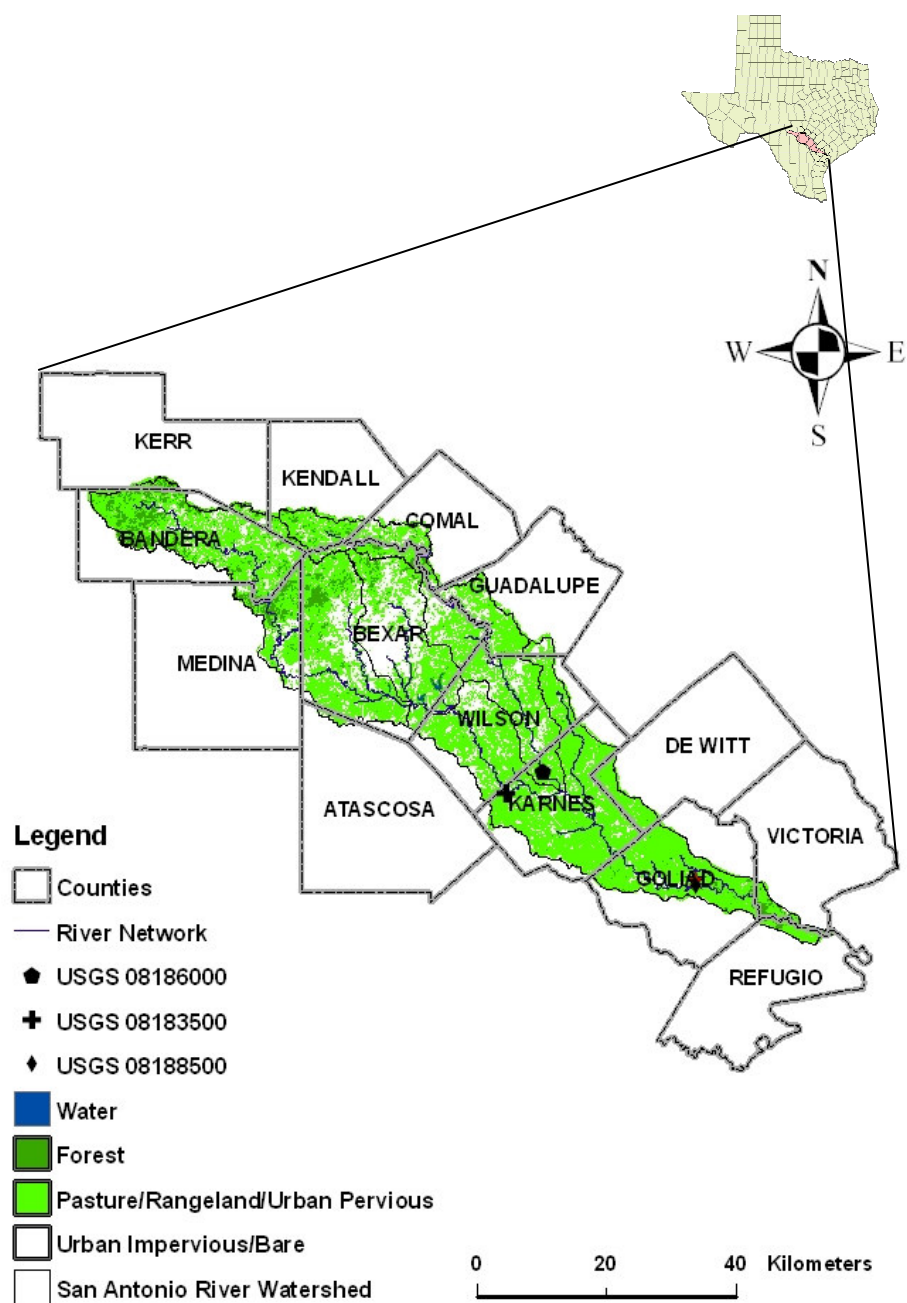


Figure III-1: San Antonio River watershed with gauging stations, weather stations, and various counties in the watershed.

Northwest of the city, the terrain slopes to the Edwards Plateau and to the southeast it slopes downward to the Gulf Coastal Plains. Soils are blackland clay and silty loam on the Plains and thin limestone soils on the Edwards Plateau.

San Antonio-Guadalupe estuary is an important estuary in the Gulf of Mexico region. It provides a critical coastal habitat that is essential ecologically and economically. Important species such as bluecrabs depend on this estuary for their survival. It provides significant economic backbone to the region by providing environment for fisheries, tourism, shipping, and marine biotechnology. It is also a critical habitat for Whooping Crane, which is a migratory bird and an endangered species. This bird migrates from Canada to this estuary during winter. Texas Water Development Board (TWDB) has made recommendations for the flow requirements for the entire Guadalupe Estuary/San Antonio Bay, which receives flows from both the San Antonio and Guadalupe River Watersheds. The minimum flow recommended was 1271 million m^3/year and the maximum flow was 1591 million m^3/year (TPWD, 1998). Past studies (particularly historical flow analysis) on freshwater inflows to Texas bays and estuaries (Longley, 1994) suggested that the largest fraction of freshwater inflows to the Guadalupe Estuary comes from gaged portions of the Guadalupe River Basin. These areas contribute approximately 58% (1653 million m^3/year) of the total freshwater inflows to the estuary; 57 % came from gaged portions of the Guadalupe River alone. Gaged portion of the San Antonio River contributed about 23 % (656 million m^3/year) of total freshwater inflows. No study separated the contributions of the individual watersheds (San Antonio and

Guadalupe River) or modeled the effect of land use change on the environmental flow availability. Past study also did not assess seasonal flows which may be more important than yearly/monthly flows (Longley, 1994).

The City of San Antonio is located in the south-central portion of Texas and in Bexar County. As the 8th largest city in the U.S., San Antonio is currently experiencing rapid urbanization and population growth on average of 1.8 % per year (U.S. Census Bureau, 2005). This population growth is increasingly impacting rural areas by accelerating land subdivision and reducing the average size of land parcels (Conner and James, 1996). It is predicted population around the city of San Antonio by 2020 will be approximately 2,172,950 (counties include Bexar, Comal, Guadalupe, Wilson, Atascosa, Bandera, Kendall, and Medina) (Texas State Data Center, 2005; Nivin and Perez, 2006).

3.3.2 Land Use Change

This watershed is experiencing rapid human growth. There has been a decline in rangeland and forest in this watershed. Analysis of LANDSAT imageries of the entire watershed for the years 1987, 1999 and 2003 suggested an increase in impervious surface from 6% in 1987 to 14% in 2003. Bexar County experienced maximum increase in impervious surface. In watershed scale, forest area decreased from 3545 square kms in 1987 to 2525 square kms in 2003.

3.4 Data

3.4.1 Hydrological Data and Rainfall Data

Daily average stream flow data was obtained for USGS 08183500 and USGS 08186000 (Figure III-1) present at the midway of the river from USGS website, for environmental flow analysis in river. Also, daily stream flow data was obtained for USGS 08188500 (Figure III-1), the most downstream gauging station in the San Antonio River, from USGS website, for freshwater inflow analysis to the estuary. The present study characterized the San Antonio River flow regime (seasonal flows in particular) using 64 years (1940 – 2003) from all the three stations. A digital filter technique (Nathan and McMahon, 1990; Lyne and Hollick, 1979; Arnold and Allen, 1999; Mau and Winter, 1997) was used in this study to separate baseflow from total stream flow. This technique is objective and reproducible (Arnold and Allen, 1999). The equation of this filter is given in equation 1 and 2.

The present study characterized the San Antonio River flow regime (seasonal flows in particular) using 64 years (1940 – 2003) of data. Data from daily average flow, and daily base flow were aggregated into three distinct seasonal periods (Dec-Mar, Apr-Jul, and Aug-Nov), for each year. Additionally, precipitation data was also analyzed using data obtained from National Climatic Data Center (NCDC) for the site NCDC COOPID

413618, very close to the most downstream gauging station (Figure III-1). This precipitation data was used for assessing the rainfall variation during the study period.

3.5 Methodology

Continuous wavelet transforms (CWT) was conducted on the flow data obtained for various gauging stations spatially located in the watershed. Data from 1940 to 2003 was used for gauging stations USGS 08188500 (the most downstream gauging station in the river), 08186000, and 08183500. These two gauging stations were located midway of the main stem Analysis was conducted on seasonal total flow, seasonal baseflow, seasonal runoff, maximum seasonal total flow, maximum seasonal baseflow, maximum seasonal runoff, minimum seasonal total flow, minimum seasonal baseflow. Analysis was also conducted on rainfall data. Wavelet toolbox in MATLAB was used for the present analysis. Each time series was analyzed using a Morlet wavelet function. The wavelet power spectrum was given by (WPS) (White et al., 2005).

$$\Psi_0(\eta) = \pi^{-1/4} e^{i\omega_0\eta} e^{-\eta^2/2} \quad (8)$$

where ω_0 is the non-dimensional wave number and η is a time parameter (non-dimensional, also could represent other metrics such as distance).

The convolution shown in equation 8 can be accomplished at all N based on a discrete Fourier transform calculated as:

$$W_n(s) = \sum_{k=0}^{N-1} \hat{x}_k \hat{\psi}(s\omega_k) e^{i\omega_k n \delta t} \quad (9)$$

where ω is the angular frequency and $\hat{\psi}(s\omega)$ is the Fourier transform of $\psi(t/s)$ in the continuous limit.

Wavelet analysis of the hydrologic stream flow data helped in understanding the cyclic changes and patterns present in the time series. It will help in linking these cyclic changes to the river basin water management to obtain the required estuarine ecological health.

3.6 Results and Discussions

3.6.1 Total Seasonal Flow

Analysis of total seasonal environmental flows at USGS gauging station number 08186000 suggested, maximum flows observed for Dec-Mar (winter season) was about 244 million cubic meters in 1992; for Apr-Jul (spring/summer season) was about 275 million cubic meters in 2002; and for Aug-Nov (fall season) was about 273 million cubic meters in 1998. Similarly, minimum flow was observed for Dec-Mar was 4 million cubic meters in 1954; for Apr-Jul was about 1 million cubic meters in 1971; and for Aug-Nov was about 3 million cubic meters in 1954.

Similarly, total seasonal environmental flow at USGS gauging station number 08183500 suggested, maximum flows observed for Dec-Mar was about 796 million cubic meters in 1992; for Apr-Jul was about 997 million cubic meters in 1987; and for Aug-Nov was about 627 million cubic meters in 1973. Likewise, minimum flows observed for Dec-Mar was about 27 million cubic meters in 1954; for Apr-Jul was about 19 million cubic meters in 1956; and for Aug-Nov was about 20 million cubic meters in 1954.

Total seasonal freshwater inflow at USGS gauging station number 08188500, the most downstream stream gauging station, suggested, maximum flow observed for Dec-Mar was about 1148 million cubic meters in 1992 (Figure III-2); for Apr-Jul was about 1425 million cubic meters in 1987; for Aug-Nov was about 1053 million cubic meters in 1967. Likewise, minimum flow observed for Dec-Mar was about 34 million cubic meters in 1954; for Apr-Jul was about 26 million cubic meters in 1956; and for Aug-Nov was about 27 million cubic meters in 1954.

Morlet continuous wavelet transformations were performed over the signals obtained for total seasonal flow. Multi scale temporal variability was observed in the signals. In general, analysis of total seasonal flow at all the three gauging stations showed presence of dominating features in flows for Apr-Jul at USGS 08186000; Dec-Mar, Apr-Jul, and Aug-Nov at USGS 08183500; Dec-Mar, and Apr-Jul at USGS 08188500, the most downstream station. Higher frequencies were observed in 10-15 years period (Figures III-3, 4, and 5) repeated every 10-15 years, suggesting presence of some cyclic phenomena.

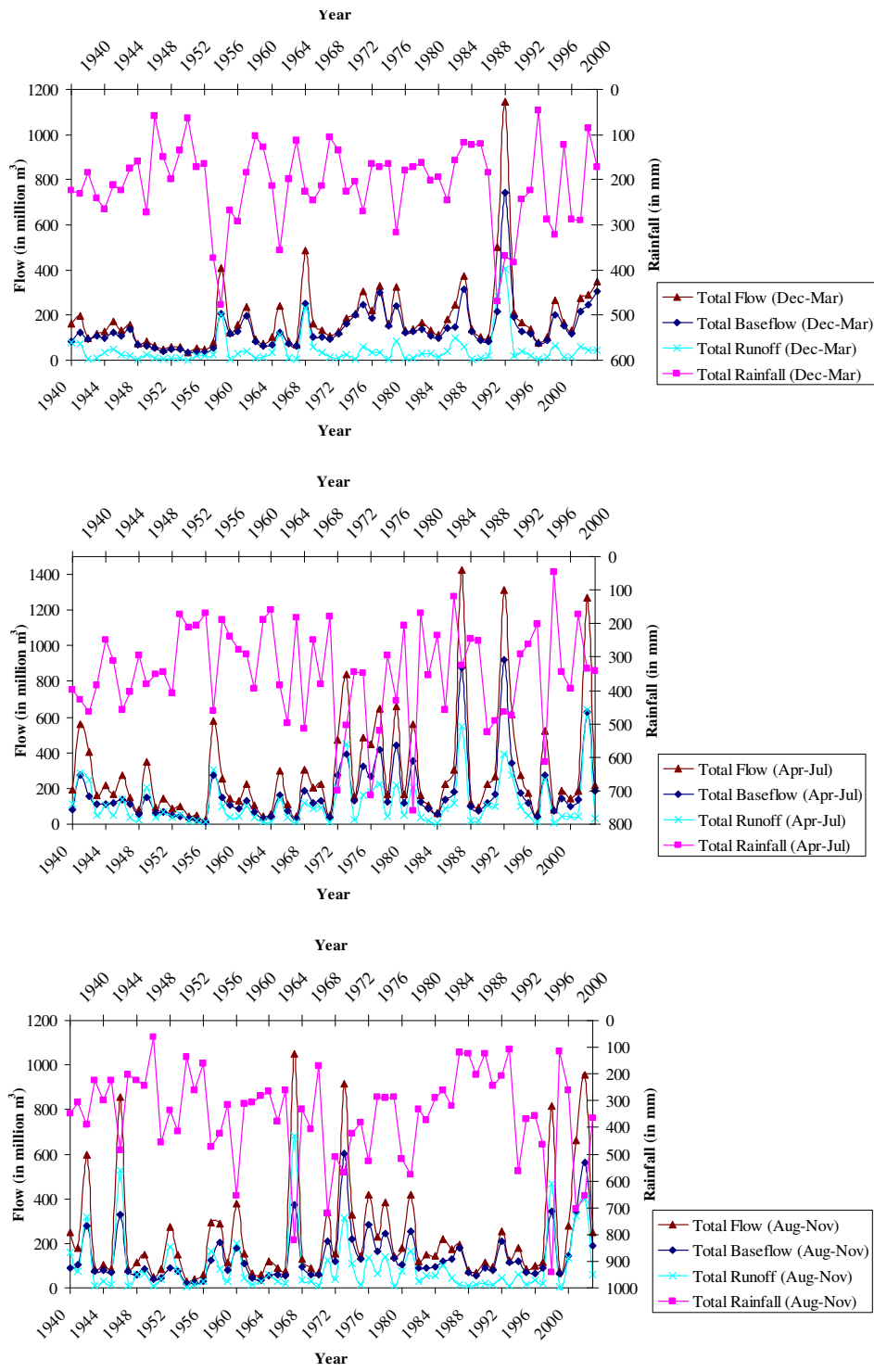


Figure III-2: Total seasonal environmental flow, total baseflow, total runoff, and total rainfall magnitudes from 1940-2003 as monitored in USGS gauging station 08188500 and NCDC 413618 station.

Dominating features were also observed in 17-23 years period in all of the seasonal flows, at all the gauging stations. These signals were repeated in 20-30 years cycle. We observed similar higher frequencies in the time series around 16 years, as observed by Labat et al., 2004.

3.6.2 Total Seasonal Baseflow

Analysis of total seasonal baseflows at USGS gauging station number 08186000 suggested, maximum flows observed for Dec-Mar was about 112 million cubic meters in 1992; for Apr-Jul was about 106 million cubic meters in 2002; and for Aug-Nov was about 83 million cubic meters in 1973. Similarly, minimum flow was observed for Dec-Mar was 3 million cubic meters in 1954; for Apr-Jul was about 1 million cubic meters in 1971; and for Aug-Nov was about 2 million cubic meters in 1954.

Total seasonal baseflow data at USGS gauging station number 08183500 suggested, maximum flows observed for Dec-Mar was about 538 million cubic meters in 1992; for Apr-Jul was about 647 million cubic meters in 1992; and for Aug-Nov was about 420 million cubic meters in 1973. Likewise, minimum seasonal baseflows observed for Dec-Mar was about 22 million cubic meters in 1954; for Apr-Jul was about 11 million cubic meters in 1956; and for Aug-Nov was about 15 million cubic meters in 1954.

Similarly, analysis of total seasonal freshwater inflow at USGS gauging station number 08188500, the most downstream stream gauging station, suggested, maximum seasonal baseflow flow observed for Dec-Mar was about 743 million cubic meters in 1992 (Figure III-2); for Apr-Jul was about 920 million cubic meters in 1992; for Aug-Nov was about 604 million cubic meters in 1973. Likewise, minimum seasonal baseflow observed for Dec-Mar was about 32 million cubic meters in 1954; for Apr-Jul was about 14 million cubic meters in 1956; and for Aug-Nov was about 20 million cubic meters in 1954.

Morlet wavelet analysis on the signals indicated presence of multi scale temporal variability in the data series. In general, analysis of total seasonal base flow at all the three gauging stations suggested presence of dominating features in flows for Apr-Jul at USGS 0818600; Dec-Mar, Apr-Jul, and Aug-Nov at USGS 08183500; Dec-Mar, Apr-Jul, and Aug-Nov at USGS 08188500, the most downstream station. Higher frequencies were observed in 10-15 years period (Figures III-6, 7, and 8) repeated every 10-15 years, suggesting presence of some cyclic phenomena. Dominating features were also observed in 17-23 years period in all of the seasonal flows, at all the gauging stations.

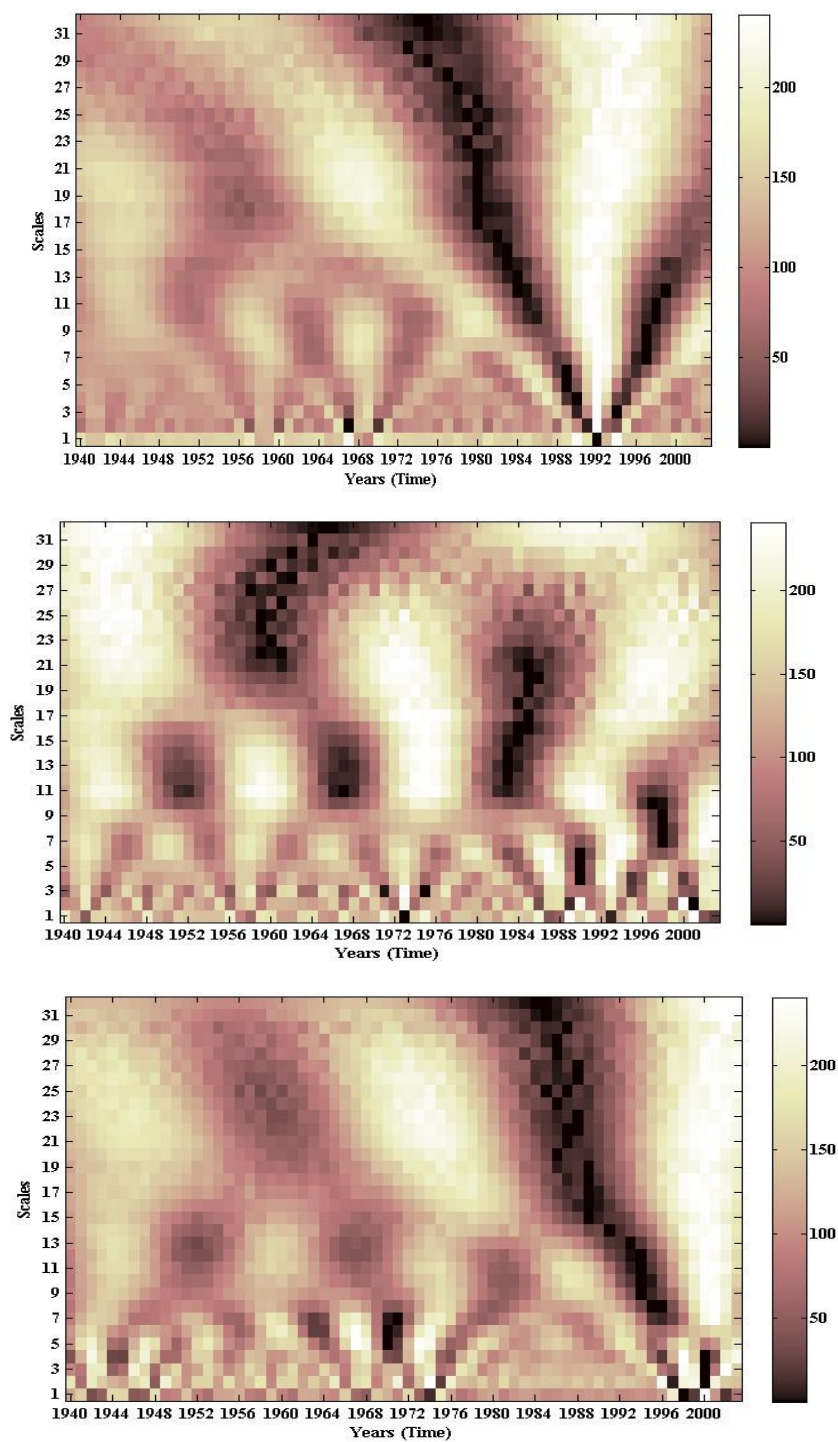


Figure III-3: Scale and period of total seasonal flow for (from top to bottom) Dec-Mar, Apr-Jul, and Aug-Nov obtained from USGS 08186000 gauging data.

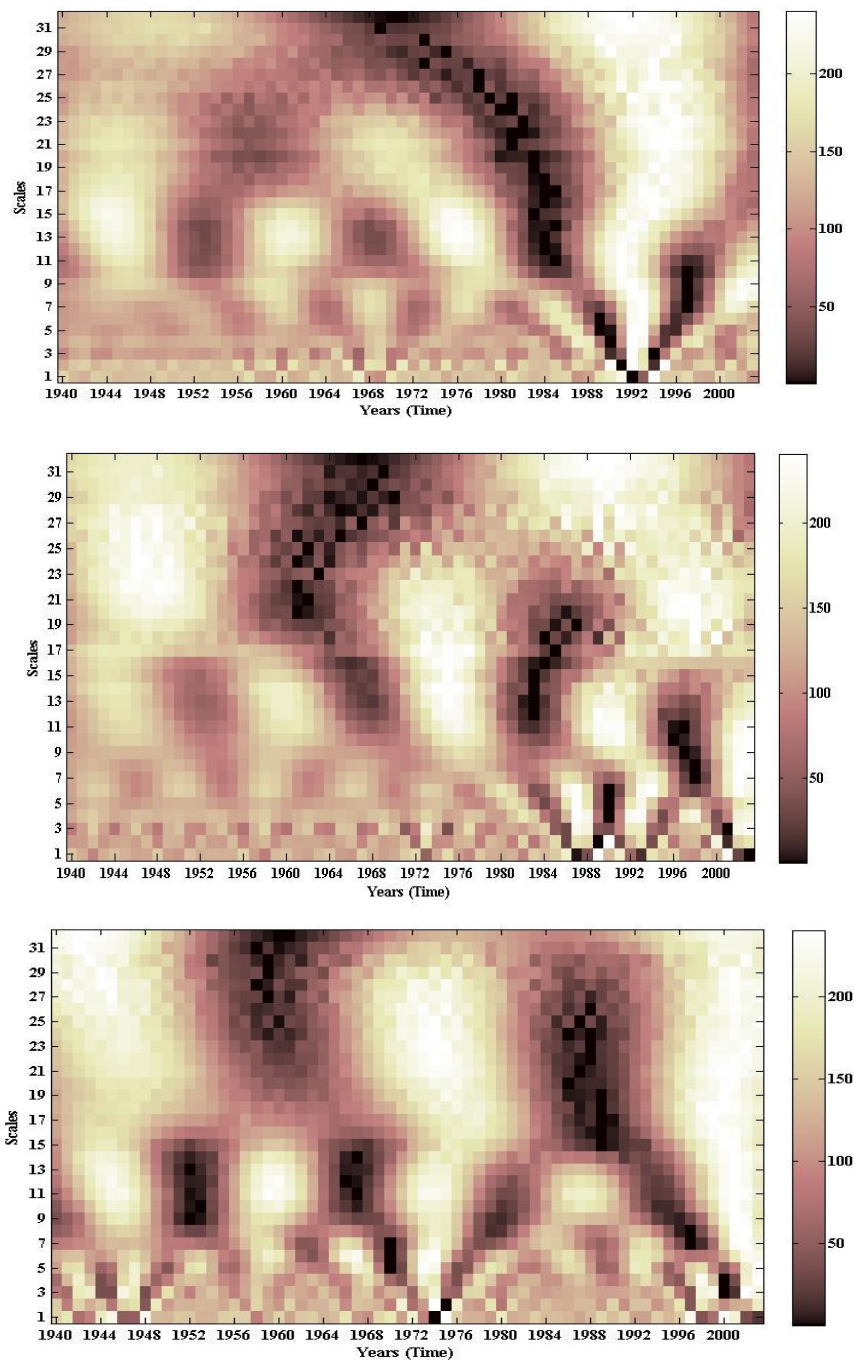


Figure III-4: Scale and period of total seasonal flow for (from top to bottom) Dec-Mar, Apr-Jul, and Aug-Nov obtained from USGS 08183500 gauging data.

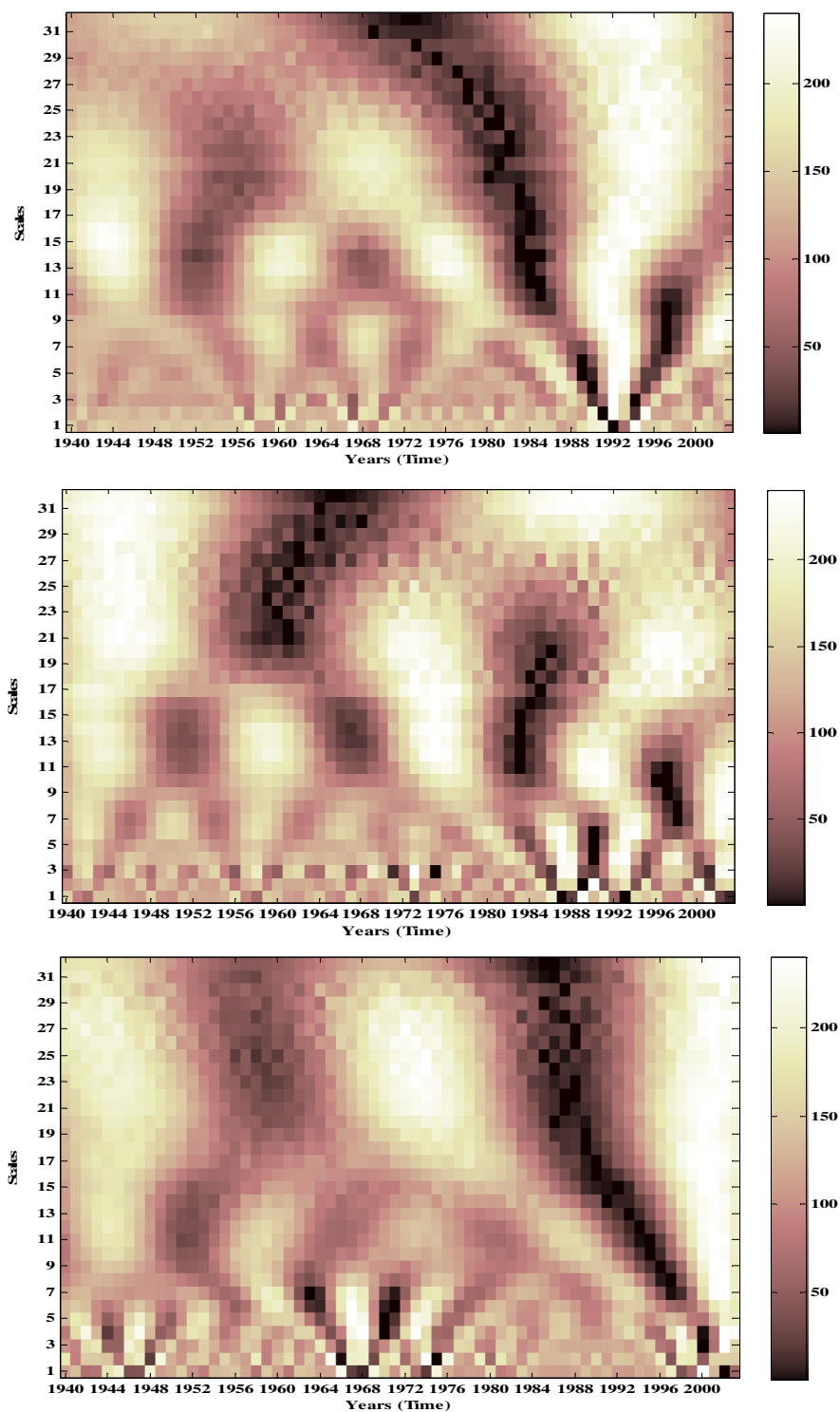


Figure III-5: Scale and period of total seasonal flow for (from top to bottom) Dec-Mar, Apr-Jul, and Aug-Nov obtained from USGS 08188500 gauging data.

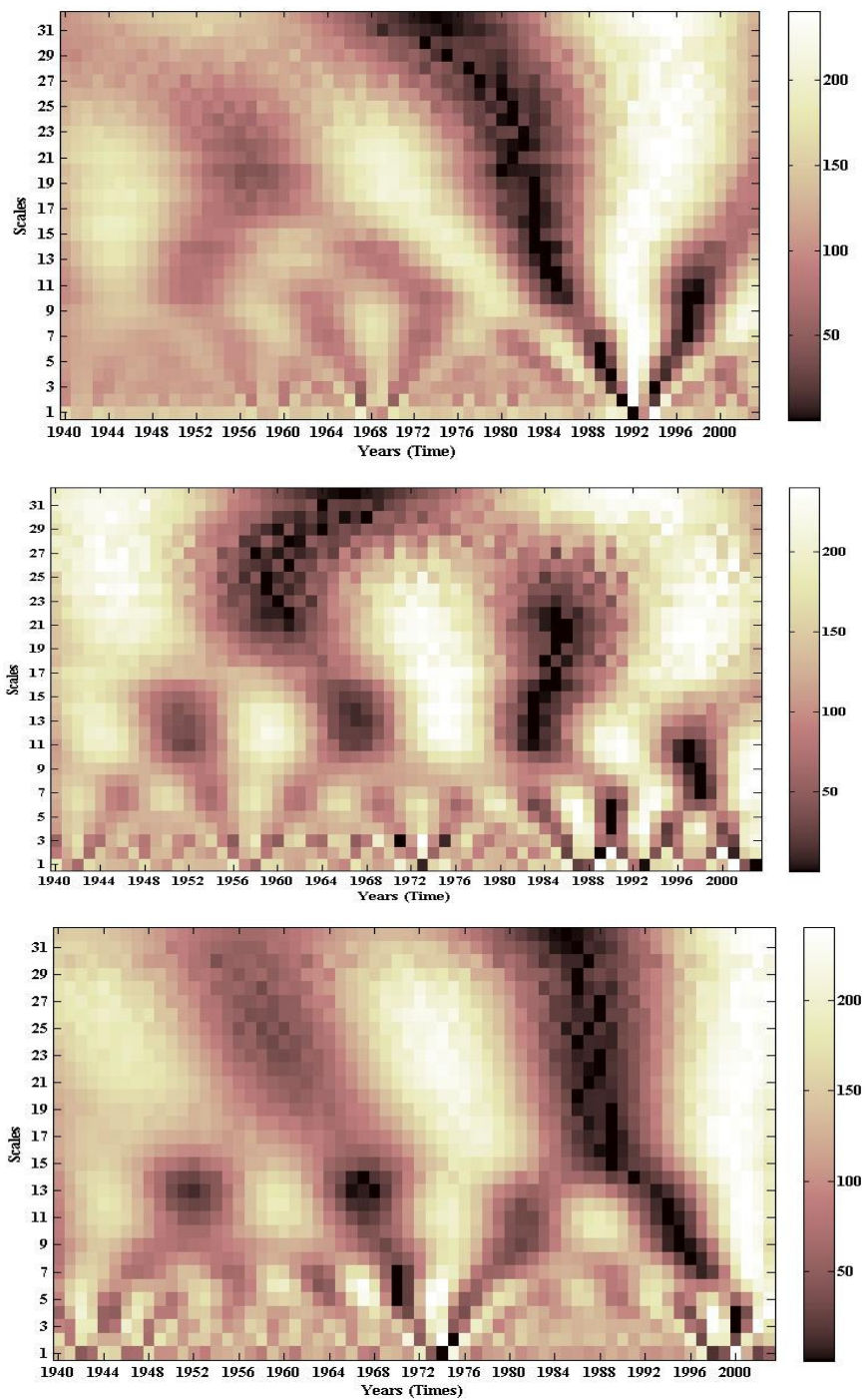


Figure III-6: Scale and period of total seasonal base flow for (from top to bottom) Dec-Mar, Apr-Jul, and Aug-Nov obtained from USGS 08186000 gauging data.

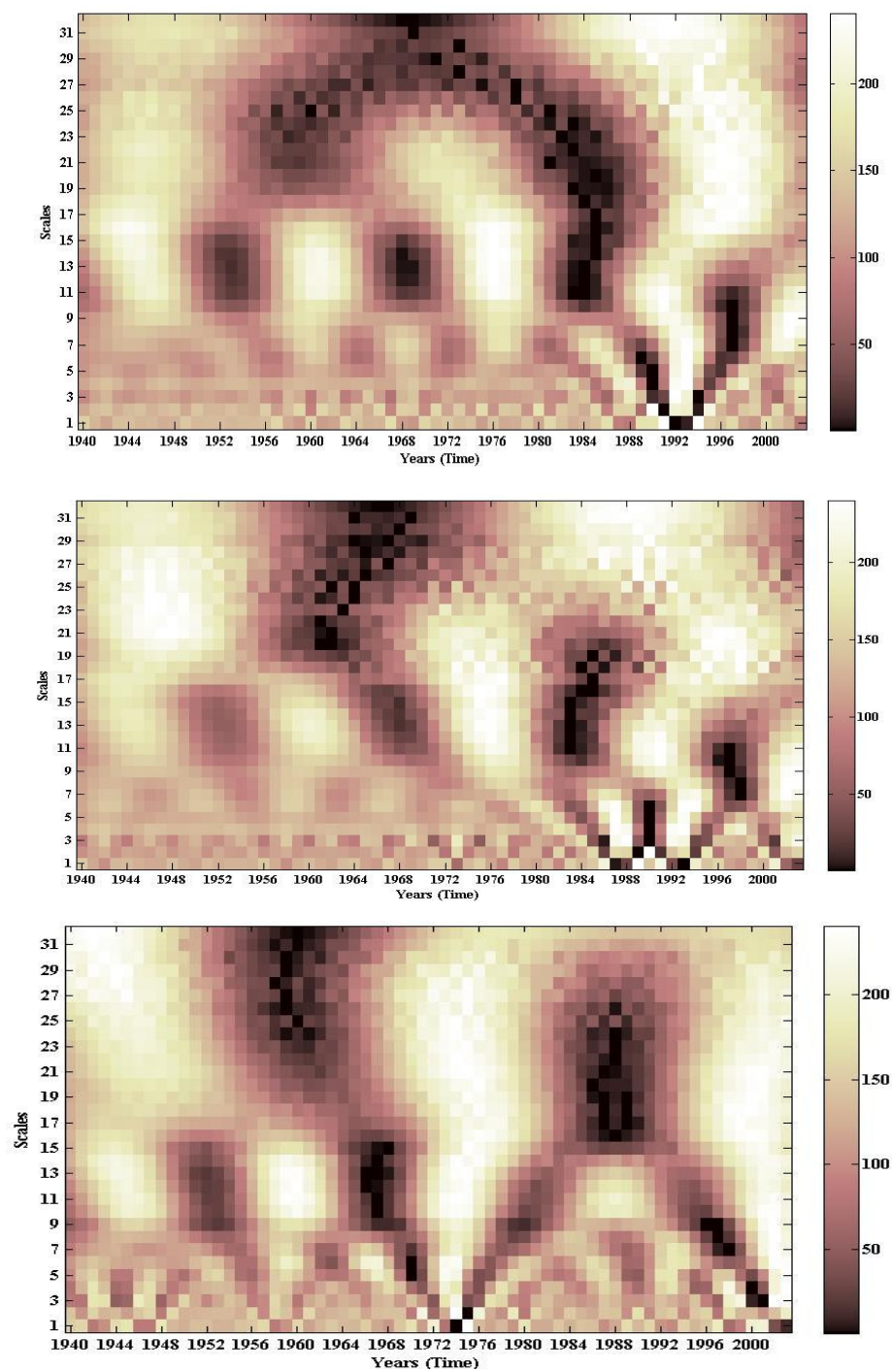


Figure III-7: Scale and period of total seasonal base flow for (from top to bottom) Dec-Mar, Apr-Jul, and Aug-Nov obtained from USGS 08183500 gauging data.

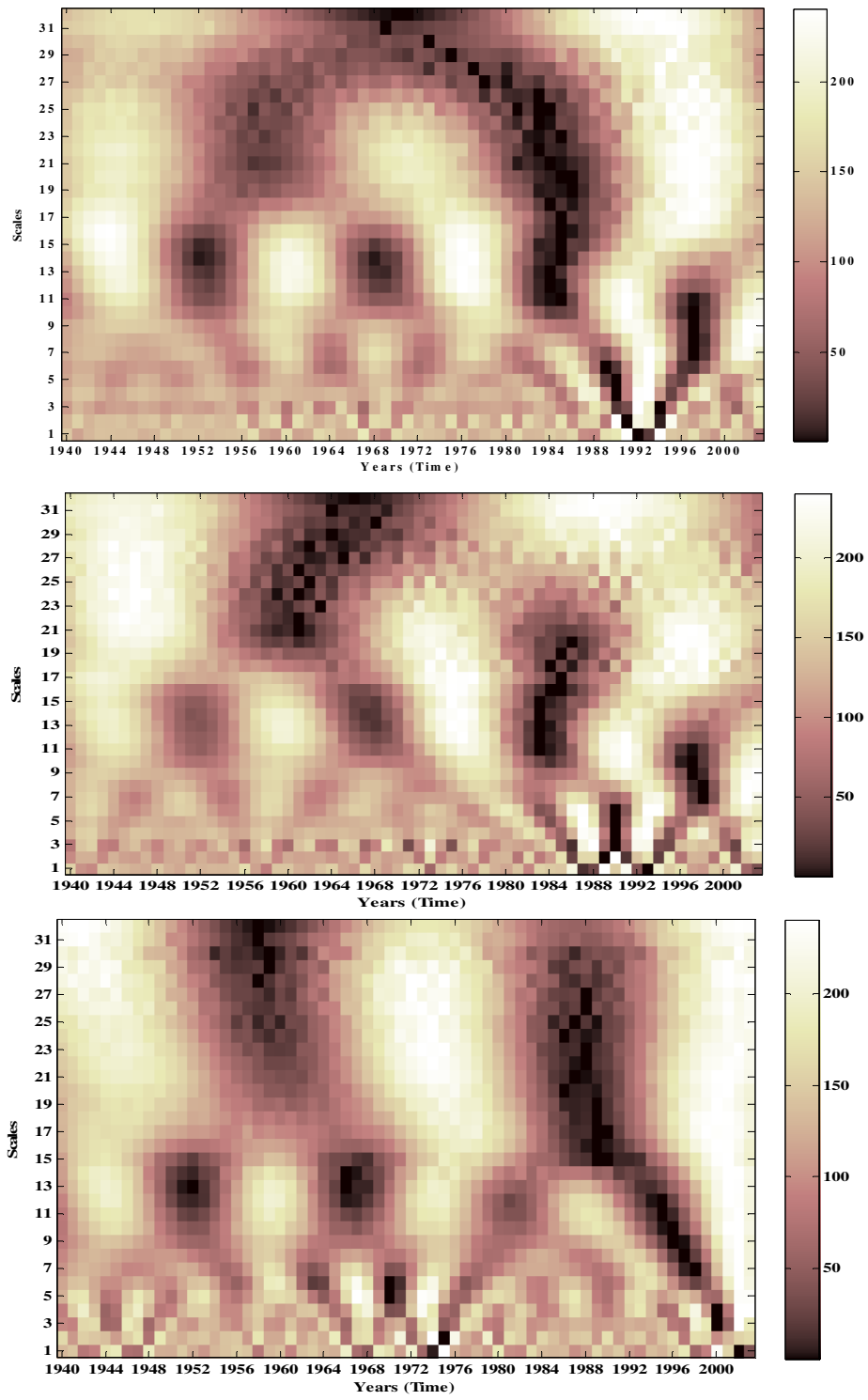


Figure III-8: Scale and period of total seasonal base flow for (from top to bottom) Dec-Mar, Apr-Jul, and Aug-Nov obtained from USGS 08188500 gauging data.

These signals were repeated in 20-30 years cycle. We observed similar higher frequencies in the time series around 16 years, as observed by Labat et al., 2004.

3.6.3 Minimum Seasonal Total Flow

Analysis of minimum seasonal total flows at USGS gauging station number 08186000 indicated, maximum flows observed for Dec-Mar was about 0.17 million cubic meters in 2003; for Apr-Jul was about 0.19 million cubic meters in 2003; and for Aug-Nov was about 0.17 million cubic meters in 2003 as well.

Minimum seasonal total flow data at USGS gauging station number 08183500 suggested, maximum flows observed for Dec-Mar was about 1.69 million cubic meters in 1992; for Apr-Jul was about 2.24 million cubic meters in 1992; and for Aug-Nov was about 1.40 million cubic meters in 1973.

Similarly investigation of minimum seasonal total inflow at USGS gauging station number 08188500, the most downstream stream gauging station, suggested, maximum of minimum seasonal total flow observed for Dec-Mar was about 2.0 million cubic meters in 1992; for Apr-Jul was about 2.54 million cubic meters in 1992; for Aug-Nov was about 1.78 million cubic meters in 1973. Likewise, minimum of minimum seasonal total flows observed for Dec-Mar was about 0.12 million cubic meters in 1956; for Apr-Jul was

about 0.005 million cubic meters in 1956; and for Aug-Nov was about 20 million cubic meters in 1956.

Wavelet analysis on the signals indicated presence of multi scale temporal variability in the data series. In general, analysis of minimum seasonal total flows at all the three gauging stations suggested presence of dominating features in flows for Dec-Mar, Apr-Jul and Aug-Nov at USGS 0818600; Dec-Mar, Apr-Jul, and Aug-Nov at USGS 08183500; Dec-Mar, Apr-Jul, and Aug-Nov at USGS 08188500, the most downstream station. Higher frequencies were observed in 10-15 years period (Figures III-9, 10, and 11) repeated every 10-15 years, suggesting presence of some cyclic phenomena. Dominating features were also observed in 17-23 years period in all of the seasonal flows, at all the gauging stations. These signals were repeated in 20-30 years cycle. There is some shifting of higher frequencies at lower scales after 1980 for several variables (Figures III-9, 10, and 11).

3.6.4 Minimum Seasonal Baseflow

Analysis of minimum seasonal baseflow revealed similar information as of minimum seasonal total flow. Baseflow is a part of total flow.

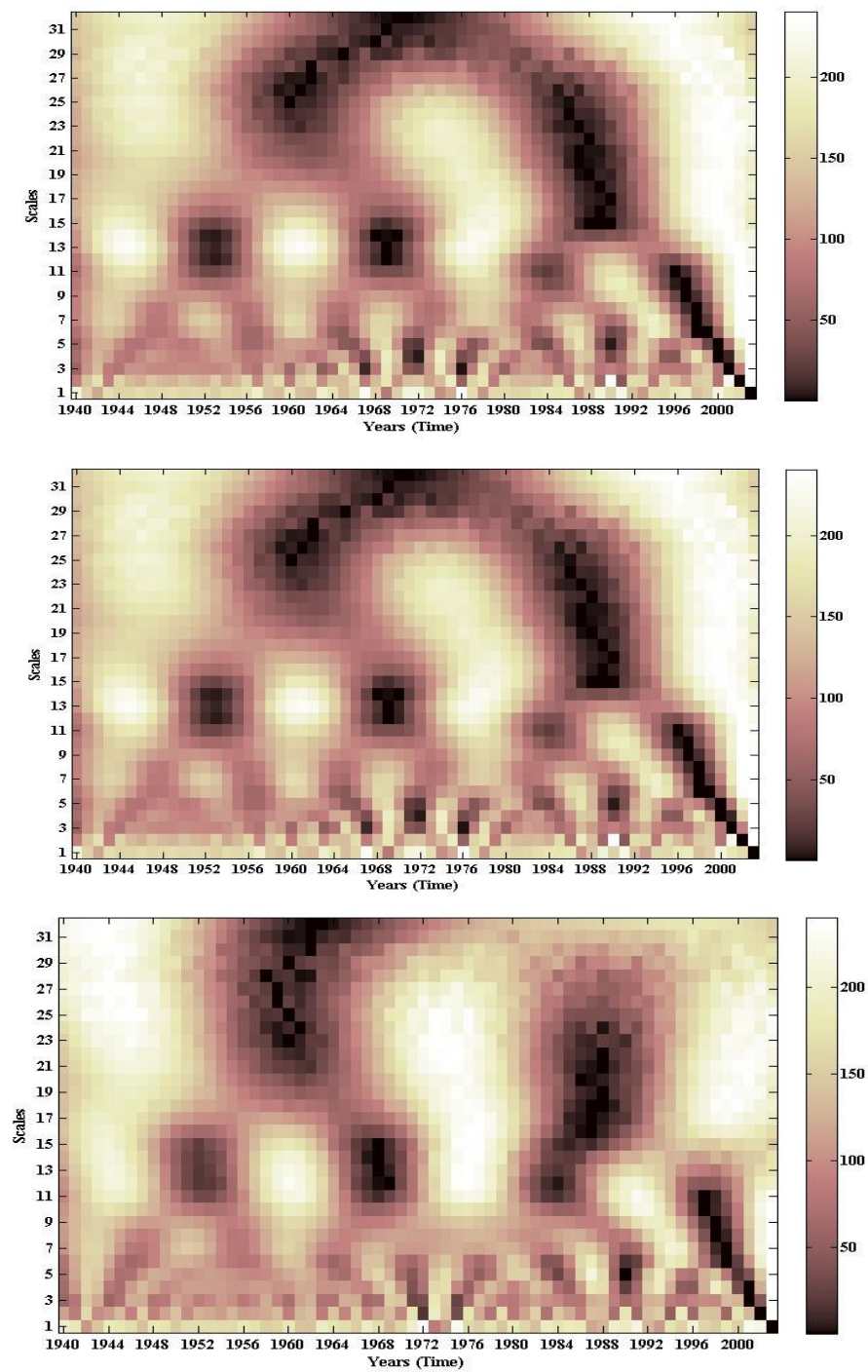


Figure III-9: Scale and period of minimum seasonal total flow for (from top to bottom) Dec-Mar, Apr-Jul, and Aug-Nov obtained from USGS 08186000 gauging data.

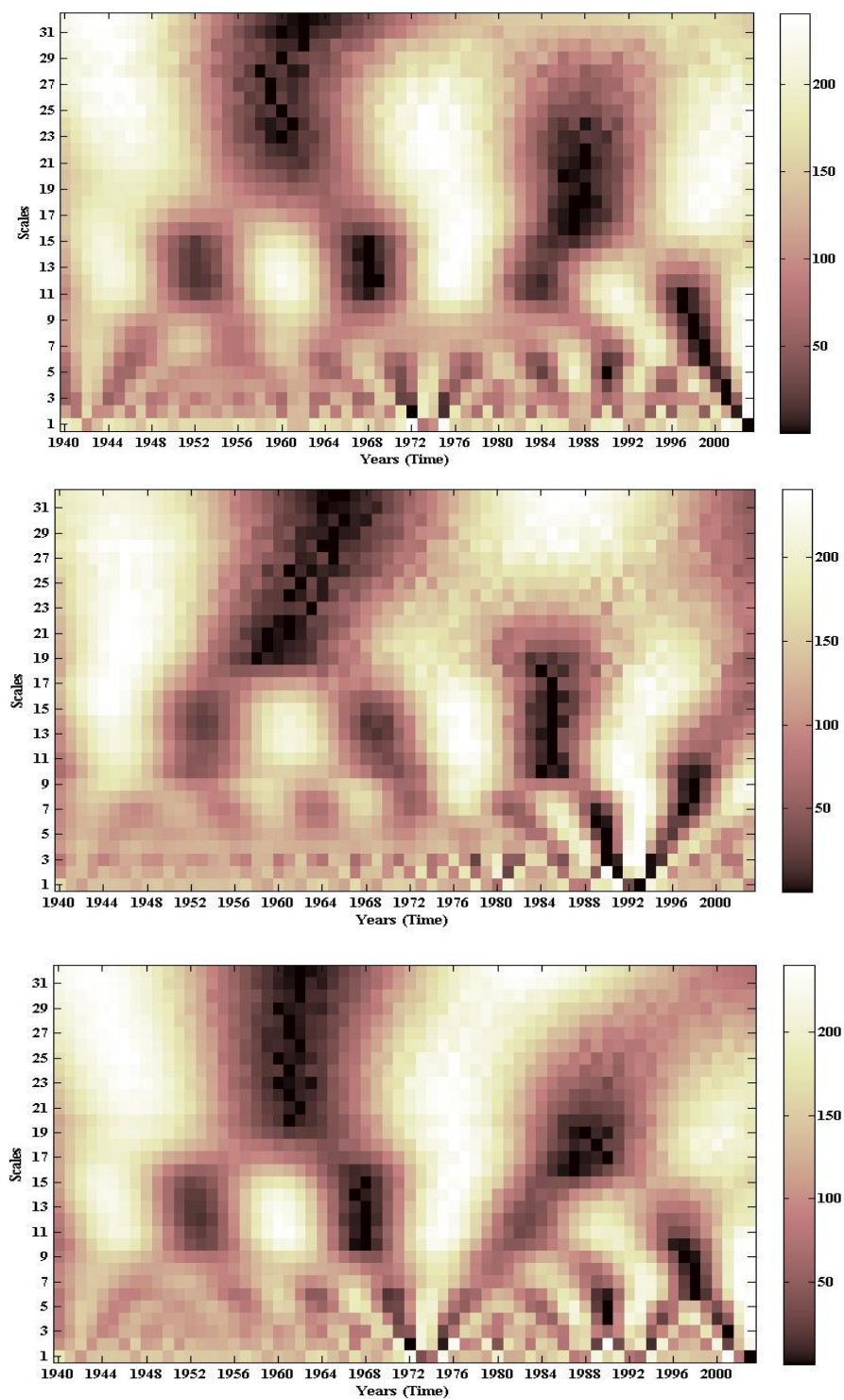


Figure III-10: Scale and period of minimum seasonal total flow for (from top to bottom) Dec-Mar, Apr-Jul, and Aug-Nov obtained from USGS 08183500 gauging data.

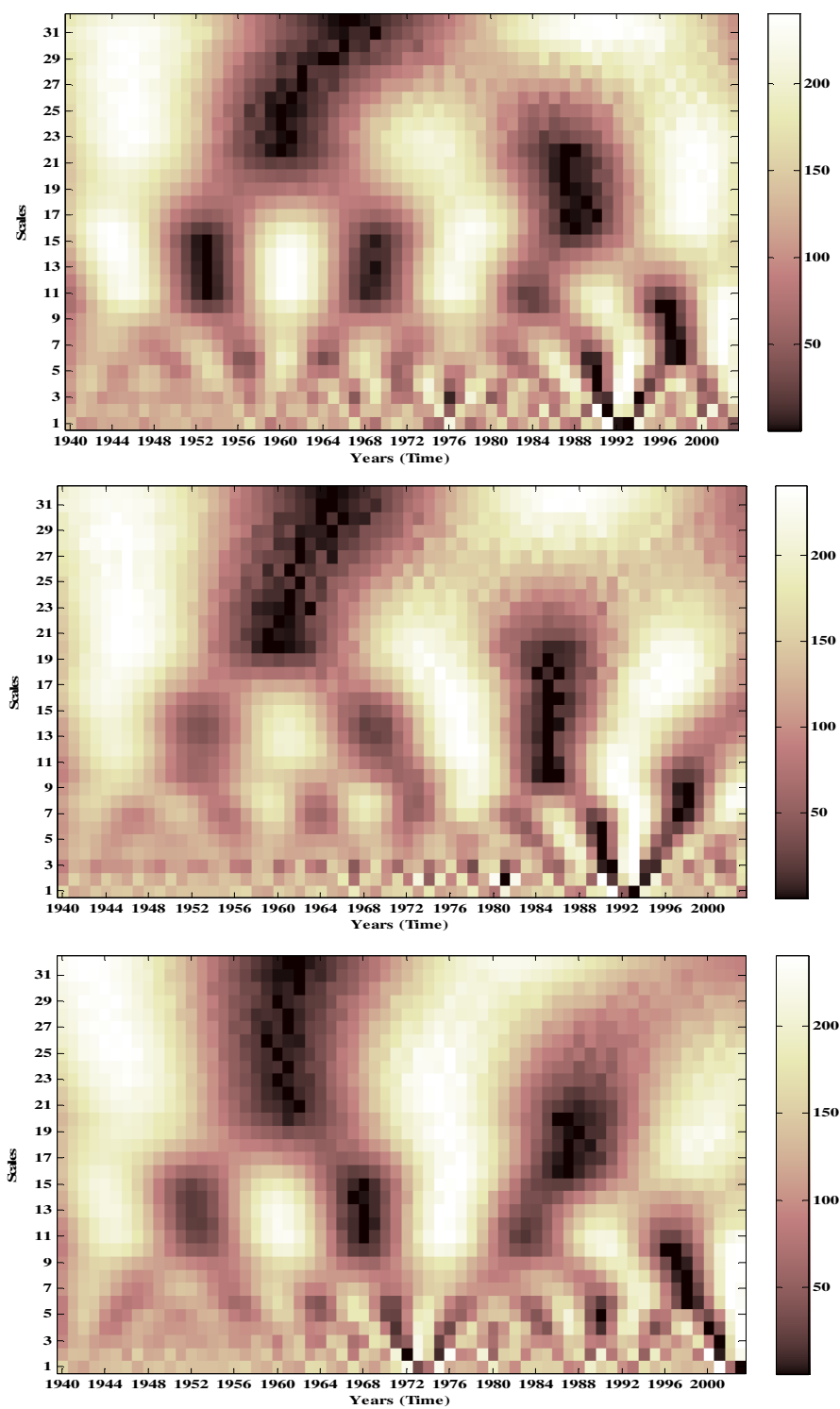


Figure III-11: Scale and period of minimum seasonal total flow for (from top to bottom) Dec-Mar, Apr-Jul, and Aug-Nov obtained from USGS 08188500 gauging data.

3.6.5 Maximum Seasonal Total Flow

Analysis of maximum seasonal total flows at USGS gauging station number 08186000 indicated, maximum flows observed for Dec-Mar was about 48 million cubic meters in 1991; for Apr-Jul was about 50 million cubic meters in 1942; and for Aug-Nov was about 108 million cubic meters in 1998 as well.

Maximum seasonal total flow data at USGS gauging station number 08183500 suggested, maximum flows observed for Dec-Mar was about 44 million cubic meters in 1991; for Apr-Jul was about 130 million cubic meters in 2002; and for Aug-Nov was about 114 million cubic meters in 1998.

Further analysis of maximum seasonal total inflow at USGS gauging station number 08188500, the most downstream stream gauging station, suggested, maximum of maximum seasonal total flow observed for Dec-Mar was about 62 million cubic meters in 1991; for Apr-Jul was about 149 million cubic meters in 2002; for Aug-Nov was about 292 million cubic meters in 1967. Likewise, minimum of maximum seasonal total flows observed for Dec-Mar was about 0.41 million cubic meters in 1954; for Apr-Jul was about 1.63 million cubic meters in 1963; and for Aug-Nov was about 1.44 million cubic meters in 1999.

Wavelet analysis on the signals suggested presence of multi scale temporal variability in the data series. In general, analysis of maximum seasonal total flows at all the three gauging stations suggested presence of dominating features in flows for Apr-Jul at USGS 0818600; Apr-Jul at USGS 08183500. In the above variables, higher frequencies were observed in 10-15 years period (Figures III-12, 13, and 14) repeated every 10-15 years, suggesting presence of some cyclic phenomena. Dominating features were also observed in 17-23 years period in all of the seasonal flows, at all the gauging stations. These signals were repeated in 20-30 years cycle.

3.6.6 Maximum Seasonal Baseflow

Analysis of maximum seasonal base flows at USGS gauging station number 08186000 suggested, maximum flows observed for Dec-Mar was about 24 million cubic meters in 1958; for Apr-Jul was about 12 million cubic meters in 2002; and for Aug-Nov was about 14 million cubic meters in 1998 as well.

Analysis of maximum seasonal base flows at USGS gauging station number 08183500 suggested, maximum flows observed for Dec-Mar was about 16 million cubic meters in 1986; for Apr-Jul was about 38 million cubic meters in 2002; and for Aug-Nov was about 19 million cubic meters in 1998.

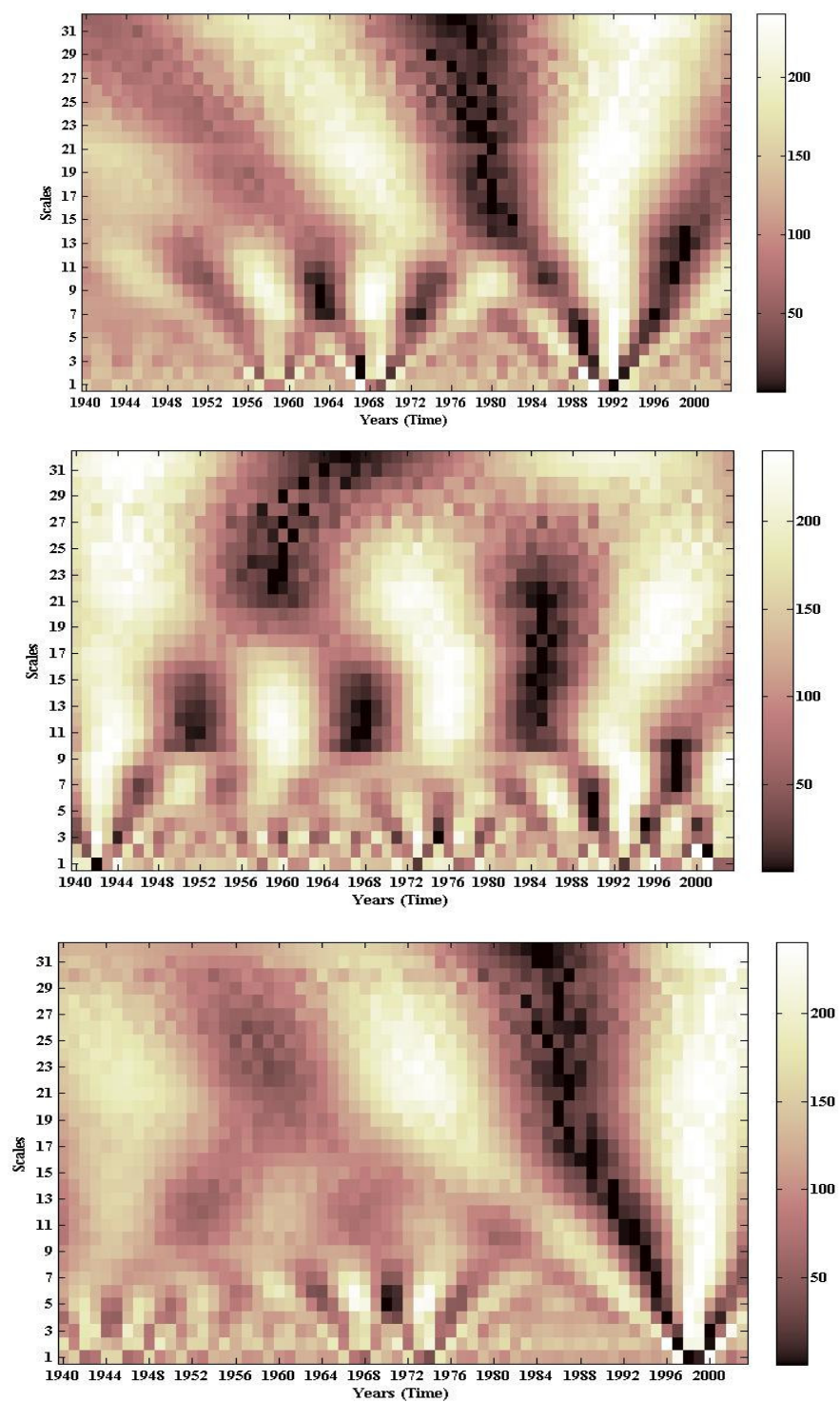


Figure III-12: Scale and period of maximum seasonal total flow for (from top to bottom) Dec-Mar, Apr-Jul, and Aug-Nov obtained from USGS 08186000 gauging data.

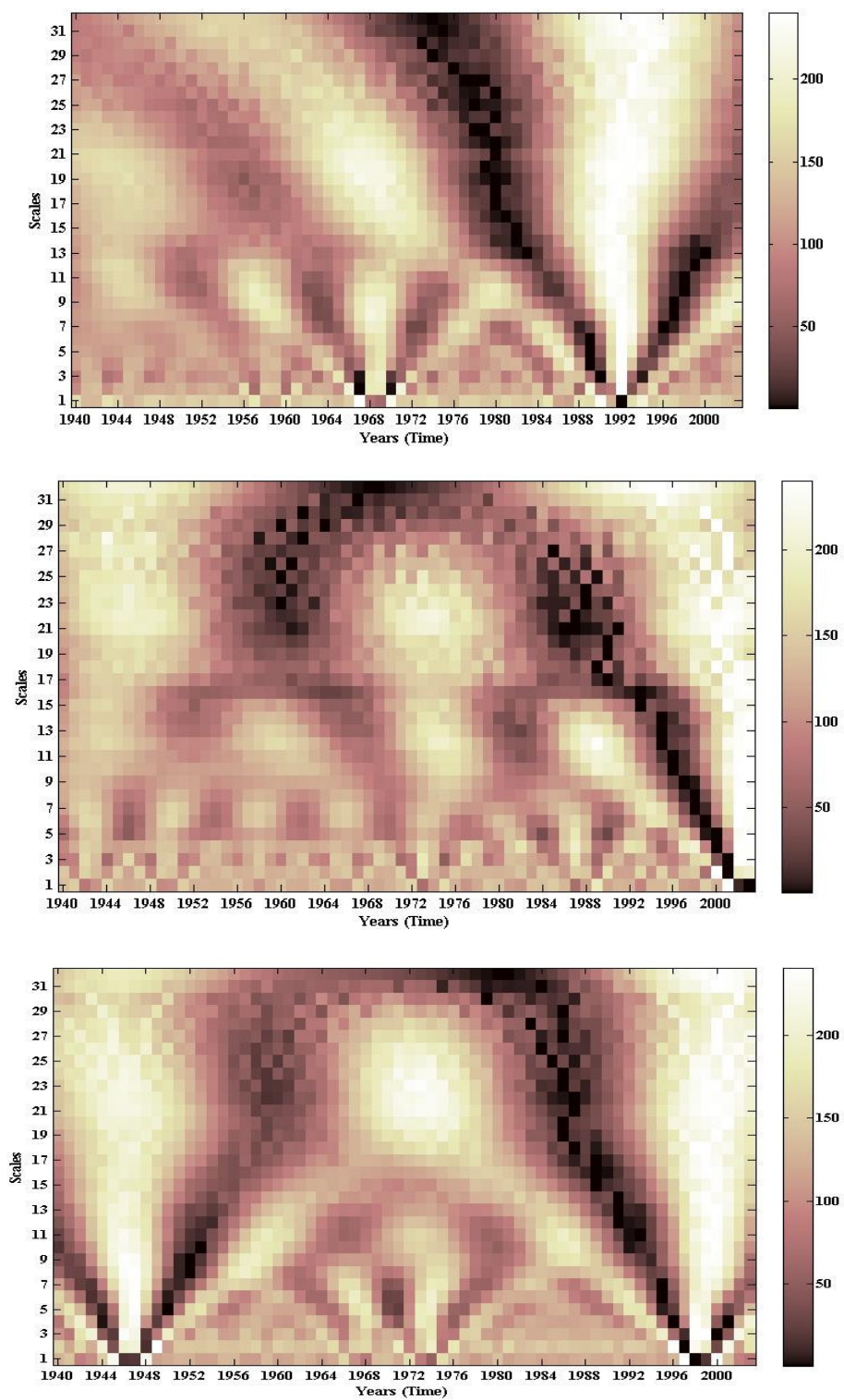


Figure III-13: Scale and period of maximum seasonal total flow for (from top to bottom) Dec-Mar, Apr-Jul, and Aug-Nov obtained from USGS 08183500 gauging data.

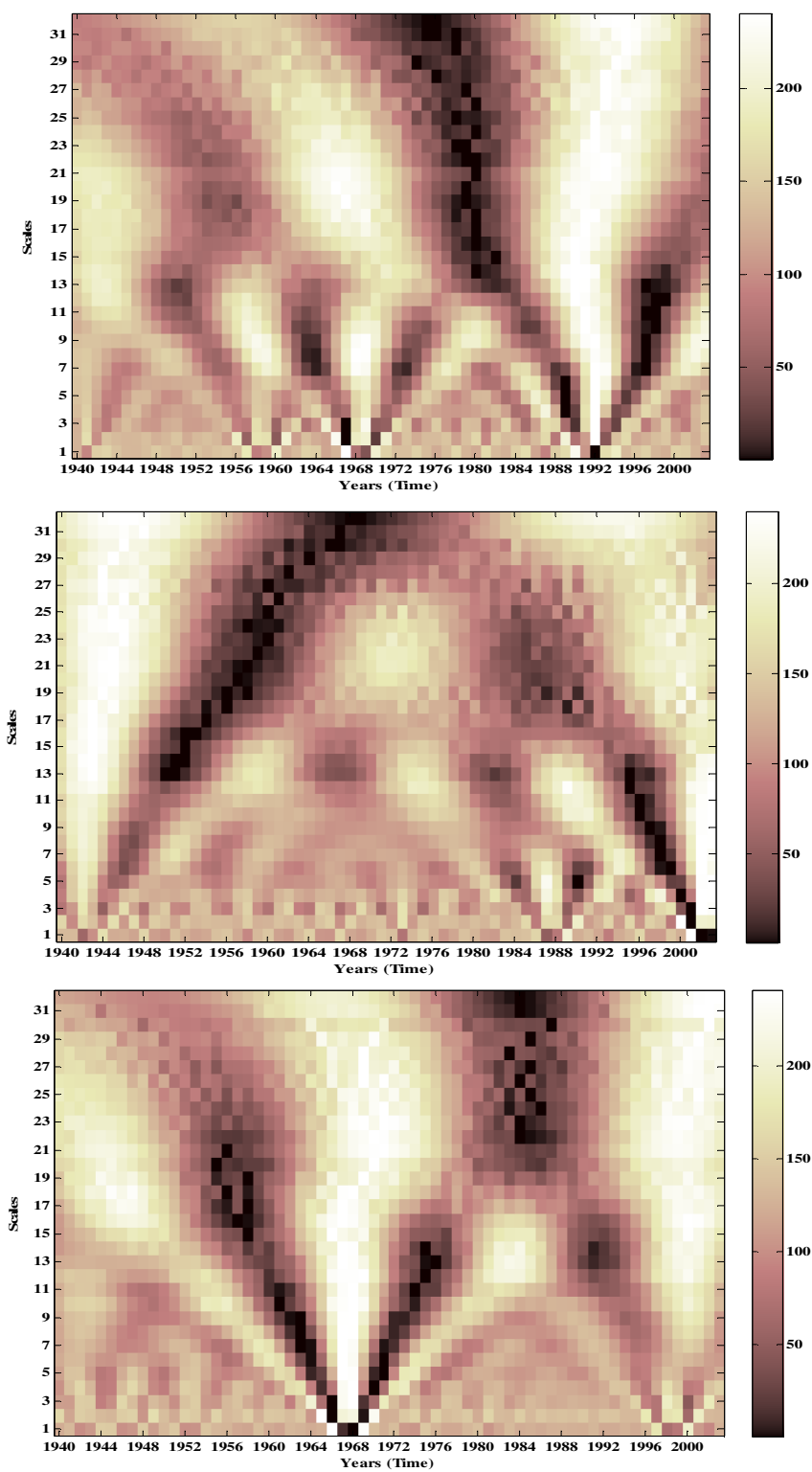


Figure III-14: Scale and period of maximum seasonal total flow for (from top to bottom) Dec-Mar, Apr-Jul, and Aug-Nov obtained from USGS 08188500 gauging data.

Analysis of maximum seasonal base flows at USGS gauging station number 08188500, the most downstream stream gauging station, suggested, maximum of maximum seasonal base flow observed for Dec-Mar was about 31 million cubic meters in 1958; for Apr-Jul was about 46 million cubic meters in 2002; for Aug-Nov was about 48 million cubic meters in 1967. Likewise, minimum of maximum seasonal base flows observed for Dec-Mar was about 0.07 million cubic meters in 1954; for Apr-Jul was about 0.49 million cubic meters in 1967; and for Aug-Nov was about 0.35 million cubic meters in 1954.

Wavelet analysis on the signals suggested presence of multi scale temporal variability in the data series. In general, analysis of maximum seasonal base flows at all the three gauging stations suggested presence of dominating features in flows for Apr-Jul at USGS 0818600; Apr-Jul at USGS 08188500. In the above variables, higher frequencies were observed in 10-15 years period (Figures III-15, 16, and 17) repeated every 10-15 years, suggesting presence of some cyclic phenomena. Dominating features were also observed in 17-23 years period in all of the seasonal flows, at all the gauging stations. These signals were repeated in 20-30 years cycle. Some higher frequencies were also observed in non repetitive cycle in Dec-Mar flows for all the three stations; however they suggested presence of multi scale temporal variability.

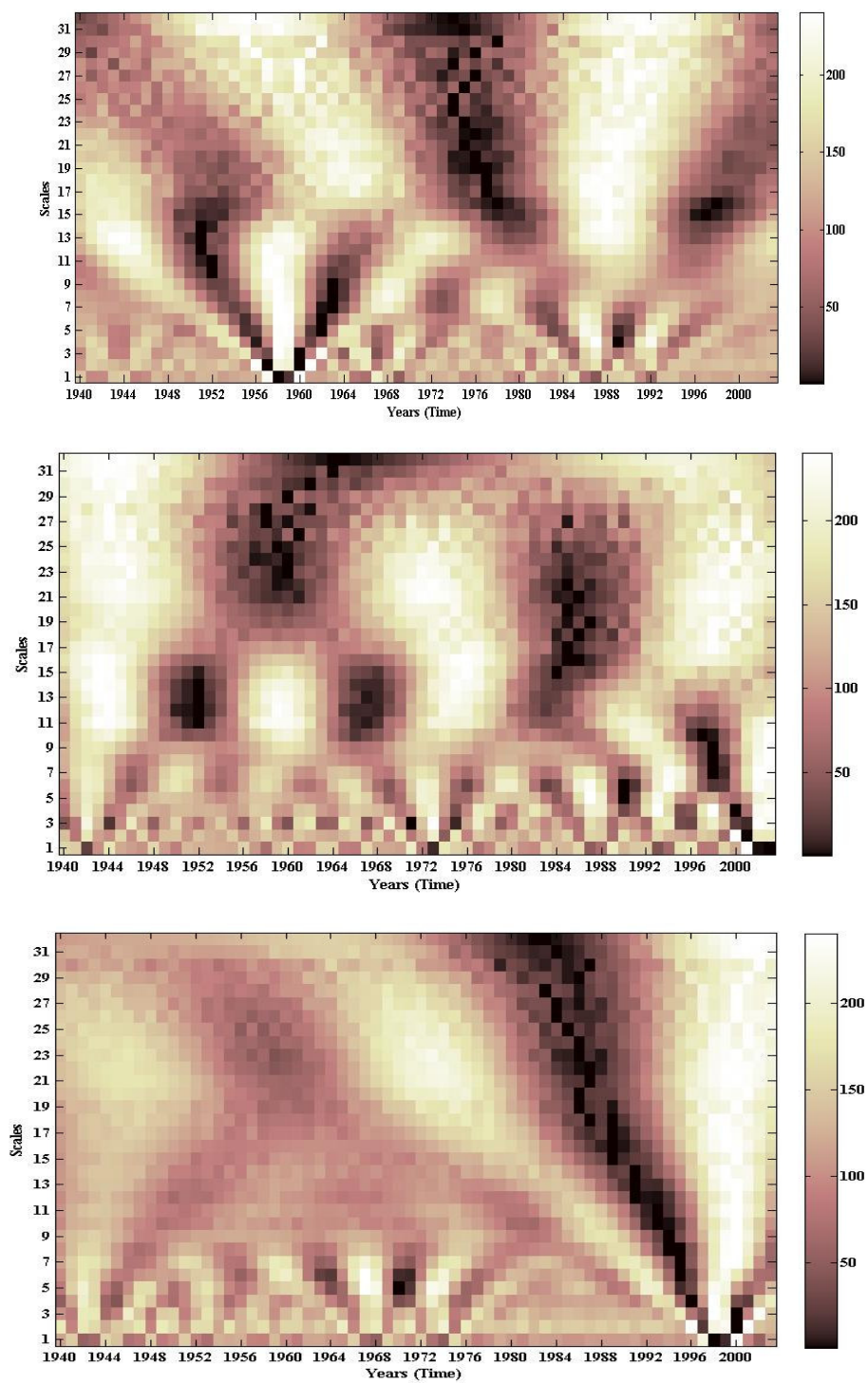


Figure III-15: Scale and period of maximum seasonal baseflow for (from top to bottom) Dec-Mar, Apr-Jul, and Aug-Nov obtained from USGS 08186000 gauging data.

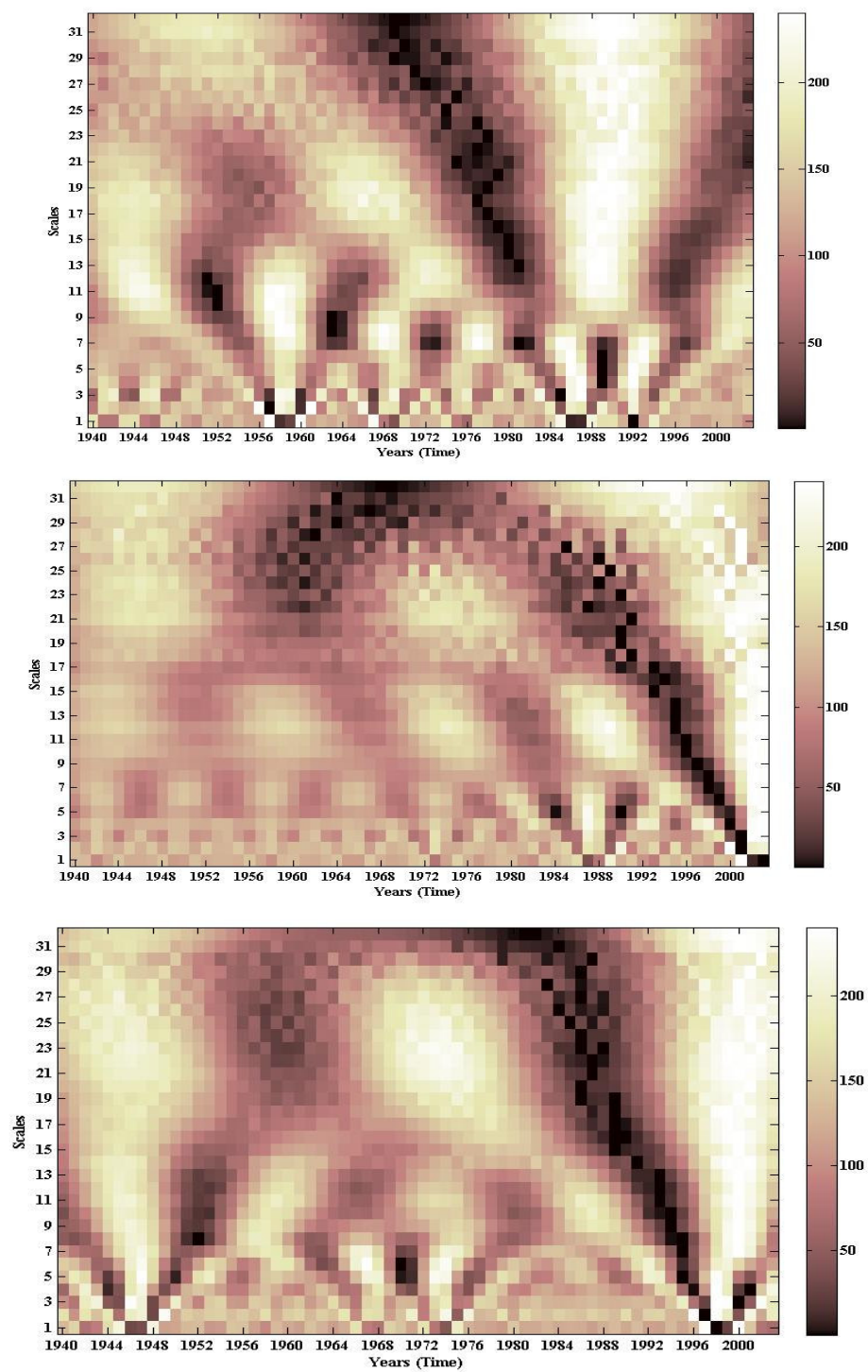


Figure III-16: Scale and period of maximum seasonal baseflow for (from top to bottom) Dec-Mar, Apr-Jul, and Aug-Nov obtained from USGS 08183500 gauging data.

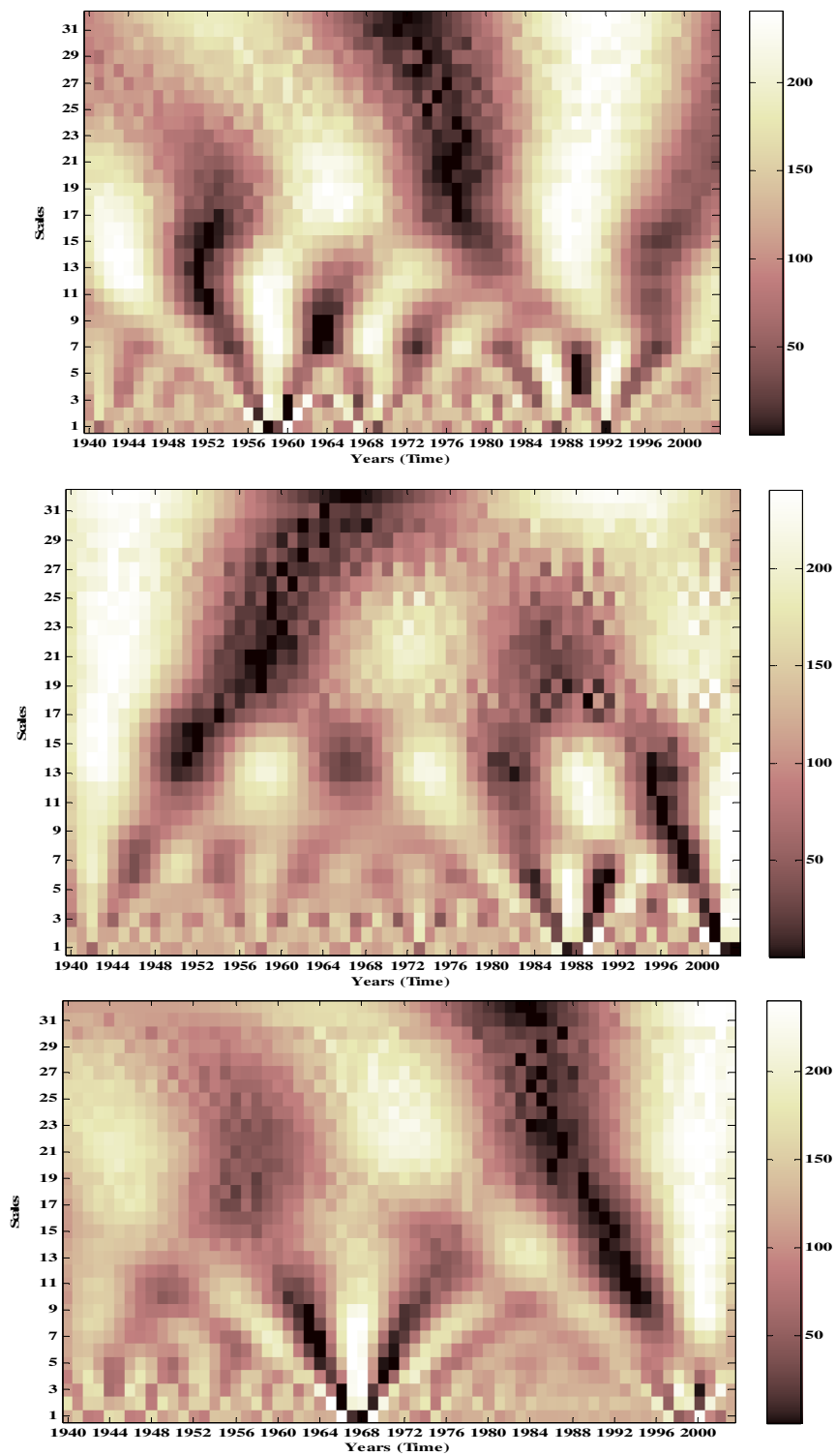


Figure III-17: Scale and period of maximum seasonal baseflow for (from top to bottom) Dec-Mar, Apr-Jul, and Aug-Nov obtained from USGS 08188500 gauging data.

3.7 Conclusion

Results obtained from this study suggested presence of dominant features at a larger scale of 17-23 years in most of the environmental flow, with 20-30 years bi-decadal oscillations. Larger scales beyond 16 years in hydroclimatic variables have been reported in past studies (Coulibay and Burn, 2005). Dominant features were also observed in 10-15 years period in most of hydrologic variables, at all the three sites, with repetitive cycle in decadal scale.

Use of continuous wavelet techniques on hydrologic variables particularly environmental flows can help in understanding various ecological processes in rivers and estuaries at different scales. This technique will allow us to understand the cyclic phenomena that correspond to the oscillations of the environmental flow signals. Specific ecological processes exist in the San Antonio Guadalupe Estuary region in which this approach would be a useful component for ecological analysis or experiment. It will be interesting to see the existence of ecological variables in larger scale of 17-23 years (as dominant in most of the hydroclimatic variables) versus the variables in smaller scales of 1-5 yrs. Since, this study suggest the presence of cyclic events of larger frequencies in 20-30 years, it will be interesting to observe the ecological cycles at this scale as well. More importantly, river basin management can be performed likewise.

CHAPTER IV
PARAMETER ESTIMATION FOR CALIBRATION AND VALIDATION OF HSPF
USING AN EVOLUTIONARY ALGORITHM AND INVERSE MODELING

4.1 Overview

Parameter estimation is an essential process in the calibration and validation of hydrologic models. This study explores the possibility of using a genetic algorithm (GA) to estimate the parameters for the Hydrologic Simulation Program in FORTRAN (HSPF) a model frequently used in hydrology and water quality modeling. The estimated parameters will be used to calibrate a model to optimize freshwater inflows from the San Antonio River Watershed to the San Antonio-Guadalupe estuary along the Gulf Coast of Texas. GA is a search algorithm based on natural selection and the mechanics of genetic evolution in pursuit of the ideas of adaptation and its use is a relatively new methodology for estimating the parameters in hydrologic models. GA is robust and has been proven theoretically and empirically to find the optimal or near optimal solution. A GA is used to search through combinations of parameters to achieve the set that is “best” in terms of satisfying an objective function. The objective function was formulated to minimize the mean absolute error between corresponding simulated and observed freshwater inflows. The calibration process was achieved through the following steps: (1) HSPF parameters are coded as “genes” in the chromosomes. (2) The population of the chromosomes is

initialized. (3) The fitness of each chromosome is evaluated by using the decoded parameter values as inputs to HSPF. (4) The RMSE between the observed and simulated streamflow is calculated. (5) Chromosomes undergo a selection process where the fittest “survive” and the weakest “die”. (6) Surviving chromosomes undergo reproduction by the process of crossover. (7) The generated offspring are subjected to mutation. (8) The process repeats from step 3 until the optimum solution is achieved. The parameters coded as genes for calibration were the lower zone nominal storage, soil infiltration capacity index, ground water recession coefficient, upper zone nominal storage, fraction of ground water inflow to deep recharge, lower zone ET parameter, and interflow inflow parameter. Simulated results were compared using three indices, Nash-Sutcliffe coefficient, mean absolute error, and root means square error. The simulated results were also compared in wavelet domain to assess the scale and localization of the signals. Obtained parameter values were well within the range cited in literature. Overall Nash-Sutcliffe coefficients in all the simulations were over 0.5, suggesting the simulated flows to be in good agreement with observed flows. This study suggested GA can be coupled with HSPF for model calibration. However, it is computationally intensive. The present method is useful because one can automate the calibration processes and overcome numerous simulation processes such as in HSPEXP.

4.2 Introduction

Hydrologic Simulation Program in FORTRAN (HSPF) is a watershed scale hydrologic model used extensively by researchers and water resources professionals in modeling watershed processes (Im et al., 2004) and investigating water resources problems. HSPF is a continuous, lumped parameter model software that simulates hydrologic and associated water quality processes on pervious and impervious land surfaces, in streams, and in reservoirs (Bicknell et al., 1996). The model has three modules: pervious land (PERLND), impervious land (IMPLND), and reaches (RCHES). Each of these modules requires several parameters to simulate hydrology and water quality.

Before these models can be used for simulating real world scenarios, they must be calibrated for conditions in the watershed of interest. Since hydrology drives other watershed processes such as water quality, model calibration is an important step. Model calibration is a parameter optimization process, which has traditionally been conducted by trial-and-error methods, in a wide range of parameter search space. The trial-and-error method can further be refined by performing sensitivity analysis of the parameters that control the model objective functions e.g., stream flow, water quality. In this process, the user adjusts the parameter, starting with the most sensitive parameter and proceeding to the next sensitive parameter, until the simulated output adequately reflects observed data for an objective function of interest.

Calibrating multiple parameters simultaneously from the parameter search space (rather than looking at one parameter at a time) may be achieved by using several optimization techniques (Nicklow, 2000). Optimization processes are search processes, where the algorithm searches for the best parameters for the desired outcome. In HSPF, calibration is usually accomplished using the HSPF-Expert System (HSPEXP) (Lumb et al., 1994). This system allows users to edit the *.uci file (which is the input file for HSPF, and has all the information that a model needs to run HSPF, plot the results and compare with observed values. Error statistics are computed and suggestions are made on which parameters to change to improve calibration. HSPEXP uses over 35 rules and 80 conditions for calibration. The rules are divided into four phases-- annual volumes, low flows, storm flows, and seasonal flows. Artificial Intelligence (AI) is used to get an estimate of initial values for model parameters. This again is a sort of trial-and-error method, where the modeler spends lot of time in repeating simulations; however, it provides valuable advice to improve the calibration.

In addition to AI, there are several optimization algorithms including direct search, simulated annealing, dynamic programming, greedy algorithm, genetic algorithm, and scattered search, to address parameter search in a large space (Srivastava et al., 2002). A Genetic algorithm (GA) is one such method widely used by researchers for optimization problems (Holland, 1975; Ines and Droogers, 2002; Srivastava et al., 2002; Liong et al., 1996), including those in hydrologic models. GA is a search algorithm and also an

evolutionary algorithm mathematically represented, that mimic the processes of natural selection and evolution (Goldberg, 1989; Carrol, 1997; Reeves, 1993).

In GA, the parameters that control the outcome of the optimization are mathematically termed as decision variables. Combinations of decision variables form a population. Each individual in the population is a “chromosome”. Chromosomes are composed of bits termed as “genes”, which are the decision variables. Therefore, each chromosome contains all possible information of the decision variables pertinent to the problem domain, i.e. a single chromosome is one possible combination of values for all the parameters used in the calibration. Traditionally in GA applications, the genes are the values of the parameters (decision variables) that are expressed in binary code (0s and 1s) (Ines and Droogers, 2002; Goldberg, 1989); however other encodings are also possible.

As an example of a binary GA application, let us consider the HSPF parameter Ground Water Recession Coefficient (AGWRC) which has a range of 0.85 to 0.99. AGWRC would first be discretized into finite lengths based on the accuracy required in the optimization, 0.01 for example. Once the number of binary bits is designed in a chromosome, it can be converted to decimal value with base 10. Then the decimal value can be used to get the original value (between max and min values) of the binary string. The above description is for one parameter. For several parameters that control the output, each parameter is coded in binary and then combined to form a single chromosome that has the information about the decision variables.

GAs are robust and can thoroughly and efficiently scan the search space for the optimal solution of the combinatorial problem. They can quickly detect the area of optimal solution or near optimal space. Sometime it takes several iterations for a GA to find an optimal solution, which depends on the objective function framed for the problem. The objective function determines the “fitness” of the chromosome. The fitness function serves as an environment for the existence of the population in each generation. The fitter individuals that survived the test of the environment tend to reproduce and produce offspring that are expected to express better genetic traits in the next generation. Each chromosome is evaluated for fitness (as described by the fitness function). Depending on the fitness, different individuals are “mated” to produce progenies for the next generation (Goldberg, 1989). Mating is a process where either of a pair of individuals brought together for breeding. For example in case of parameters, the chromosomes (decision variables) are brought together to exchange information between them. During mating it is assumed that, fitter individuals have higher probability of producing more and better offsprings. GAs undergo various biological processes such as crossover, mutation, and elitism.

Crossover is a biological process in which there is exchange of genetic material from both the parents. It improves the genetic traits in future generations; therefore, it adds variety to the pool. GAs mimic these biological process as well. Since, crossover provides better genetic trait in each successive generation, it helps the algorithm to search near optimal solution space, with each successive generation. For example in case of parameters,

values of the parameters between the individuals (chromosomes) are randomly exchanged during crossover. Crossovers are of two types: single point crossover, and uniform crossover. In single-point crossover the position of the chromosome is randomly selected at some point in the chromosome length, whereas in uniform crossover individual bits in the string are compared between two parents. The bits are exchanged with 50% fixed probability.

In addition to crossover, GAs mimics the biological process of mutation. Mutation introduces diversity, by randomly infusing new genetic materials into the population. For example in case of parameters, values of the parameters are randomly altered in the chromosome, i.e. random alteration of parameters infuses new genetic material. There are two basic mutation approaches: jump mutation and creep mutation. In jump mutation each bit in the string is allowed to mutate based on some probability, where as creep mutation explores the immediate vicinity of the current population in the solution space. Elitism is another feature where the fittest individual from the population is transferred to the next generation.

Crossover and mutation are controlled by their probability value. Crossover and mutation happens only when the random number is less than or equal to probability of crossover, or to probability of mutation, respectively. If this does not happen then the parent enters into the next generation. The biological processes of selection, crossover, and mutation are repeated for several generations until the best possible solution is achieved.

Below is a brief description on the complete processes of GA. In this process the fittest individual (string) survives by randomly exchanging information and arriving at the solution (Goldberg, 1989; Holland, 1975; Ines and Honda, 2005). The parameters are coded as a set of binary sub-strings to form a chromosome; further forming population. A binary GA was implemented for the present study. The bits (0s and 1s) arrangement in the chromosome is a possible combination for a possible solution of the problem (Figure IV-1) domain.

The required number of binary bits for the parameter is given by:

$$2^L = \frac{X_{\max} - X_{\min}}{\delta} \quad (10)$$

and

$$L = \frac{\ln(X_{\max} - X_{\min}) - \ln \delta}{\ln 2} \quad (11)$$

where Xmax is maximum value of the parameter (e.g., 0.99); Xmin is the minimum value of the parameter (e.g., 0.85); δ is accuracy (e.g., 0.01); and L is the length of the binary string. By calculation, value of L was determined, say 7. The number of discrete possibilities for the parameter X will be then be 128 ($= 2^7 = 2^L$). Now describing the above method in an example: say a binary representation for X = 0100110 (since L = 7) is randomly obtained. The decimal value of X with base 10 then, is:

$$0100110 = 0x2^6 + 1x2^5 + 0x2^4 + 0x2^3 + 1x2^2 + 1x2^1 + 0x2^0 = 0 + 32 + 0 + 0 + 4 + 2 + 0 = 38 \quad (12)$$

$$\Rightarrow X = 0.85 + 38 \left[\frac{(0.99 - 0.85)}{(128 - 1)} \right] = 0.891 \quad (13)$$

which is obtained from

$$X = X_{\min} + B \left[\frac{(X_{\max} - X_{\min})}{(2^L - 1)} \right] \quad (14)$$

where X is the value of the string; X_{\min} is lower bound of X ; X_{\max} is upper bound of X ; B is the decimal value of the binary string of X with base 10; and L is the length of the binary string.

The processes of calibration starts with an initial population (called chromosomes). The generated population is then subjected to evaluation based on the fitness function. After this, they undergo a process called selection to form a mating pool. The fitter population survives and the weaker dies. The survivors play a vital role in generating new offsprings for the next generation. The selected individuals (chromosomes) randomly unite and exchange hidden information (genetic information) through crossover to produce offspring. In order to randomly induce new genetic materials in the next generation, the new set of chromosome undergoes mutation.

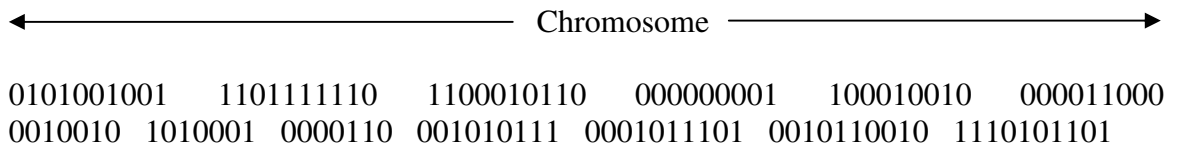


Figure IV-1: A binary representation of chromosome in GA for optimal parameter estimation in hydrologic calibration.

Most of the earlier studies on use of GA in optimization has addressed land use planning (Stewart et al., 2004), water management practices (Ines and Honda, 2005), best

management practices (Srivastava et al., 2002) and automatic calibration of distributed watershed models (Muleta and Nicklow, 2005). Past studies have not addressed parameter optimization in HSPF for surface water quantity. Therefore, the overall objective of this study is to assess the plausibility of using GA for automatic calibration of HSPF.

The present study has used modified- μ GA (Carroll, 1997) for present problem domain. It is different than the μ GA in a sense that it introduces creep mutation to randomly alter the sub-strings of a chromosome. Higher restarting criterion is set to increase the rate of population restart. During restart, the elite chromosome is preserved and the rest of the population is randomly generated (Ines and Honda, 2005; Ines and Droogers, 2002; and Carroll, 1997). This study used a binary tournament selection with shuffling. In this method, the position of the chromosomes in the population is randomly shuffled. Like chromosome at position A is shuffled with those at position B and vice versa. By definition, binary tournament proceeds by selecting two chromosomes from the shuffled population. The two selected chromosomes compete for a position in the mating pool according to their fitness. The chromosome with higher fitness value is selected and it joins the mating pool. The present study used creep mutation. It is a kind of mutation that occurs at the real space (base 10). The binary sub-strings are mutated between their minimum and maximum values. This is different than jump mutation because lesser perturbation is introduced to the micro-population.

4.3 Methodology

4.3.1 Study Area

The San Antonio River Basin encompasses 10,826 km² (Figure IV-2) from the headwaters of the Medina River to the point at which the San Antonio River joins with the Guadalupe River before emptying into the Gulf of Mexico, approximately 390 river km (Figure IV-2). This study area is located between latitude 29.91° N and 28.51° N and longitude 99.57° W and 97.01° W. The watershed drains through some portion of 8 counties: Kerr, Kendall, Comal, Guadalupe, Dewitt, Victoria, Refugio, and Medina Counties (Figure IV-2). Major tributaries to the San Antonio River are Leon Creek, Salado Creek, Cibolo Creek, and Medina Creek. Population in this river basin has increased in the last 30 years primarily due to the growth of the City of San Antonio. It is predicted that the population around the city of San Antonio by 2020 will be approximately 2.2 million (Texas State Data Center, 2005; Nivin and Perez, 2006). To the northwest of the city, the terrain slopes to the Edwards Plateau and to the southeast it slopes to the Gulf Coastal Plains. Average slope of this watershed is about 1.38 degrees. Soils are blackland clay and silty loam on the Plains and thin limestone soils on the Edwards Plateau. Analysis of 2003 processed LANDSAT imageries (Figure IV-2)

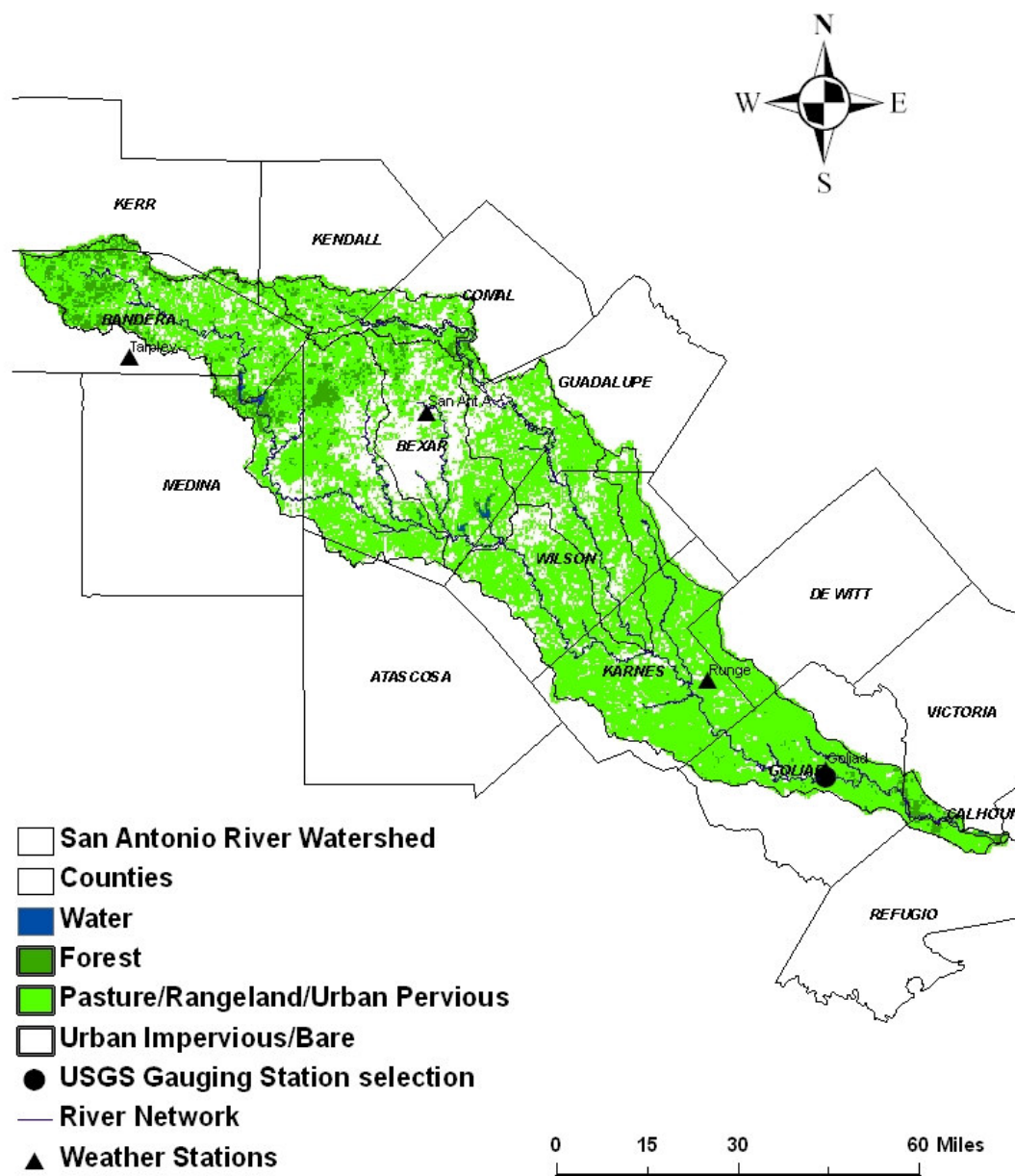


Figure IV-2: San Antonio River watershed with 2003 land use, gauging stations, weather stations, and various counties in the watershed.

suggested approximately 60% of the watershed is dominated by pasture/rangeland, followed by 24% forest, 14% urban impervious/bare, and 2% water. Historically, this region has experienced an average annual rainfall of about 890 mm. Edwards Aquifer which is a karst system, is the sole source of water supply to the City of San Antonio (both industrial and domestic uses) and near by areas. This aquifer crosses the watershed about half way from the headwaters of the river.

4.3.2 Model Description

BASINS was developed by the U.S. EPA's Office of Water to support environmental and ecological studies (USEPA, 2001). BASINS is interfaced through an ARCVIEW framework (USEPA, 2001). It is composed of databases (e.g., databases for soil, weather stations, and point sources), assessment tools such as PLOAD (pollutant load), an in-stream water quality model such as QUAL2E, a watershed delineation tool, and several watershed scale models such as HSPF and SWAT. BASINS software is used to pre-process the data required to run the respective model. It converts the input data into a format that is required by the watershed model.

In HSPF, modules are divided into pervious land (PERLND), impervious land (IMPLND), and reaches (RCHRES). Each land segment is considered a lumped catchment. However, spatial variability can be mimicked by dividing the river basin into many hydrologically homogeneous land segments. Runoff is simulated from each land

segment independently, using meteorological input and watershed parameters. Simulation is based on an hourly time step. The simulation is based on mass balance approach (Paul et al., 2004). In the IMPLND module, water is partitioned as overland flow, evaporation, or surface detention storage. In the PERLND module, precipitation in form of water is divided into direct runoff, direct evaporation, surface storage followed by evaporation, surface storage followed by interflow, and infiltration to the subsurface area. The subsurface is divided into upper zone, lower zone and deep groundwater zone compartments. Water received by the subsurface zone is either stored, evaporated or flows to the subsequent lower zone. Water in groundwater zone is assumed to be lost from the system.

Based on literature, various parameters control water balance (hydrology) in HSPF (Moore et al., 1988; Laroche et al., 1996, Im et al., 2004; USEPA 2000) (Table IV-1). The parameters are lower zone nominal storage (LZSN), soil infiltration capacity index (INFILT), ground water recession coefficient (AGWRC), upper zone nominal storage (UZSN), fraction of ground water inflow to deep recharge (DEEPPFR), lower zone ET parameter (LZETP), and interflow inflow parameter (INTFW). LZSN is related to precipitation pattern and soil characteristics in the area; INFILT is the parameter that effectively controls the overall separation of the available moisture from precipitation (after interception) into surface, subsurface flow and storage, and it is primarily a function of soil characteristics where the value are related to SCS hydrologic soil groups; AGWRC, is the ratio of current groundwater discharge to that from 24 hours earlier;

Table IV-1: Various model parameter that control water quantity in HSPF, their length in the chromosome, and accuracy.

Parameters	Description	Length (L) of the Parameter	Accuracy (δ)
LZSN	Lower Zone Nominal Storage (in)	10	0.01
INFILT	Soil Infiltration Capacity Index (in/hr)	9	0.001
AGWRC	Ground Water Recession Coefficient (per day)	7	0.001
DEEPFR	Fraction of Ground Water Inflow to Deep Recharge	9	0.001
UZSN	Upper Zone Nominal Storage (in)	10	0.001
INTFW	Interflow Inflow Parameter	10	0.01
LZETP	Lower Zone ET Parameter	10	0.001

UZSN is related to land surface characteristics, topography, and LZSN; DEEPFR is the fraction of infiltrating water which is lost to deep aquifers; LZETP is the index to lower zone evapotranspiration; INTFW is the coefficient that determines the amount of water which enters the ground from surface detention storage and becomes interflow.

4.3.3 Data Description

The San Antonio River watershed is located within the Hydrologic Cataloging Boundaries (HUC) 12100301, 12100302, 12100303, and 12100304. Soils data from the STATSGO soils database and topography data to create a digital elevation model (DEM) for above mentioned HUC were obtained from EPA's BASINS web site (USEPA, 2001). Reach Network file Version 3 a comprehensive set of digital spatial data that contains information about surface water features such as lakes, ponds, streams, rivers, and wells was also obtained from BASINS. Recent land use land cover data (2003) sets were processed using ENVI and imported to BASINS. LANDSAT imageries were obtained from US Geological Survey. ENVI 4.2 was used to processes the images and ARCGIS was used for geospatial analysis.

San Antonio watershed was subdivided into 44 hydrologically connected sub-watersheds using the DEMs and the Automatic Watershed Delineation tool available with BASINS 3.0. Factors like land use, slope, soil, and climate were considered during watershed delineation. Too many sub-watersheds in HSPF allow too many operations, thereby

increases computing time. Also HSPF can only handle about 200 operations. Too many sub-watersheds provide opportunity for too many operations; resulting malfunctioning of the model. Therefore, selecting 44 sub-watersheds was the optimal solution. Four weather stations National Climatic Data Center (NCDC) COOPID 418845, 417945, 417836, and 413618 were selected to represent weather data for HSPF simulation. Weather stations were selected on the basis of availability of long term hourly data (hourly precipitation, and daily evapotranspiration) (Figure IV-2) from 1996-2005. The necessary meteorological data to run HSPF is stored in watershed data management (WDM) file. For the present study HSPF needed hourly precipitation and hourly potential evapotranspiration. These two weather variables control water quantity. WDMUtil tool was used to arrange the data in model readable format (USEPA, 2001). It is software that helps user in importing data in the required format, using several available scripts. The Thiessen polygon method was used to distribute rainfall across the watershed (Figure IV-3). Daily evapo-transpiration was disaggregated into hourly evapotranspiration using WDMUtil tool.

Historical daily mean stream flow data for USGS gauging station 08188500 was obtained from the USGS web site (USGS, 2006) for the simulation period (2000-2005). This station is the outlet of the San Antonio Watershed. This stream flow data was used in model calibration and validation.

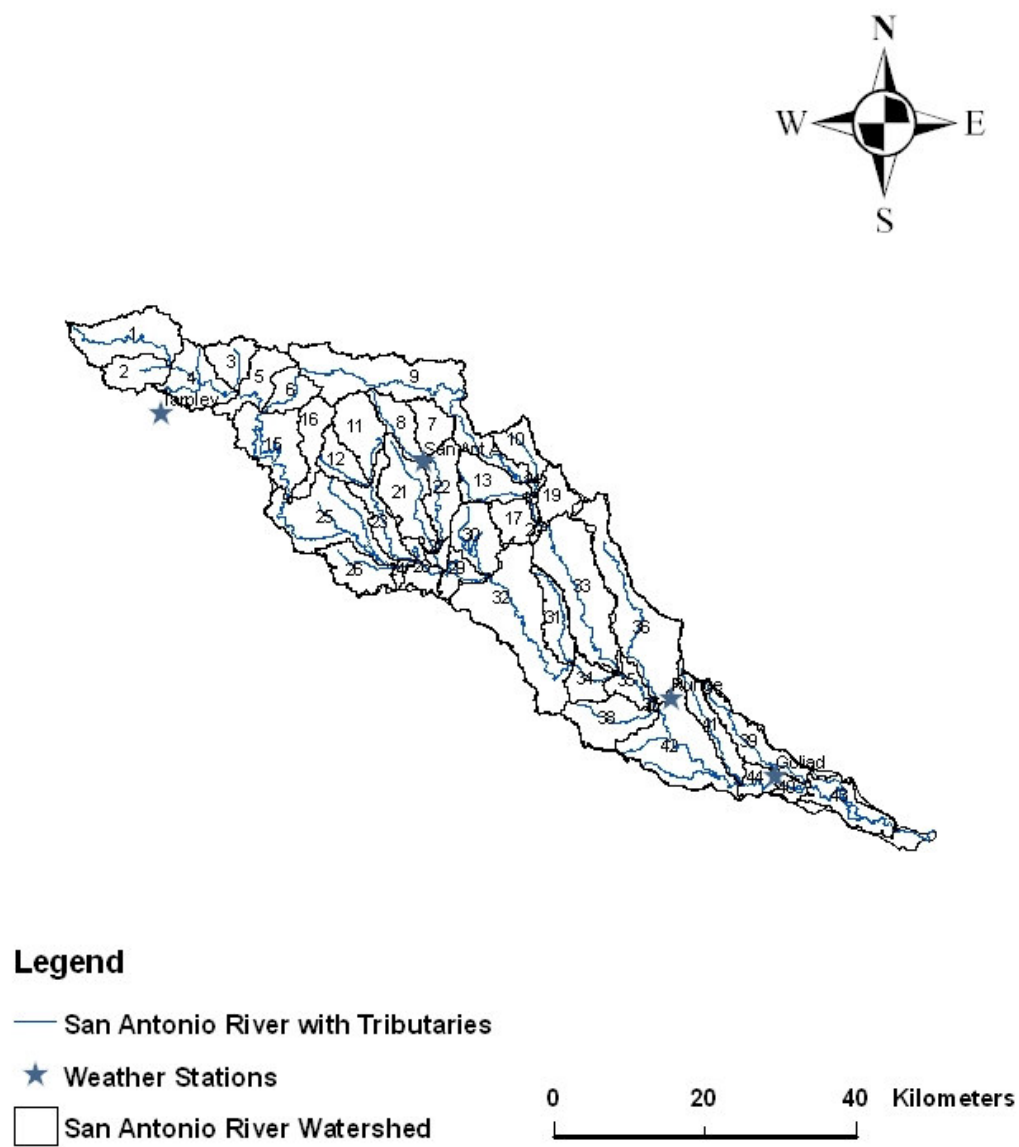


Figure IV-3: San Antonio River watershed with weather stations and the sub-basins associated with the weather stations.

4.3.4 Operation of Genetic Algorithms

The present study loosely coupled HSPF and GA (Figure IV-4). Seven different parameters were coded in binary form and the population was initialized. The binary values were decoded to real values in the next step, in order to provide input values to HSPF. HSPF performed simulation and the simulation result was evaluated using the fitness function. If the optimum value for the parameter was not reached, then genetic operators conducted their functions. The loop continued until the optimal parameters were obtained.

4.3.5 Model Calibration Using GA

Seven parameters were identified as having the most influence on predicting water quantity in HSPF, LZSN, INFILT, AGWRC, UZSN, DEEPFR, LZETP, and INTFW (Table IV-1) (Im et al., 2004; Engelmann et al., 2002; Paul et al., 2004). The ranges for each parameter for the San Antonio River watershed are given in table IV-1. These parameters were coded to form chromosomes. The length (L) of each parameter with accuracy (δ) was determined using equation 2. Table IV-1 shows the value of L and δ for each parameter. The total length of the chromosome was 117. Ten individuals were created in each generation. Two thousand generations were used for parameter estimation (Ines and Honda, 2005). The total simulation time was approximately one million seconds.

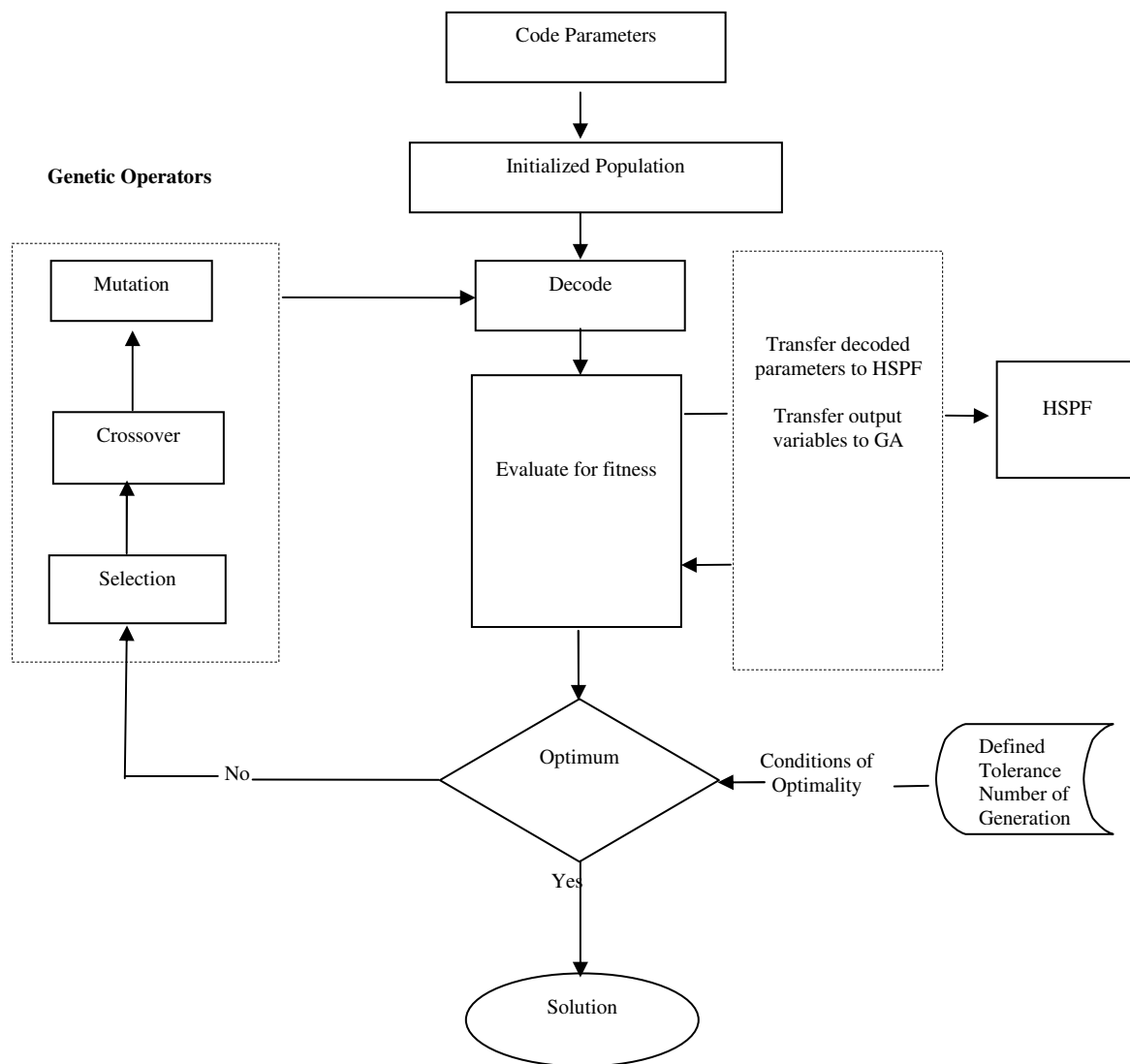


Figure IV-4: A figure showing GA linked with HSPF (Modified from Ines and Droogers, 2002).

The model simulations were executed for daily average flow (cms) from 01/01/2000 to 12/31/2004. The model calibration period was limited to the daily average flow from 01/01/2002 to 12/31/2004. The first two years of simulation were used for “Warming up”. The simulated values were matched to the observed values in a method know as inverse modeling (Ines and Droogers, 2002). The mean absolute error (MAE) and Nash-Sutcliffe model efficiency (E) were used as the objective functions in GA-HSPF. MAE is given by

$$MAE = \frac{\sum_i^n |O_i - S_i|}{n} \quad (15)$$

where O_i is observed daily flow for the i^{th} day; S_i is the simulated daily flows for the i^{th} day and n is the total number of days. The closer MAE is to zero, the better is simulation results (Weglarczyk, 1998; Legates and McCabe, 1999).

Nash-Sutcliffe model efficiency (E) (Nash and Sutcliffe, 1970) is a dimensionless indicator that is widely used in model verification. A positive value of E exhibits an acceptable fit between the observed and simulated values and therefore the model can be considered to be a better predictor of the system (Paul et al., 2004). E value above 0.5 is considered good agreement between O_i and S_i , as documented in literature (Santhi et al., 2001). E is calculated as:

$$E = 1 - \frac{\sum_i^n (O_i - S_i)^2}{\sum_i^n (O_i - O')^2} \quad (16)$$

where, the parameters are described above, and O' is the mean of observed daily flow.

The calibrated model output (simulated daily flow) was also compared with observed flow in wavelet domain (Kumar and Foufoula-Georgiou, 1997, Torrence and Compo, 1998). For this purpose Morlet Wavelet was selected (Anctil and Coulibaly, 2004). Analysis of signals, such as flow in wavelet domain helps in identifying dormant frequencies in the time series and the location of such frequencies (present in scale) (Sahoo and Smith, 2007).

4.3.6 Model Validation

Model was validated to assess if the parameters value represent watershed conditions. Validation of the model was conducted by using observed daily stream flow data for the years 2001 and 2005. Indices such as mean absolute error and Nash-Sutcliffe coefficient was used for model validation.

4.4 Results and Discussions

Hydrologic calibration was reached after 2000 generations. However, after only 250 generations the fitness no longer increased indicating optimal parameters had been found (Figure IV-5). The optimal parameters values were then obtained. Initial, final and literature values for the seven parameters are shown in Table IV-2. The GA generated parameter values are in line with literature and possible parameter values outlined in EPA BASINS Technical Note 6. In the present study DEEPFR value obtained from HSPF-GA linked model is 0.7. This value is not within the parameter values described in EPA BASINS Technical Note 6. However, Paul et al., 2004 has used 0.7 (DEEPFR value) in similar studies in the same region. It was expected to have a higher DEEPFR value because of presence of Edwards Aquifer, a karst system (presence of limestone) that crosses in the middle part of the region. The parameter DEEPFR, is the fraction of infiltrating water which is lost to deep aquifers. Presence of such karst system in the region tends to loose water to deep aquifers.

The calibration results suggested that GA was able to simulate daily flow. Visual observation and comparison of observed and simulated flow (Figure IV-6) suggested that GA-HSPF was able to simulate most of the flows; however, it was not able to match the high flow events perfectly. This could possibly be attributed to the spatial variability of rainfall that the weather stations used for this study, were unable to capture. The model

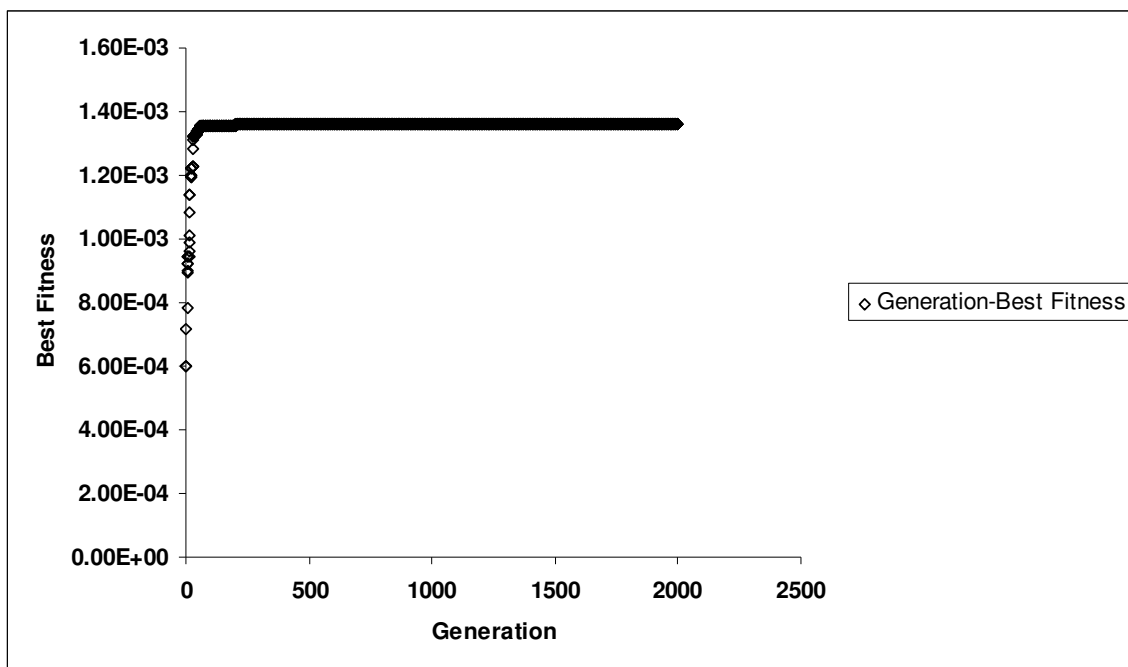


Figure IV-5: Graph showing generations versus best fitness that suggest model improvement over time.

Table IV-2: Various parameter values obtained from GA-HSPF, and their comparison with literature.

Parameters	Description	Initial Value	Final Value	Moore et al. (1988)	Chew et al. (1991)	Laroche et al. (1996)	Engelmann et al. (2002)	Im et al. (2004)
LZSN	Lower Zone Nominal Storage (in)	6.5-6.0	14.0-14.9	4.9	5.0	14.2	5.0	4.3-5.8
INFILT	Soil Infiltration Capacity Index (in/hr)	0.16	0.49-0.50	0.004-0.02	0.05-0.17	0.23	0.04	0.047-0.075
AGWRC	Ground Water Recession Coefficient (per day)	0.98	0.85-0.98	0.98	0.98	0.99	0.99	0.88-0.91
UZSN	Upper Zone Nominal Storage (in)	1.12	2.0	0.2	0.01-0.06	0.76	0.7	0.35-1.0
DEEPFR	Fraction of Ground Water Inflow to Deep Recharge	0.1	0.7	-	-	-	0.18	0.05-0.45
LZETP	Lower Zone ET Parameter	0.1	0.8	0.3-0.55	0.2-0.6	0-0.8	0.42	0.2-0.7
INTFW	Interflow Inflow Parameter	0.75	1.0	1.0	0.75-1	9.83	0.5	1-1.7

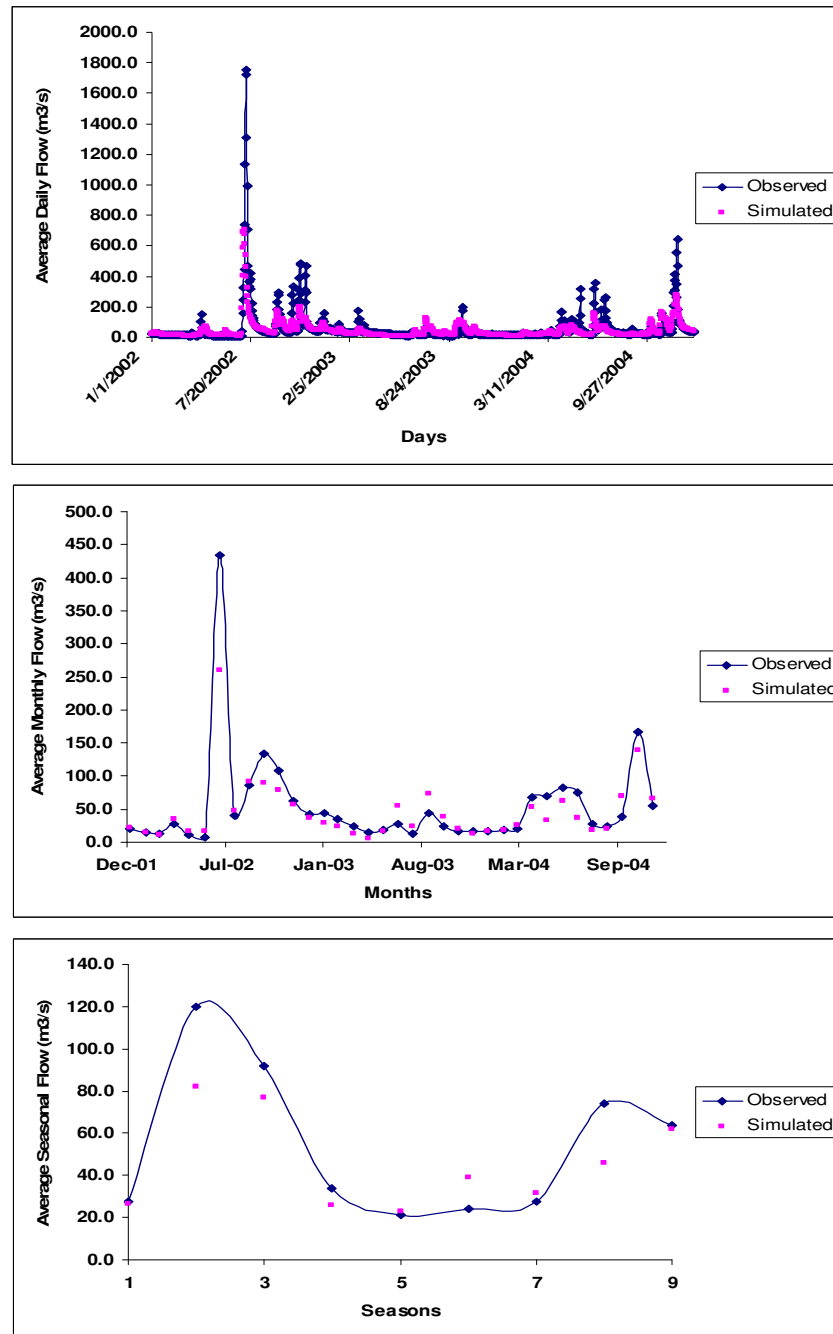


Figure IV-6: From top to bottom: Average observed daily and average simulated daily flow; average observed monthly and average simulated monthly flow; average observed seasonal and average simulated seasonal flow; average observed yearly and average simulated year.

was calibrated for daily flow; however, average monthly flow, average seasonal flow, and average yearly flow was used to verify the accuracy of the model.

Three indices were used to verify the results of the simulation. The model efficiency (E), MAE and RMSE for average daily observed flow and average daily simulated flow was found to be 0.52, 25.81 m³/s, and 82.19 m³/s, respectively. E, MAE, and RMSE for average monthly observed and average daily simulated flow for the calibration period was found to be 0.92, 17.73 m³/s, and 34.03 m³/s, respectively (Figure IV-6). Similarly, E, MAE, and RMSE for average seasonal observed flow and average seasonal simulated flow was found to be 0.72, 12.44 m³/s, and 17.40 m³/s, respectively (Figure IV-6). Likewise estimated E, MAE, and RMSE for average yearly observed and average yearly simulated was found to be 0.72, 9.72 m³/s, and 11.54 m³/s, respectively (Figure IV-6). Since, overall E in all the cases (daily flow, monthly flow, seasonal flow, and yearly flow) was above 0.5, the simulated flows are considered to be in good agreement with observed stream flow (Santhi et al., 2001; Paul et al., 2004). In all these cases (average monthly, average seasonally, and average yearly) of flows, GA was not able to simulate the high flows. The possible reason could be attributed to climatic forcings that were not accounted for, by the model.

The daily simulated flow (2002-2004) was compared with daily observed flow (2002-2004) in wavelet domain (Figure IV-7). Results suggested that similar frequencies were present in lower scale (1-53 days). Highest frequencies were present in all the scales in

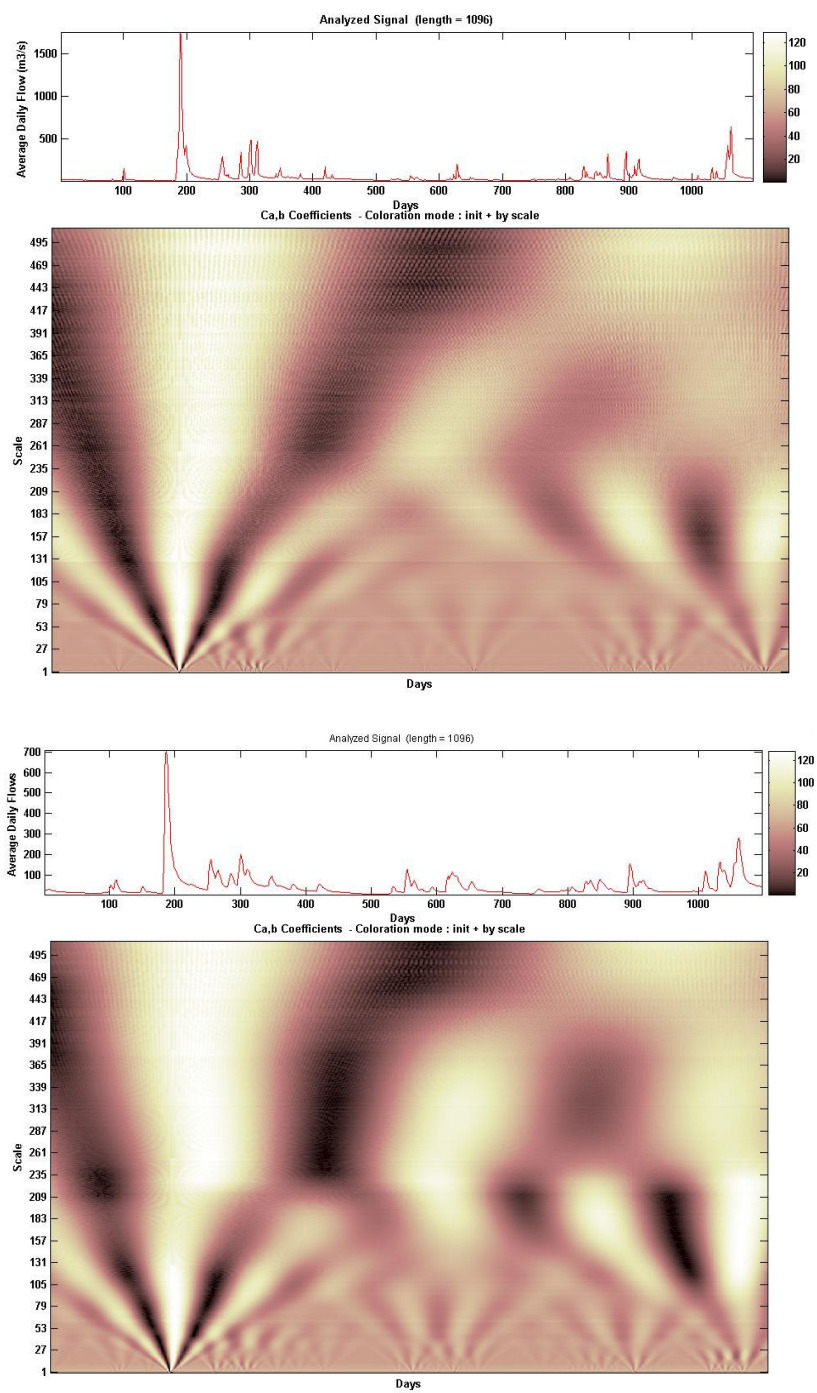


Figure IV-7: From top to bottom: Observed daily flow and simulated daily flow (2002-2004) in wavelet domain.

both simulated and observed flow. Highest frequencies were also present in 183-235 days scale in both the observed and simulated flows. Thus, wavelet analysis suggested that the model can provide reasonable information about the flow frequencies and location of the flow frequencies in the time series. Detail analysis of coefficients in all the scales present in both observed and simulated signals (flows) will further strengthen the model.

The calibrated model was validated for the year 2001 and 2005. All 12 months were used for 2001 validation year; however, only 11 months (January through November) were used for validation in 2005. The required data such as hourly precipitation, and hourly evapotranspiration was only available until November 2005, for the weather stations used in this study. Results were validated by simulating daily flows for the two years. Further, average monthly flows were also estimated for the two years. E, MAE, and RMSE for observed and simulated daily flow for the year 2001 was found to be 0.58, 20.73 m³/s, and 50.91 m³/s, respectively (Figure IV-8). Similarly, E, MAE, and RMSE for observed and simulated monthly flow for the year 2001 was found to be 0.71, 15.30 m³/s, and 22.95 m³/s, respectively (Figure IV-8). E, MAE, and RMSE for observed and simulated daily flow for the year 2005 was found to be 0.61, 6.17 m³/s, and 11.51 m³/s, respectively (Figure IV-9). Similarly, E, MAE, and RMSE for observed and simulated monthly flow for the year 2005 was found to be 0.90, 3.57 m³/s, and 4.66 m³/s, respectively (Figure IV-9). Four weather stations were used for the current study, since the weather data required by the model was not available at any other stations; this

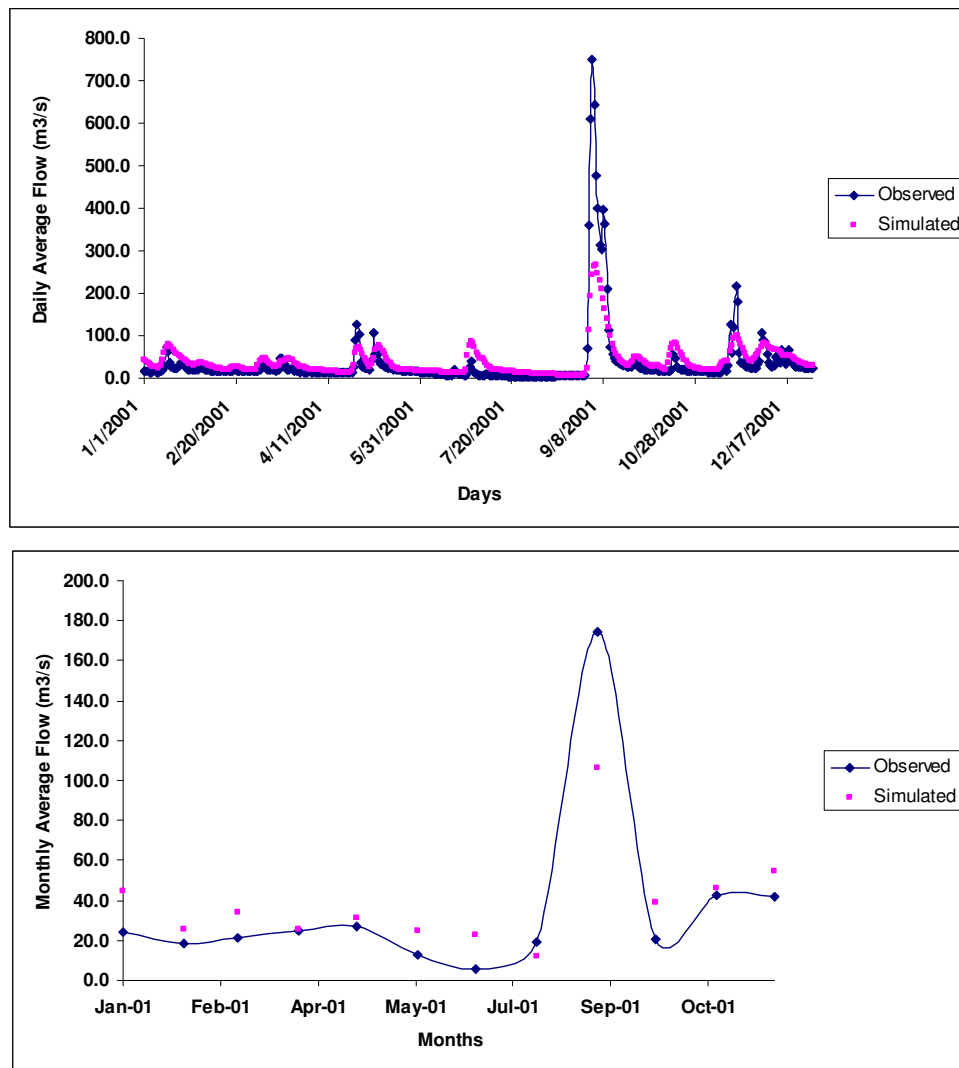


Figure IV-8: From top to bottom: Average observed daily and average simulated daily flow; average observed monthly and average simulated monthly flow for the validation year 2001, at the watershed outlet.

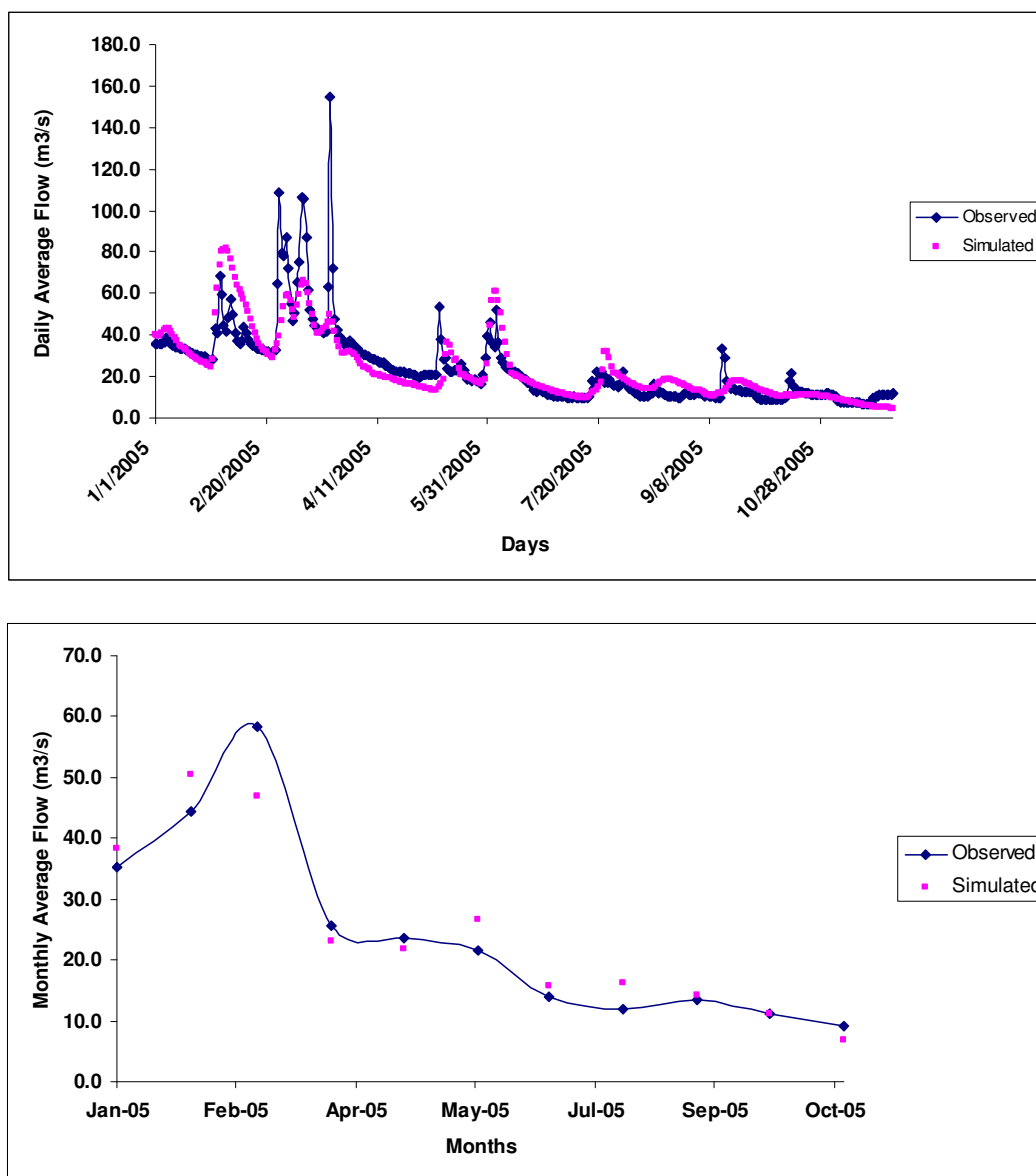


Figure IV-9: From top to bottom: Average observed daily and average simulated daily flow; average observed monthly and average simulated monthly flow for the validation year 2005, at the watershed outlet.

might have contributed significantly to the differences between the simulated stream flow and the observed flow.

The daily simulated flow (2001) was compared with daily observed flow (2001) in wavelet domain (Figure IV-10) and also to 2005 (Figure IV-11). Results suggested that similar frequencies were present in lower scale (1-22 days). Highest frequencies were present in all the scales in both simulated and observed flow at about 250 day. Comparison of daily flow and simulated flow for the year 2005 in wavelet domain revealed similar coloration at all scale. Similar frequencies were observed in lower scale (1-15 days). Detail analysis of coefficients in all the scales present in both observed and simulated signals (flows) will further strengthen the model.

4.5 Conclusion

Earlier study (Paul et al., 2004) have used HSPEXP for calibration, where the model is run several times to get appropriate parameter values. However, in this research the optimal parameters were obtained from the search space, thus reducing the tedious processes of time consuming simulation. The present study is computationally intensive, since GA uses a wide search space. However, this is efficient because it automated the whole calibration process. GA has been successfully implemented in various optimization problems. In the present problem, GA effectively searched the parameter values for hydrologic calibration. The parameter values were well within the values

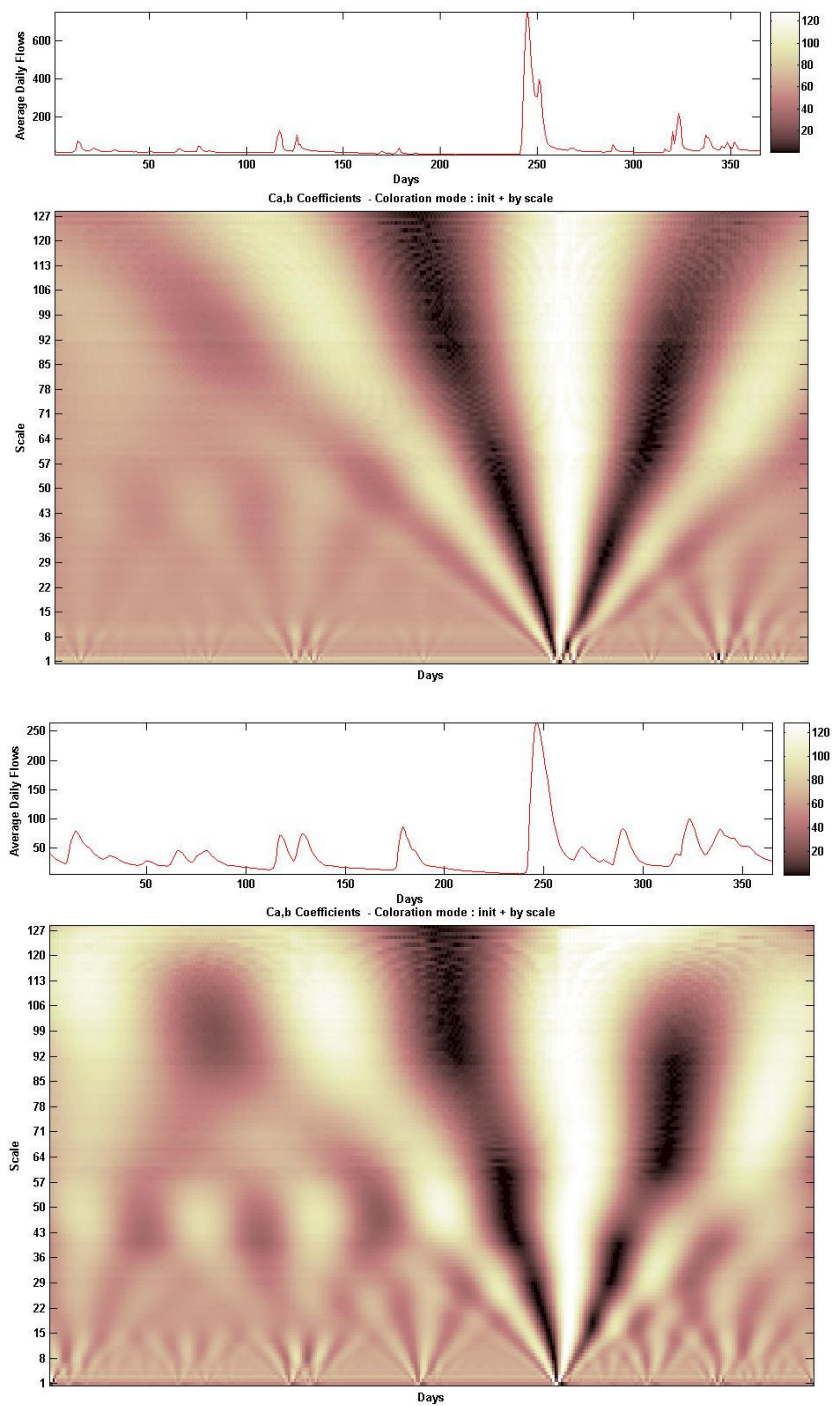


Figure IV-10: From top to bottom: Observed daily flow and simulated daily flow (2001) in wavelet domain.

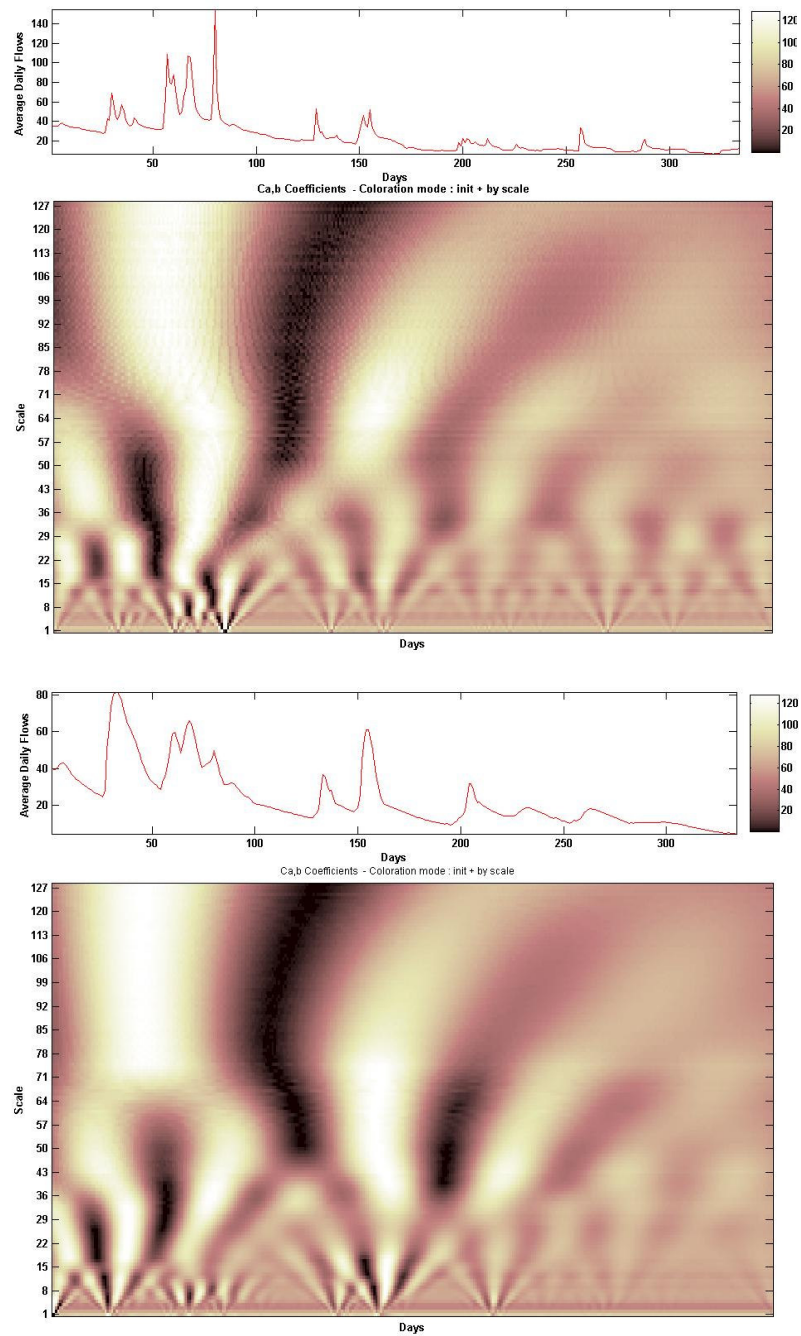


Figure IV-11: From top to bottom: Observed daily flow and simulated daily flow (2005) in wavelet domain.

reported in literature and BASINS TECHNICAL Note 6. GA coupled with HSPF was not able to simulate some of the peak flows. We attributed this, to lack of adequate weather stations in the watershed; for which the entire spatial variability in climatic forcings were not captured. Further, improvement in algorithm is needed to see the efficacy when GA is coupled with HSPEXP.

CHAPTER V
MODELING THE EFFECTS OF LAND COVER/LAND USE CHANGE AND
PRECIPITATION VARIABILITY ON FRESHWATER INFLOWS

5.1 Overview

Adequate environmental flows are needed to maintain the ecological integrity of the estuaries. The environmental flows from a watershed are influenced by changes in land use/land cover, variability in precipitation, and water regulations. San Antonio, TX, the 8th largest city in the US, is likely to affect environmental flows to the San Antonio Bay/Guadalupe Estuary, in the San Antonio River basin. Rapid urbanization has changed the land use and land cover in this river basin. The present study used satellite remote sensing techniques to assess the effect that this change has in the regional hydrology. LANDSAT satellite data for the years 1987, 1994, and 2003 were used in an unsupervised ISODATA classification to quantify changes in land use/land cover. In order to quantify the effect of land use/land cover change on environmental flow (flow volume in the San Antonio river in particular), the model was calibrated using the remotely sensed data from 2003; and then, only land use/land cover data for the year 1999, and 1987 were changed in subsequent simulations. After assessing the impact of LULC change, original weather data such as hourly precipitation and evapotranspiration for the respective year was introduced to the model to assess the impact of precipitation variability on freshwater inflows. Simulation result suggested that increase in impervious

surface altered the hydrograph by increasing the peak flows. Wavelet analysis of the time series suggested that increase in impervious surface (LULC change) altered the location of lower frequencies. LULC change also altered the low flow events in the time series. A significant variation in rainfall amount was observed between 2003 and 1999. Rainfall also influenced the hydrograph by altering the position of the hydrograph. With less rainfall, less water drained to the estuary. The predicted daily time series for flow was then aggregated for monthly flow analysis. Present study will help water resources managers and regulators assess the effect that urbanization potentially has on environmental flows.

5.2 Introduction

Freshwater inflows are the environmental flows that are required for estuarine health and maintenance. Estuaries are the connecting link between terrestrial and marine ecosystems, and provide a critical coastal habitat that is essential ecologically and economically to the world economy (Alongi, 1998; Kennish, 2001). Important species such as finfish and shellfish depend on estuaries for their survival and contribute more than 90% of the total fisheries activity in the Gulf of Mexico (Kennish, 2000). Estuarine and coastal marine fisheries return more than \$23.0 billion annually to the US economy (Kennish, 2000). The State of Texas has approximately 590 km of coastline and in late 1990s, coastal industries contributed \$ 5.4 billion to the Texas economy (Kennish, 2000).

Hydrology is the most critical element of in stream flow studies. It is used to assess hydraulic function, water quality, channel maintenance and riparian forming processes, and physical habitat for target aquatic species. A flow regime encompasses the seasonality and periodicity of flows. Hydrologic/hydraulic technical evaluations have as their aim understanding and quantifying the magnitude, frequency, timing and duration of these flows, the degree to which the natural flow regime has been altered, and impacts of land and water use on the flow regime.

The productivity of estuarine systems depends on the timing and magnitude of freshwater inflow along with the associated nutrients, metals, and organic matter delivered from the terrestrial environment (TWDB, 1994). Freshwater inflows are essential to ecological processes including dilution of salt water creating a unique habitat for several species, regulation of bay water temperature, and marine biogeochemical cycles. Variations in freshwater inflows can alter the ecology of the estuarine environment and potentially hamper productivity. Freshwater inflows are influenced by the land cover/land use (LCLU), climate variability and water management practices in the contributing watershed, particularly in watersheds that are experiencing rapid human induced disturbances.

LCLU change (LCLUC) can alter hydrology at the local, regional, continental and global scales. With increasing urban growth, LCLUC can modify the amount of flow through changes in infiltration, storm flow, evapotranspiration, and groundwater storage

(Bhaduri et al., 2001). Impervious surface is one of the important land cover characteristics in urban area, which is developed by human activity. Impervious surfaces increase the frequency and intensity of downstream water quantity and quality (Legesse et al., 2003; Waylen and Poveda, 2002).

The amount of precipitation also plays a pivotal role in freshwater availability to estuaries. Analysis of environmental flows in several river basins has been studied to relate it to precipitation variability. Increase in discharge in conterminous U.S, suggested that the U.S is getting wetter, but less extreme. (Lins and Slack, 1999; Peterson et al., 2002; Costa et al., 2003; Copeland et al., 1996).

Remotely sensed data from satellite imagery provides a source of reliable data for land use classification and land cover change analysis. It has proven to be one of the most flexible and useful tools in ecological analysis. Increased availability and low-cost satellite imaging technology has made its use most practical for studying large areas. The NASA's LANDSAT (NRC, 1995) program is one of the longest running satellite data acquisition programs in the United States. Several studies have demonstrated the potential of remote sensing methods as a source of information specifically useful for analysis of the urban/suburban environment with focus on land cover/land use, socioeconomic information, and transportation infrastructure (Donnay et al., 2001; White, 1998). The authors used indices such as surface model to quantify the urban environment using remote sensing imageries and GIS technologies. Only a few studies

have focused their remote sensing analysis on application in urban land use change models (Acevedo et al., 1996; Flanagan and Civco, 2001; Brivio et al., 2002). Studies related to urban mapping have used urban impervious surfaces using ground-measured and remotely sensed data to quantify the extent of urbanization. (Donnaay et al., 2001; Smith et al., 2003) Availability of remotely sensed data with high temporal and spatial resolution, has allowed analysis methods to become more objective and suitable for application over large areas using temporally consistent datasets (Tanaka and Sugimura, 2001).

Although, the human impacts and disturbances on the global hydrologic cycle, and the potential consequences of this on climate are still in debate (Sala and Paruelo, 1997), studies suggest that land use can cause atmospheric changes (Stohlgren et al., 1998), streamflow variability (Waylen and Poveda, 2002) and modification in the dynamics of tree populations (Stohlgren et al., 1998). One of the most important land cover type characteristics of urban environments is impervious surface developed through anthropogenic activities. Impenetrable surfaces, such as rooftops, roads, and parking lots, have been identified as key environmental indicators of urban land use, water quality and water quantity. Impervious surfaces also increase the frequency and intensity of downstream runoff and decrease water quality. While there have been studies assessing the effects of climate change and land-use change on streamflow (Legesse et al., 2003), previous studies did not explicitly examine the hydrologic influence of land use conversion due to urbanization and its effect on freshwater inflow.

Previous studies (TWDB, 1998; TPWD, 1998) have determined methods for quantifying coastal freshwater inflows using computer optimization and hydrodynamic modeling as the predictive technique. The modeling quantifies theoretical estimates of minimum and maximum freshwater inflows and maximum fisheries harvest inflow for each estuary on the Texas Gulf Coast. TPWD (1998) made recommendations for the flow requirements for the Guadalupe Estuary which receives flows from both the San Antonio and Guadalupe River Watersheds. The minimum and maximum flows recommended were 1270 and 1590 million m³/year, respectively. Maximum fisheries harvest inflow was estimated to be 1418 million m³/year. Historical flow analysis of freshwater inflows to Texas bays and estuaries (Longley, 1994) suggests that the largest fraction of freshwater inflows to the Guadalupe Estuary comes from gauged portions of the Guadalupe River Basin, approximately 58% of the total freshwater inflows. Gaged portion of the San Antonio River contributed about 23 % (656 million m³/year) of total freshwater inflows. None of the studies separated the contributions of the individual watersheds (San Antonio and Guadalupe River) or modeled the effect of land use change on the environmental flow availability. Past studies also did not assess seasonal flows which may be more important than yearly/monthly flows (Longley, 1994).

Although, the San Antonio River contributes only 20-30 % of freshwater inflows to the Guadalupe Estuary (Longley, 1994), it is hypothesized that urban development will significantly alter the flow (both timing and magnitude) regime by effecting processes such as reservoir operations, return flows, ground water usage, base flow, and peak

flows. Time series analysis of flow in the San Antonio Basin suggested an increasing trend in most of the variables in the lower portion of the basin; however flows in the upper portion of the basin experienced a decreasing trend. Remotely sensed data coupled with a hydrologic model can be used to assess the impact of LULC on freshwater inflows. Hydrologic Simulation Program in FORTRAN (HSPF) is one of the watershed scale hydrologic models that are used extensively by researchers and water resources professionals in modeling watershed processes (Im et al., 2004; Wicklein and Schiffer, 2002; Brun and Band, 2000) and investigating water resources problems. HSPF was used to simulate hydrology and water quality impacts in a small urbanizing watershed (Im et al., 2004); results suggested runoff volume and peak rate increased with increase in urban area. HSPF has also been used to examine relationships between stormflow and baseflow as a function of percentage of impervious cover (Brun and Band, 2000).

The **primary purpose** of this study is to quantify the regional hydrologic budget response to change in LULC in the San Antonio River Watershed.

5.3 Methodology

LULC and precipitation effects on freshwater inflows were assessed using land cover land use classifications derived from satellite imagery coupled with a watershed scale hydrologic model. Steps in the analysis were:

1. Land use classifications were derived from LANDSAT satellite images using a ISODATA classification approach for three time periods, 1987, 1999, and 2003.
2. An HSPF model of the San Antonio River Watershed was calibrated using a genetic algorithm approach from 2002 to 2004 and validated against observations from 2001 and 2005. (see chapter IV).
3. Land use classifications from 1987 and 1999 were used to simulate hydrology using the calibrated model from step two for the period 2003.
4. Model simulated average daily flow was aggregated to estimate average monthly flow. Statistical analysis (t test) was conducted on the average monthly flows for the simulation years 1987, 1999, and 2003, to assess if the flows are statistically different.
5. Behavior of streamflow in the frequency domain was assessed using a Morlet Wavelet technique.
6. The effect of precipitation variability on water quantity was assessed by varying weather data while holding landuse constant in the HSPF model.

5.3.1 Study Area

The San Antonio River Basin encompasses 10,826 km² from the headwaters of the Medina River to the point at which the San Antonio River joins with the Guadalupe River before emptying into the Gulf of Mexico (Figure V-1). The San Antonio River begins just below Olmos Dam and runs 406 river km through four counties: Bexar,

Wilson, Karnes, and Goliad Counties. To the northwest of the city, the terrain slopes to the Edwards Plateau and to the southeast it slopes downward to the Gulf Coastal Plains. Soils are blackland clay and silty loam on the Plains and thin limestone soils on the Edwards Plateau. Population in this river basin has increased in the last 30 years primarily due to the growth of the City of San Antonio. It is predicted that the population around the city of San Antonio by 2020 will be approximately 2,172,950 (Texas State Data Center 2005; Nivin and Perez, 2006).

5.3.2 Land Cover Land Use Assessment

LANDSAT series data (5 TM and 7 ETM) were used for land cover and land use assessment. Images were obtained either from the USGS LANDSAT Image Distribution Center or from www.texasview.org, a remote sensing consortium for the State of Texas. Four paths and three rows combined to form four path/row combinations: 2640, 2739, 2740, and 2839 to cover the entire watershed area. Images were obtained for 3 years; 1987, 1999, and 2003 (Table V-1). Images from these years were selected based on data availability, adequate temporal spacing to detect significant change between time periods and cost vs. utility of images. Other factors considered while selecting images included relatively cloud free images to avoid misclassification; images from the latter part of the acquisition year to have proper picture of the entire watershed. Two images were acquired from 1985 and 1986 because of the difficulty of

obtaining cloud free images in 1987. This should not affect the results because the images covered relatively small portions of the watershed.

Environment for Visualizing Images 4.3 (ENVI 4.3) was used to process the images. Images were projected in UTM zone 14 projection systems. A resampling technique, the nearest neighbor method (Jensen, 2005; Duda et al., 2001) was used to correct the image and project it with 30 m spatial resolution where needed. To assess the accuracy of the resampled file a 2003 geo-referenced Texas Department of Transportation (TXDOT) file was used.

An ISODATA unsupervised classification technique was used to classify the images. Approximately 20 different classes were initially used for classification (Jensen, 2005) for each image, with a maximum number of iterations set at 20, and a 5% threshold change. Processing took approximately 30 minutes per image. After 20 different classes were obtained, the pixels were reclassified into 4 different classes: water, forest, pasture/rangeland/urban pervious, and urban impervious/bare. Classifications were based on the similar hydrologic responses (i.e. similar infiltration capacity) of the land use classes. In addition, these categories usually have similar spectral signatures. Digital Orthophoto Quarter Quadrangle (DOQQs) were used to assign the value to the pixel of the processed imageries. DOQQs were obtained from Texas Natural Resources Information System (TNRIS).

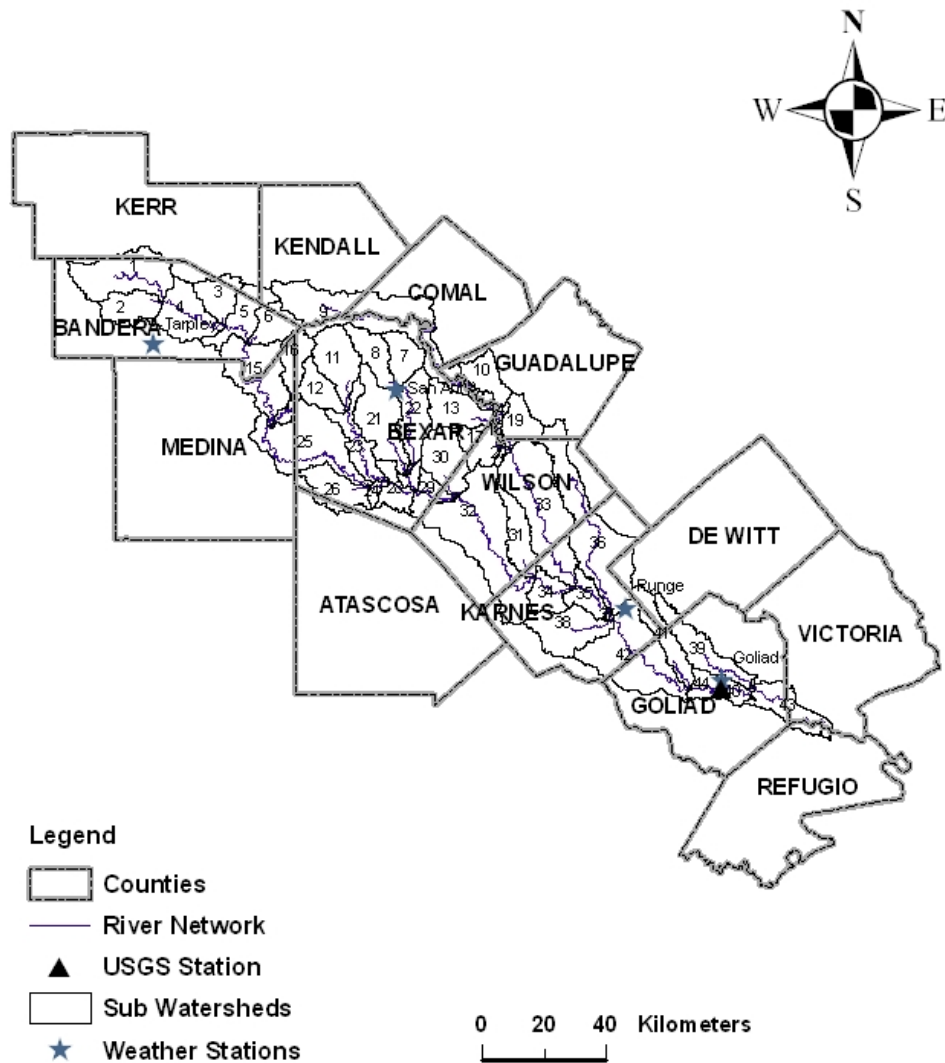


Figure V-1: San Antonio River watershed indicating USGS gauging station and NCDC weather stations used in the analysis.

Table V-1: LANDSAT series images used for the LULC change analysis in the San Antonio River Watershed.

Year	Path/Row	Acquisition Date	Satellite
1987	2640	10-17-1986	Landsat 5 TM
	2739	09-25-1987	
	2740	09-25-1987	
	2839	09-26-1986	
1999	2640	10-05-1999	Landsat 7 ETM
	2739	10-20-1999	
	2740	10-20-1999	
	2839	12-14-1999	
2003	2640	11-15-2003	Landsat 7 ETM
	2739	11-04-2003	
	2740	11-15-2003	
	2839	11-15-2003	

Accuracy assessment is an important step in image processing, providing essential information about how closely image classification matches the true land classes. DOQQs, and transportation network data were used for this purpose. About 100 different points were selected from the processed images for the respective classes. Accuracy assessment in ENVI was conducted by getting the confusion matrix (Jensen, 2005). Overall accuracy was approximately 80%, which was acceptable (Jensen, 2005).

The processed image was imported to an ARCVIEW GIS environment. The percentage of the area contributed by each land cover type, forest, for example, was estimated by multiplying the pixel size (30m x 30m) by the number of pixels assigned to that particular land cover classification and dividing it by the total watershed area. LULC change from one time period to another was then estimated from changes in these

percentages. Extent of urbanization in each county was assessed by overlying county layer on LULC layer using ArcGIS.

5.3.3 Model Description

HSPF is a continuous, lumped parameter hydrologic model (USEPA, 2001). This model can be used to simulate a wide range of hydrologic and water quality processes that occur in a watershed, including sediment transport and movement of contaminants. In HSPF, modules are divided into pervious land (PERLND), impervious land (IMPLND), and reaches (RCHRES). Each land segment is considered as a lumped catchment. However, it can mimic spatial variability by dividing the river basin into many hydrologically homogeneous land segments. It simulates runoff from each land segment independently, using different assigned meteorological input data and watershed parameters. Simulation in this software is based on an hourly time step. The simulation in HSPF is based on mass balance approach (Paul et al., 2004). In the IMPLND module, precipitation is partitioned as overland flow, evaporation, or surface detention storage. In the PERLND module, precipitation is divided into direct runoff, direct evaporation, surface storage followed by evaporation, surface storage followed by interflow, and infiltration to the subsurface area. The model divides the subsurface compartment into upper zone, lower zone and deep groundwater zone. Any amount of water that is received by subsurface zone is either stored, evaporates or flows to the subsequent lower zone. Water in groundwater zone is assumed to be lost from the system.

Since HSPF considers only two classifications, PERLND and IMPLND, the LULC classifications were lumped to PERLND and IMPLND values. Impervious and bare surface values derived from LANDSAT information were assigned to IMPLND; forest and rangeland were assigned to PERLND. This information was derived for each of the years 1987, 1999, and 2003.

The necessary meteorological data to run HSPF is stored in a watershed data management (WDM) file. For this study HSPF needed hourly precipitation and hourly potential evapotranspiration. These two weather variables control water quantity. A WDMUtil program was used to import the data in the required format, using several available scripts.

5.3.4 Data Description

The San Antonio River watershed is located within the Hydrologic Cataloging Boundaries (HUC) 12100301, 12100302, 12100303, and 12100304. Data layers including STATSGO soils data, Reach Network Version 3, and the Digital Elevation Model (DEM) for HUC 12100301 were obtained from EPA's BASINS web site (USEPA, 2003). Reach Network file Version 3 is a comprehensive set of digital spatial data that contains information about surface water features such as lakes, ponds, streams, rivers, and wells.

The San Antonio River Watershed was subdivided into 44 hydrologically connected sub-watersheds using the DEMs and the Automatic Watershed Delineation tool available with BASINS 3.0. Four weather stations, NCDC COOPID 418845, 417945, 417836, and 413618, were used to obtain weather data for HSPF simulations. Weather stations were selected on the basis of availability of long term hourly data (hourly precipitation and daily evapotranspiration). Available data was downloaded from NCDC website. A Thiessen polygon method was used using ArcInfo to determine the representative weather station for each sub-basin. Daily evapotranspiration was disaggregated into hourly evapotranspiration using the WDMUtil tool. Precipitation data and modeled evapotranspiration values for the year 1999 and 2003 were analyzed to assess variability. Pair wise comparison (student t-test) between the years was conducted on this purpose.

Historical daily mean stream flow data for USGS gauge station 08188500 was obtained from the USGS for the simulation period. This station is located at the outlet of the San Antonio River Watershed, the point at which the HSPF model was calibrated and validated.

5.3.5 Calibration and Validation

Hydrologic calibration in HSPF was conducted using a genetic algorithm (GA) approach as described in Chapter IV. Three years, 2002, 2003, and 2004, of daily average stream flow data from USGS gauging station 08188500 were used for calibration. The 2003

land use dataset was used for calibration. Model validation was conducted using 2001 and 2005 stream flow data. Mean Absolute Error (MAE), and Nash-Sutcliffe coefficient was used for model calibration and validation (See chapter IV).

5.3.6 Scenario Analysis

In order to quantify what percentage of flow is affected by LULC change and what percentage of flow is affected by rainfall variability, 10 different scenarios were conducted (Table V-2). Variations in freshwater inflows were estimated by:

$$LULC\ Change = \frac{Q_a - Q_b}{Q_a} \quad (17)$$

Where Q_a is the flow obtained from base scenario (Table V-2) and Q_b is the flow obtained from final scenario. For example, to assess the variability of flow due to LULC change, in the first simulation (Table V-2), base scenario was flow obtained by using LULC of 2003 and rainfall of 2003; and final scenario used was LULC of 1999 and rainfall of 2003. The results were obtained in percentage by multiplying 100. Similar equation (equation 2) was also used to estimate flow variability due to rainfall variation.

$$Pr\ ecipitation\ Varibility = \frac{Q_a - Q_b}{Q_a} \quad (18)$$

5.4 Results and Discussion

Analysis of land use land cover from LANDSAT series imageries suggested an increase in urban impervious/bare surface in the watershed from 1987 to 2003 (Figure V-2, Figure V-3, and Figure V-4). The increase in impervious surface has a direct relationship with urbanization (Dow and Dewalle, 2000). Increase in impervious surface was clearly marked in Bexar County. This County has been experiencing heavy urbanization. The percentage of impervious surface in the whole watershed went from 6% in 1987 to 14% in 2003 (Figure V-2, Figure V-3, Figure V-4, and Figure V-5); and, in Bexar County the percentage increased from approximately 9% to 21 % (Figure V-5). The increase in urban growth was partially matched by a decrease in forested area over several years. Forested area decreased from approximately 3548 square kms in 1987 to about 2525 square kms in 2003 over the entire San Antonio River watershed. In Bexar County forested area decreased from approximately 1010 square kms in 1987 to 700 square kms in 2003 (Figure V-5). GIS analysis suggested urban growth has occurred in the counties adjacent to Bexar County as well. Comal, Guadalupe, and Medina counties have experienced rapid urban growth due to the expansion of the City of San Antonio. Part of Comal, Guadalupe, and Medina is covered by San Antonio River Watershed. Partly change in these counties might be affecting freshwater inflows to the estuary.

Table V- 2: Scenarios used for various simulation to separate precipitation variability from LULC change effect on freshwater inflows.

Scenarios	LULC change effect	
1	2003 LULC	2003 Rainfall
2	1999 LULC	2003 Rainfall
3	1987 LULC	2003 Rainfall
4	2003 LULC	1999 Rainfall
5	1999 LULC	1999 Rainfall
6	1987 LULC	1999 Rainfall
Precipitation variation effect		
7	2003 LULC	2003 Rainfall
8	2003 LULC	1999 Rainfall
9	1999 LULC	1999 Rainfall
10	1999 LULC	2003 Rainfall

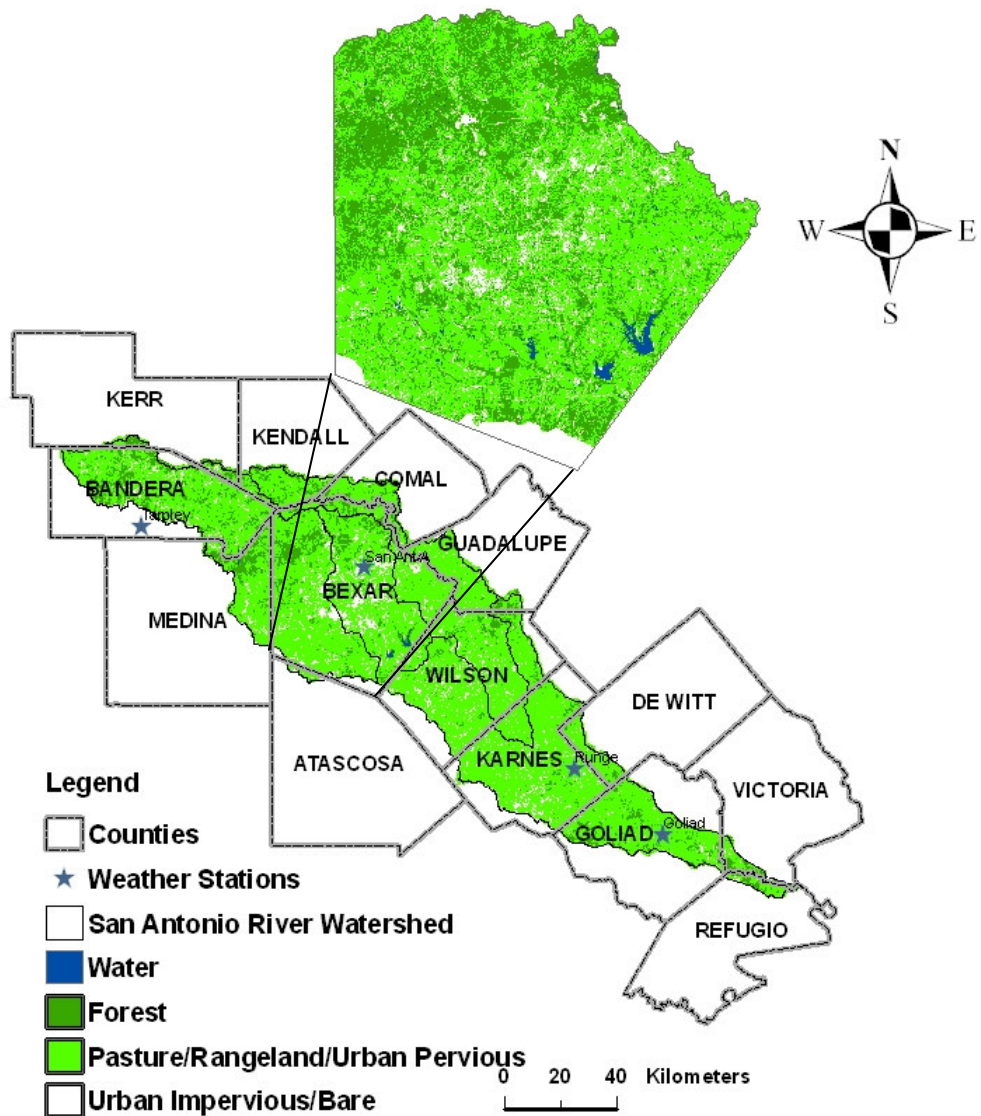


Figure V-2: San Antonio River watershed with 1987 land use land cover dataset, focusing Bexar County.

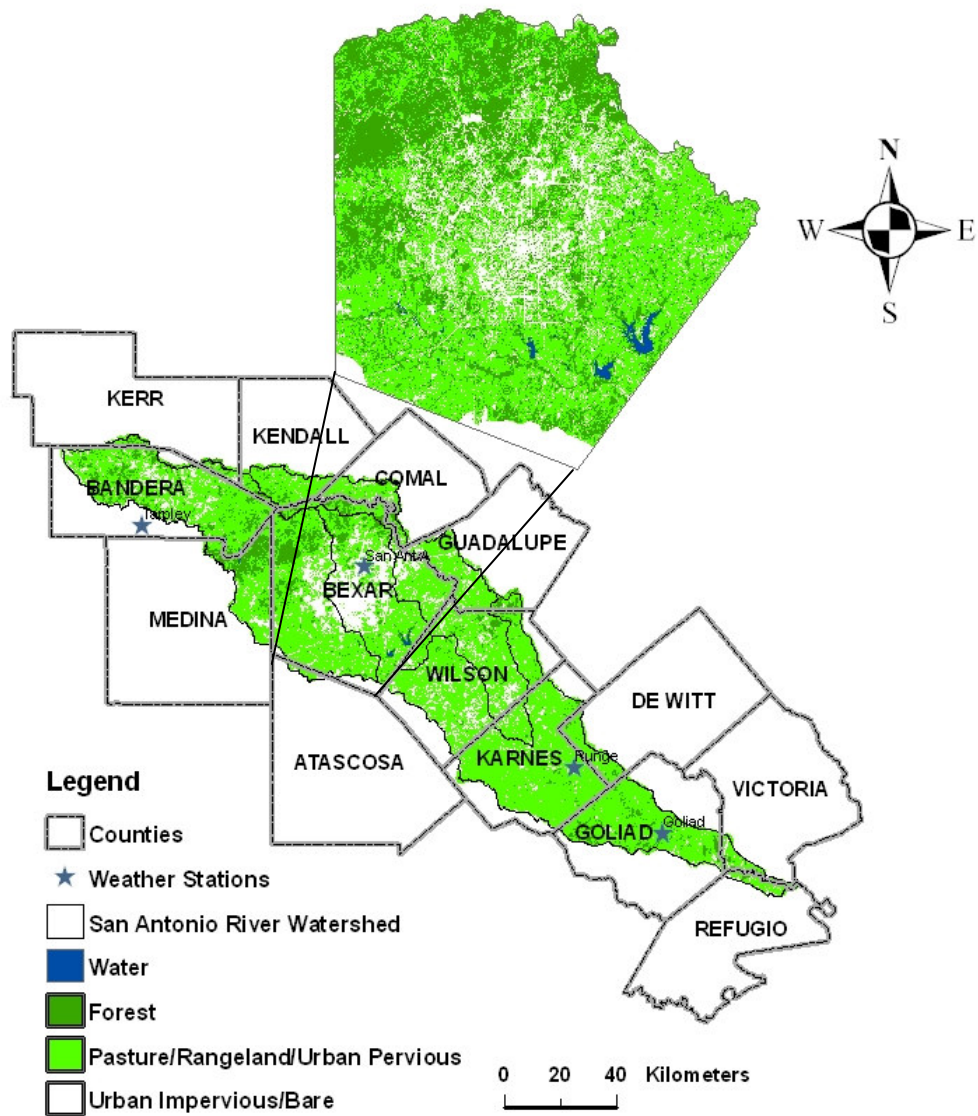


Figure V-3: San Antonio River watershed with 1999 land use land cover dataset, focusing Bexar County.

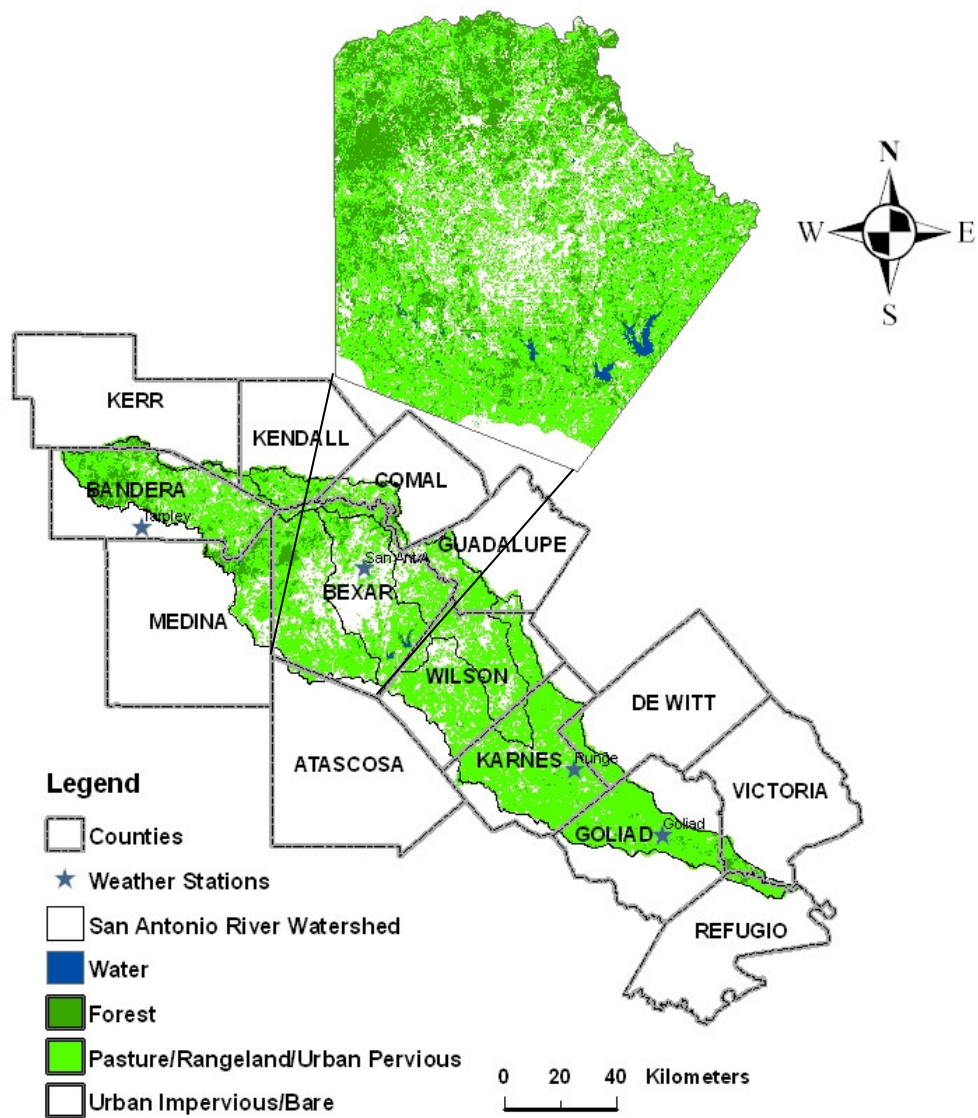


Figure V-4: San Antonio River watershed with 2003 land use land cover dataset, focusing Bexar County.

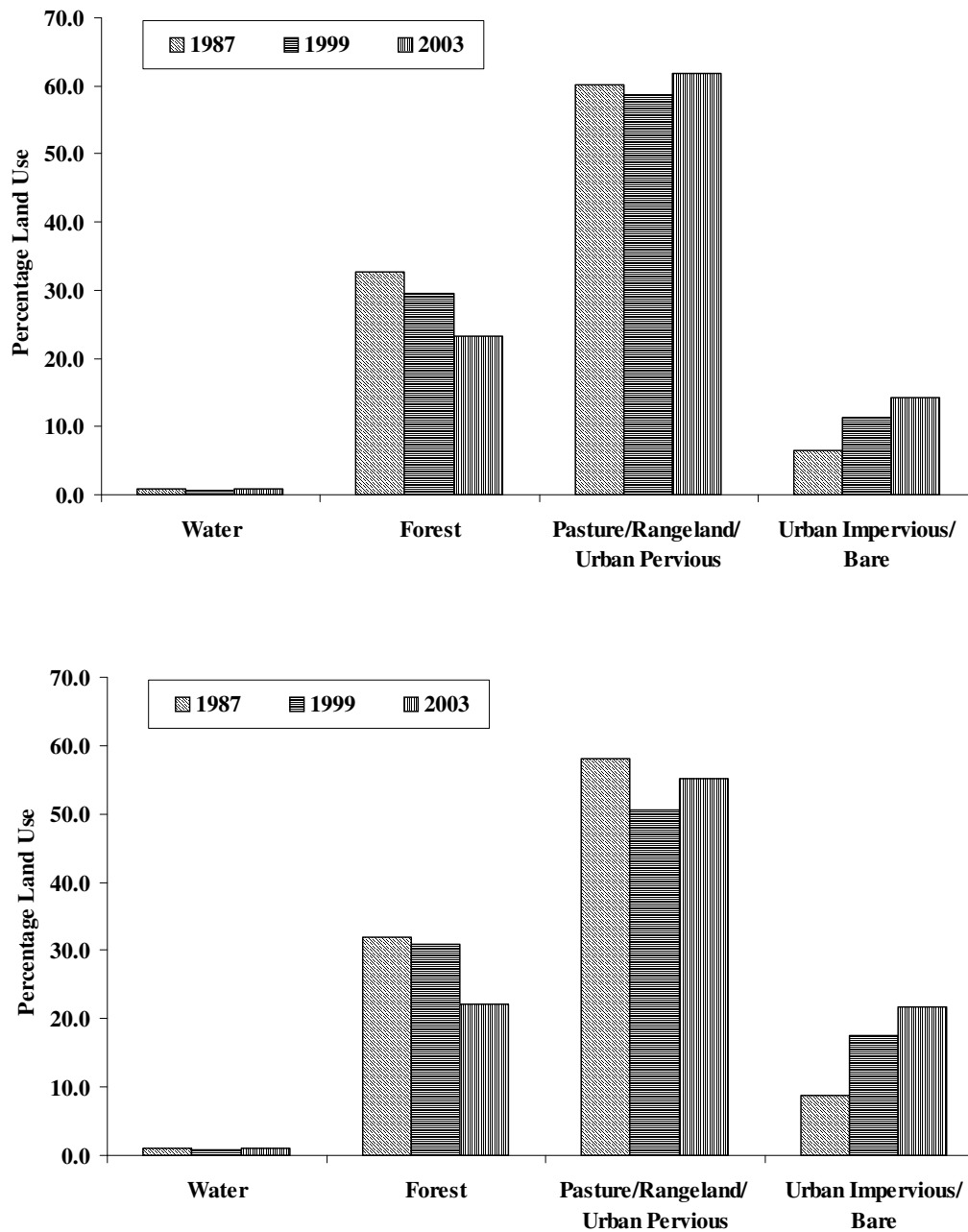


Figure V-5: Percentage change in land use from 1987 to 2003, in watershed scale (top), and in Bexar County (bottom), obtained from remote sensing and GIS analysis.

Analysis of hydro-climatic variables such as precipitation for the period 1999 and 2003 (Figure V-6) suggested a significant difference ($p < 0.1$) in daily rainfall between the two years. The watershed experienced about 482 mm of rainfall in 1999, where as it experienced about 686 mm of rainfall in 2003. In both the years May through September experienced more than two-thirds of total annual rainfall. Significant variation in rainfall was not observed within weather stations. Earlier studies have suggested rainfall to be similar in a regional or watershed scale (Bloschl et al., 2007). Similarly, statistical analysis of potential evapotranspiration suggested significant difference ($p < 0.1$) between 1999 and 2003 (Figure V-7). The watershed experienced about 1092 mm of potential evapotranspiration in 1999 and about 991 inches in 2003. Like rainfall May through September experienced more than two-thirds of total potential evapotranspiration.

Model simulation results indicated an increase in peak flows from 1987 to 1999 to 2003 (Figure V-8). Increase in peak flows could be attributed to increase in impervious surfaces, and decrease in forest (Figure V-5). Increase in impervious surface reduces infiltration, and there by increases runoff (Cheng and Wang, 2002), and alters overall water balance. Most of the studies (Bloschl et al., 2007; Im et al., 2004) suggested land use land cover change affects in local scale. However, our investigation suggested LULC might have an affect in basin scale, particularly in San Antonio River Basin. This river basin is experiencing LULC change, where urbanization is the most dominant LULC type change.

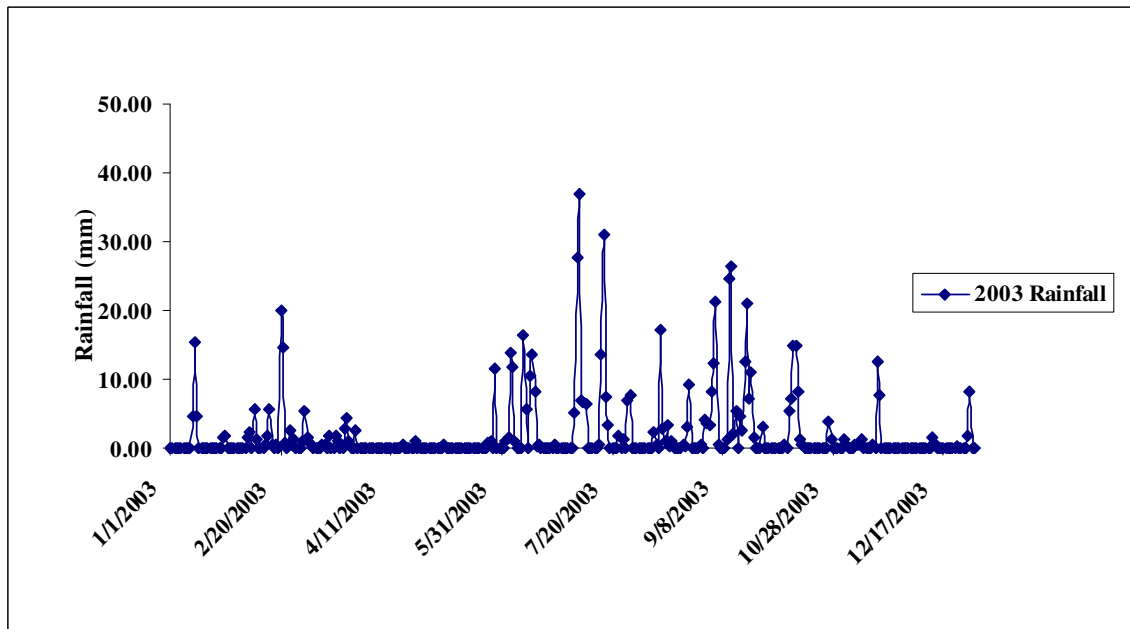
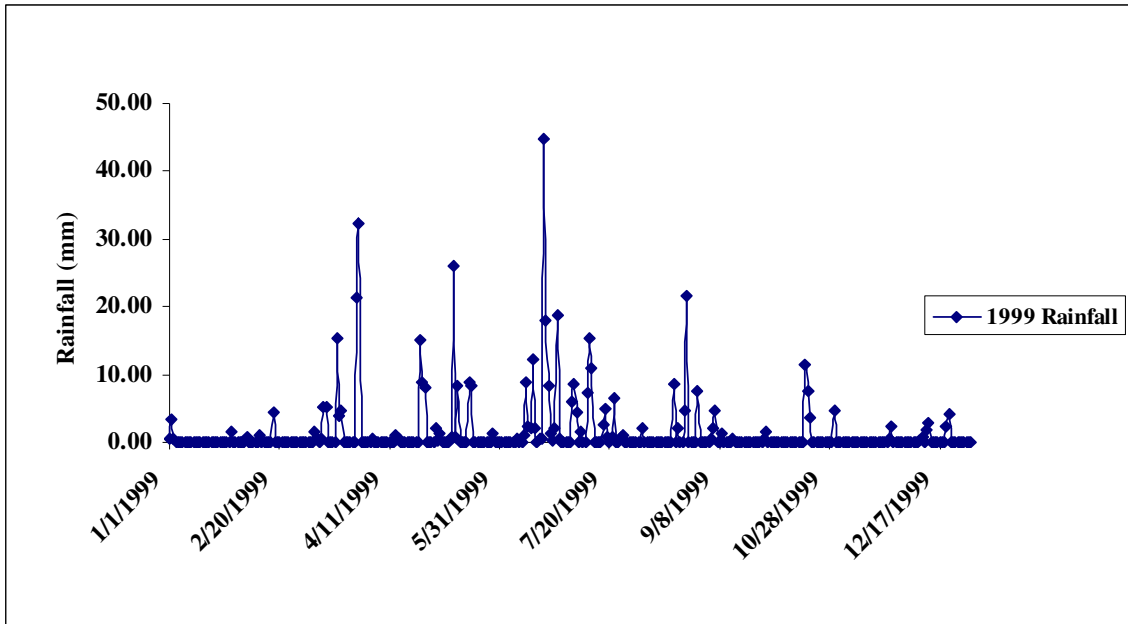


Figure V-6: Daily total rainfall for the watershed, estimated by thiesen polygon method for the year 1999, and 2003.

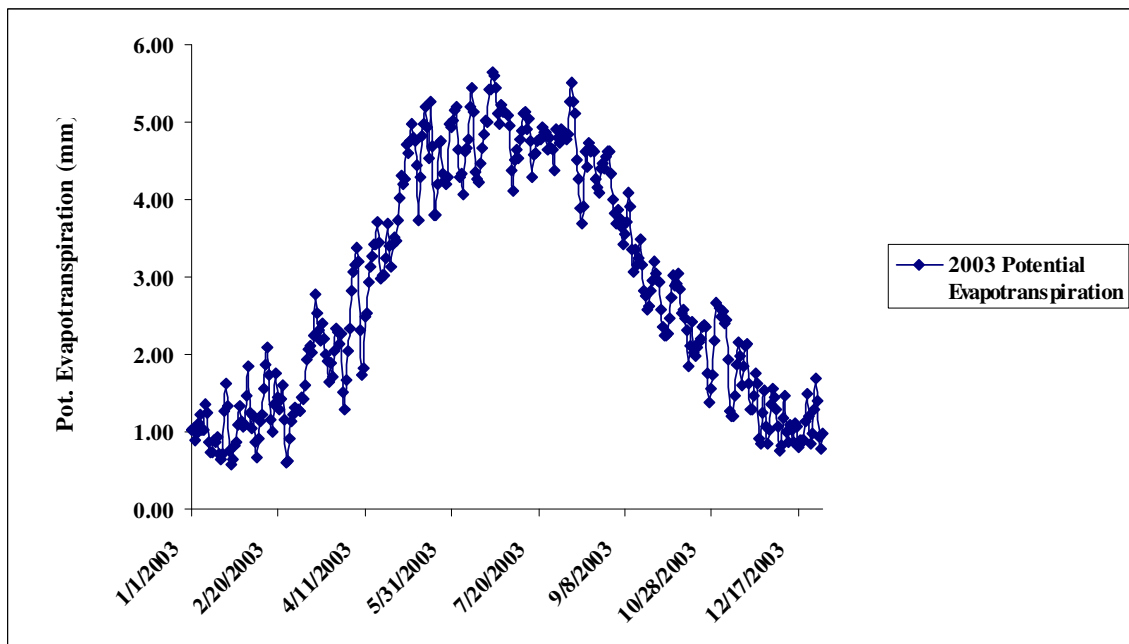
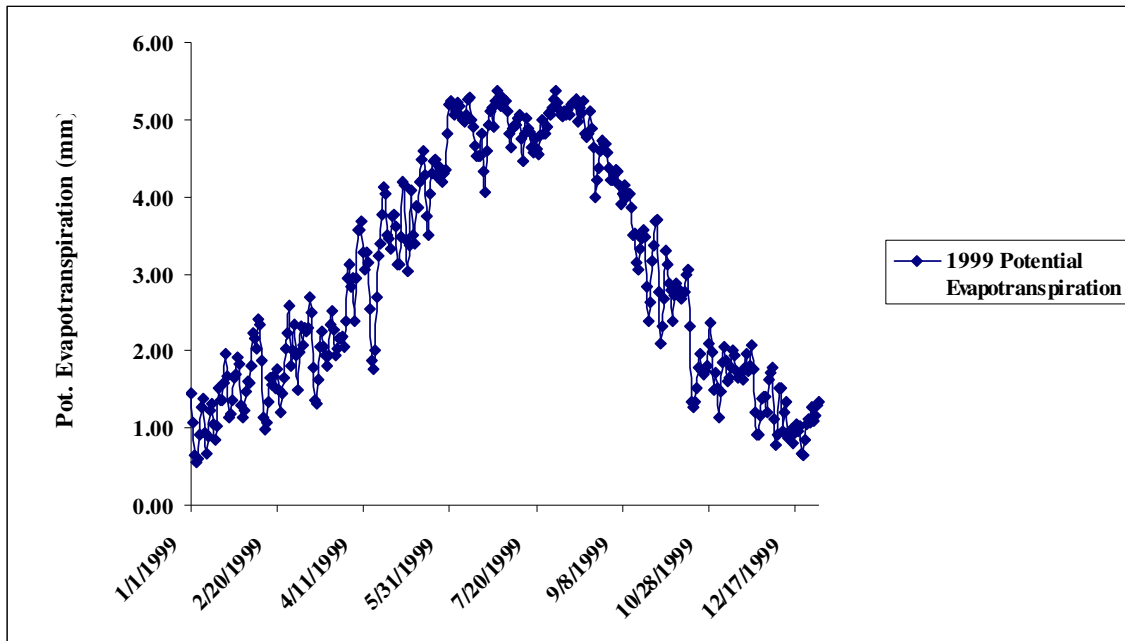


Figure V-7: Estimated daily total potential evapotranspiration for the watershed for the year 1999, and 2003.

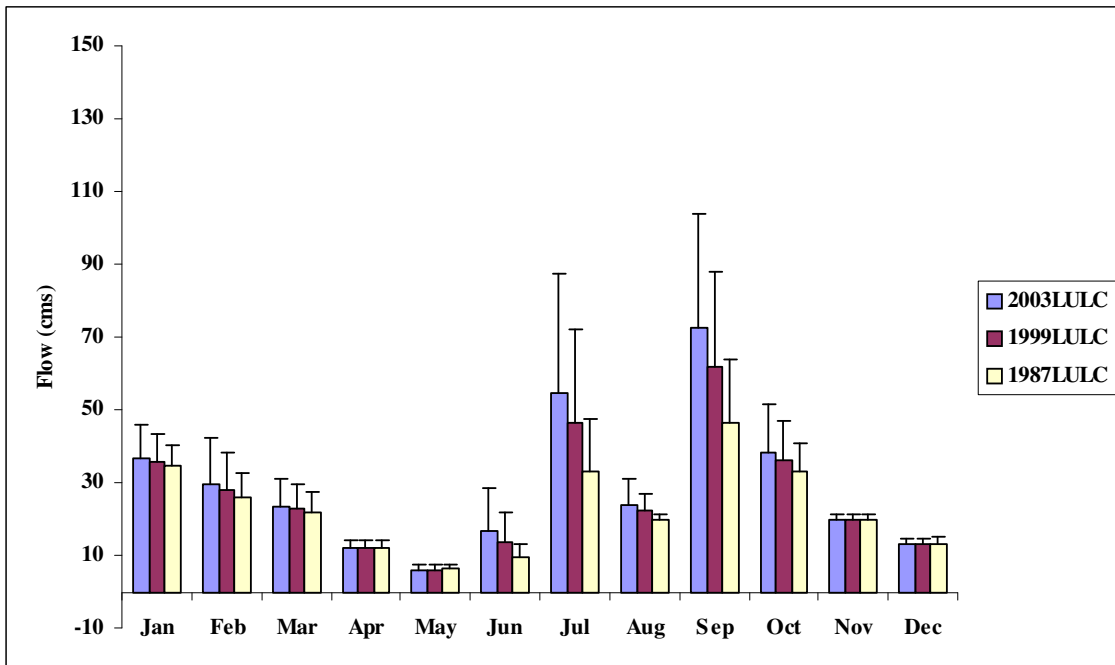
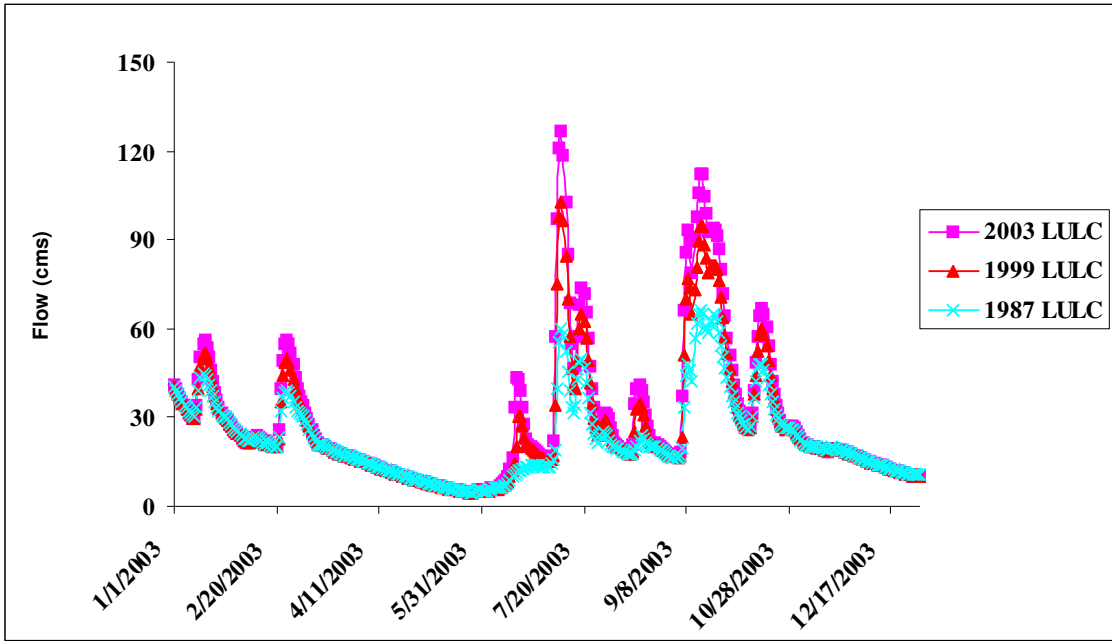


Figure V-8: Average daily flow (top) and average monthly flow (below) after changing the land use for 1999, and 1987.

Average monthly flow was calculated from the simulations for the years 1987, 1999, and 2003. Statistical analysis was conducted on the estimated monthly flows between each year. Results implied, average monthly flow increased significantly ($p < 0.1$) in most of the months from 1987 to 1999 to 2003. Significant difference was not marked for some of the months such as April, and November, while comparing average monthly flows for the years 2003 and 1999. Similarly, significant difference was not observed for the month of November, while comparing average monthly flows for the years 2003, and 1987. Flows in months such as May and December (Figure V-8) were also compared for the simulation period. These months were selected because they experienced less flow based on simulation results (Figure V-8). Investigation results suggested a statistical difference between May and December flows. Average monthly flows in May decreased from 6.28 cms in 1987 to 6.17 cms in 1999, further to 6.11 cms in 2003 (Figure V-8). Similarly, average monthly flows in December decreased from 13.13 cms in 1987 to 12.99 in 1999, further to 12.96 cms in 2003. Decrease in low flows over the simulation years (1987, 1999, and 2003) could be attributed to increase in impervious surfaces. Low flows reflect base flow. Increase in impervious surface reduces infiltration; thereby, influencing baseflow.

Morlet wavelet was used for wavelet analysis of the time series generated from LULC change for the year 1987, 1999, and 2003 (Figure V-9). Wavelet analysis is conducted to assess changes in frequency and scale of the flows. Analysis suggested, land use land cover alters the frequencies and location of the frequencies. Lower frequencies present in

1987 simulation in 2 to 32 days scale between 100-250 days has been somewhat replaced by higher frequencies in 1999, and 2003 simulations. This suggested the system was behaving flashier with increase in impervious surface over the years; meaning, there is increase in peak and dip flows. Also, analysis showed changes in lower frequencies in 64 days period. Lower frequencies at this period were observed in 1999 and 2003 simulations, suggesting more storage of water in the system in 1987 than other two years. This means, for same amount of rainfall in all the three years, rapid peaks and recession were observed in 1999 and 2003 than 1987.

Once the effect of LULC change was quantified by changing just the actual LULC datasets of 1999 and 1987 in 2003 model simulation, actual weather data sets of 1999 were introduced in the 1999 LULC scenario. The simulation resulted in quantifying variations in freshwater inflows that is due to precipitation variability. Simulation results (Table V-2) were compared, in order to estimate the percentage of variations in freshwater inflows, which could either be attributed to LULC change or precipitation variability. Variations in freshwater inflows due to LULC change was estimated by Figure V-10, and Figure V-11.

Approximately 8% of the environmental flow was attributed to LULC change, when scenario 1 and scenario 2 was taken into consideration (Figure V-10). About 12 % of the environmental flow was attributed to LULC change, when the scenario 2 and scenario 3

was taken into consideration (Figure V-10). The peak flows shifted from lower magnitudes in 1987 LULC to higher magnitudes in 2003 LULC (Figure V-10).

In all the cases rainfall was same, which means increase in peak flows could possibly be attributed to increase in impervious surface over the years (Figure V-5). Similarly, scenarios 4, 5, and 6 (Table V-2) were also considered to assess only the importance of LULC change on environmental flows (Figure V-11). Approximately 8% of the environmental flow was attributed to LULC change, when scenario 4 and scenario 5 was taken into consideration; and about 12% of the environmental flow was attributed to LULC change, when the scenarios 5 and 6 were taken into consideration.

Scenarios 7, 8 and 9, 10 (Figure V-12 and Figure V-13) were used to assess the importance of climate variability on environmental flows to estuary. Equation similar to equation 2 was used to assess this variability. Analysis of scenario 7 and scenario 8 suggested a variation of 36% in freshwater inflows due to precipitation pattern change; where as scenarios 9 and 10 suggested a variation of 63% in freshwater inflows that possibly could be attributed to precipitation variability. Visual interpretation of flow data (Figure V-12 and Figure V-13) for the LULC 2003 and 1999 suggested shift in flow pattern. This shift is due to variation in rainfall. The present study was limited by the unavailability and unsuitability of weather data for the year 1987.

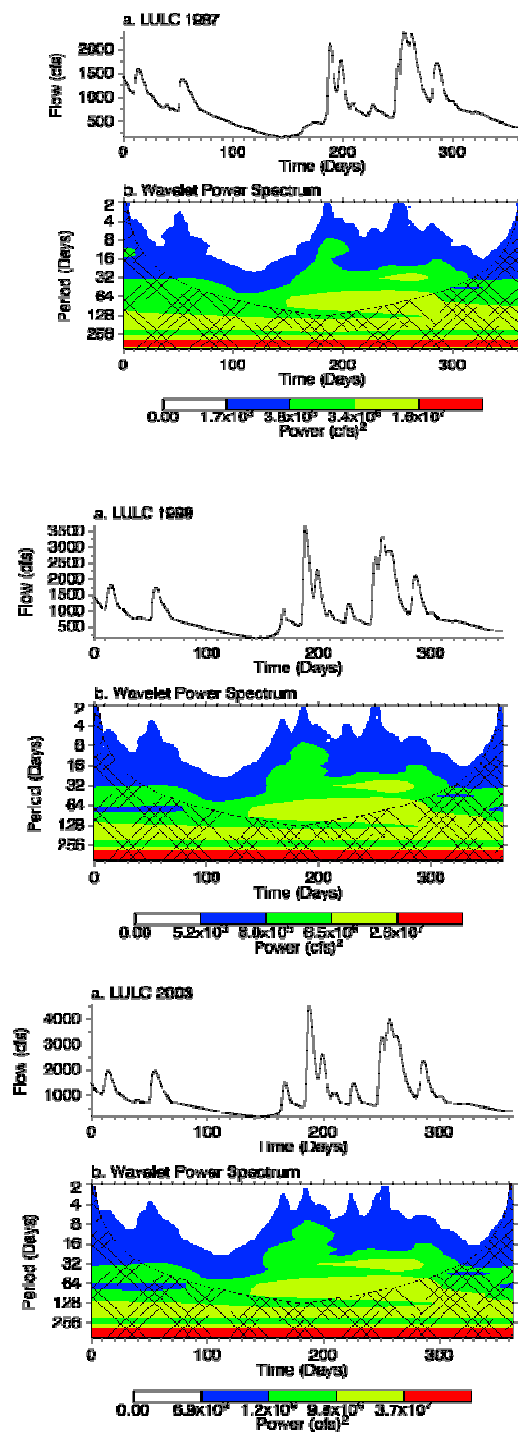


Figure V-9: Morlet wavelet analysis for various land use change; (from top to bottom) simulations results for LULC 1987, 1999, and 2003.

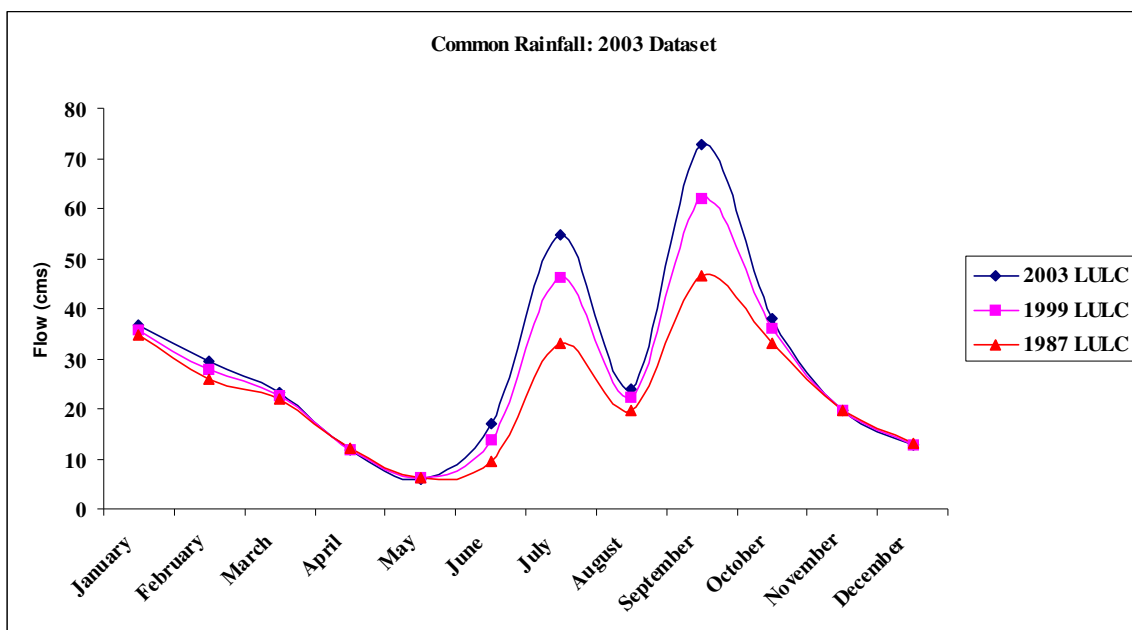
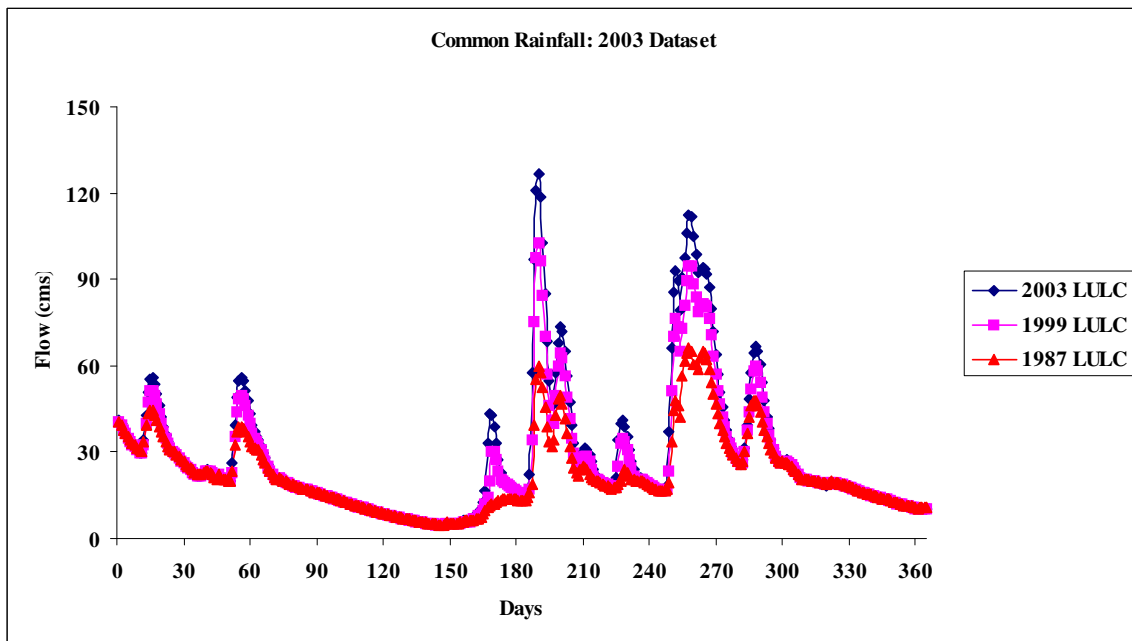


Figure V-10: Simulation results with a common 2003 rainfall dataset and respective LULC datasets of the years. Average daily flow (top) and average monthly flow (bottom) for both the years.

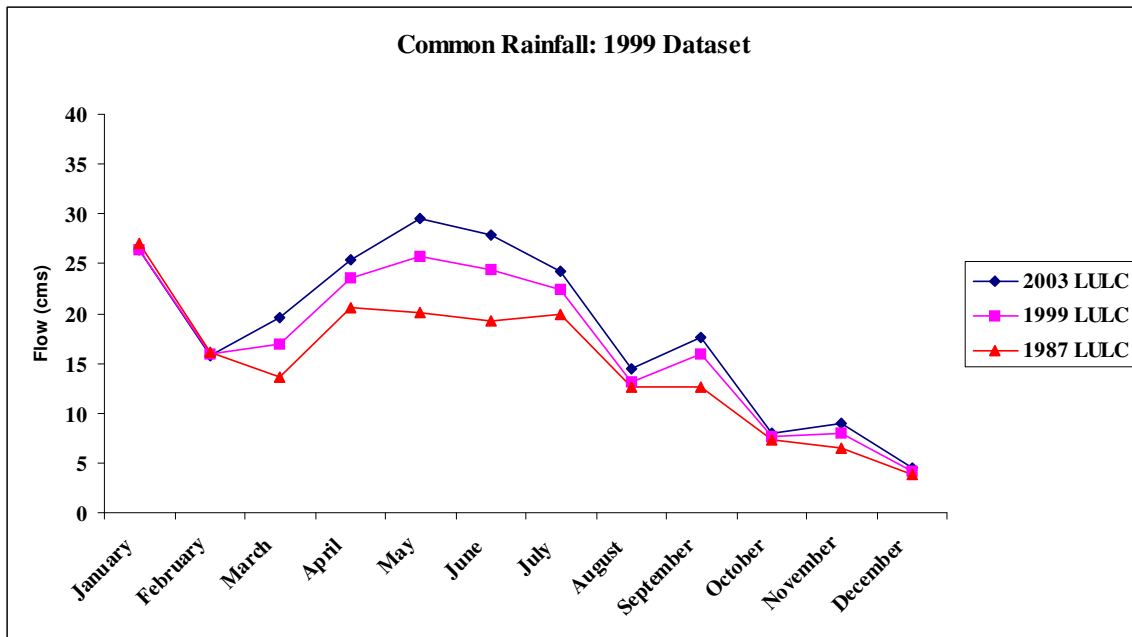
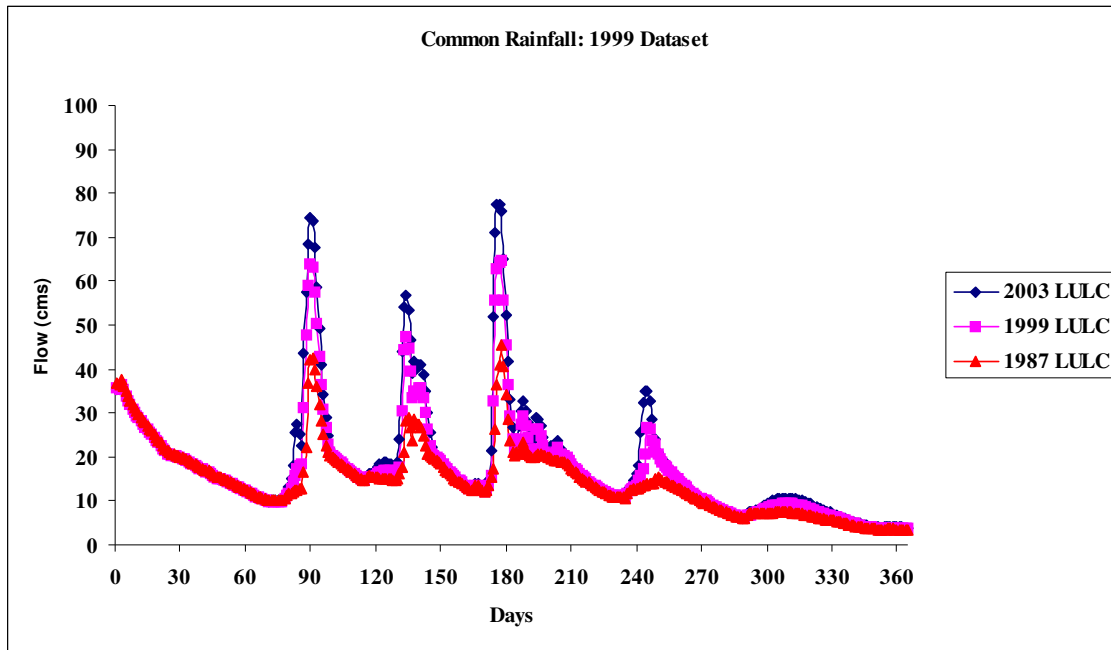


Figure V-11: Simulation results with a common 1999 rainfall dataset and respective LULC datasets of the years. Average daily flow (top) and average monthly flow (bottom) for both the years.

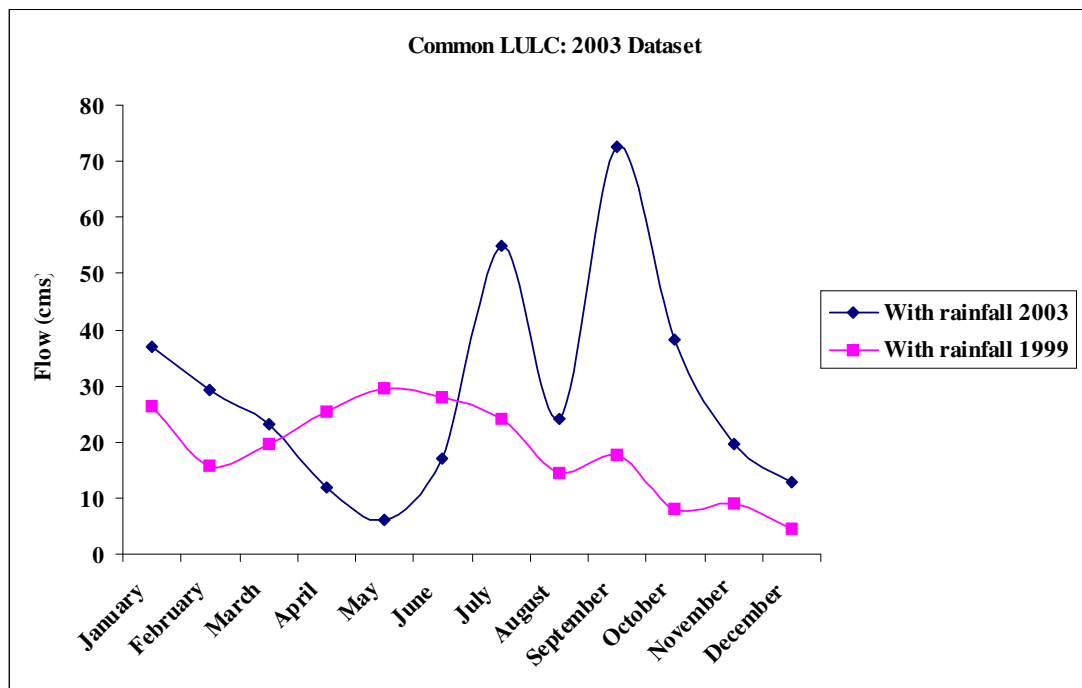
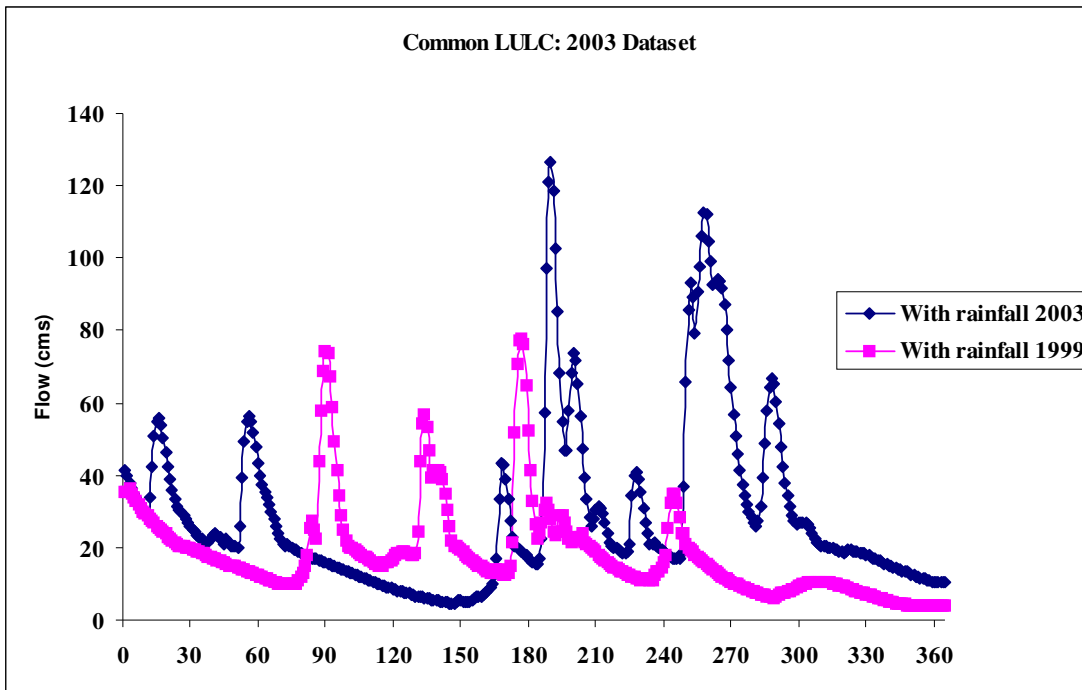


Figure V-12: Simulation results with a common 2003 LULC dataset and original hydroclimatic data for the year 1999 and 2003. Average daily flow (top) and average monthly flow (bottom) for both the years.

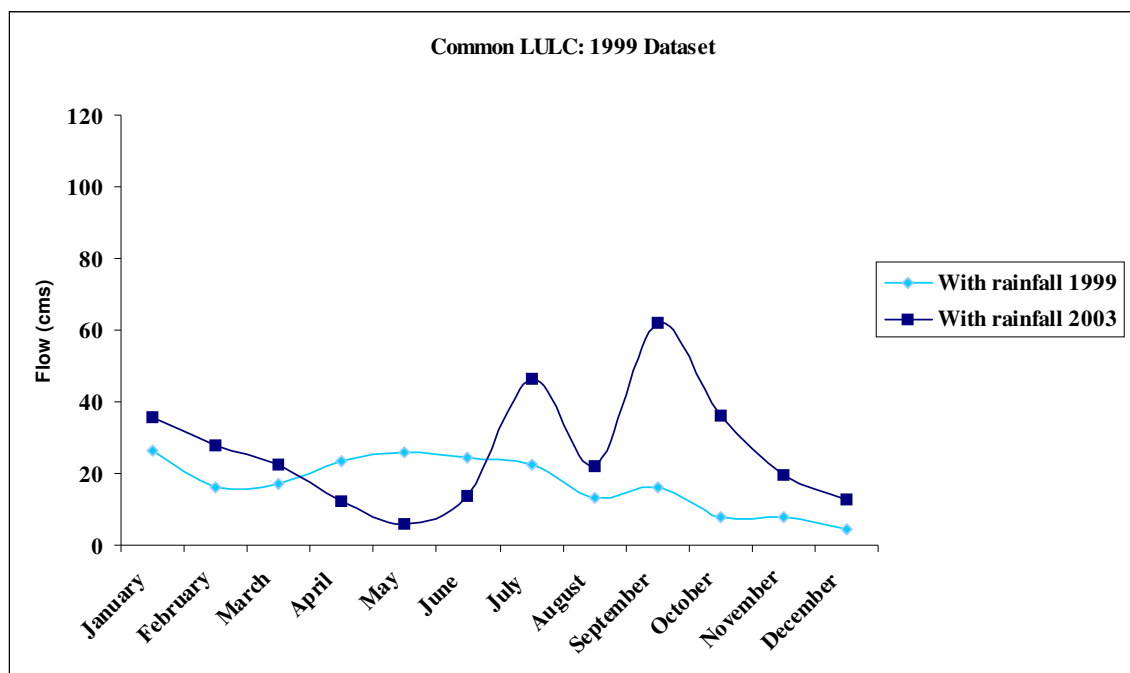
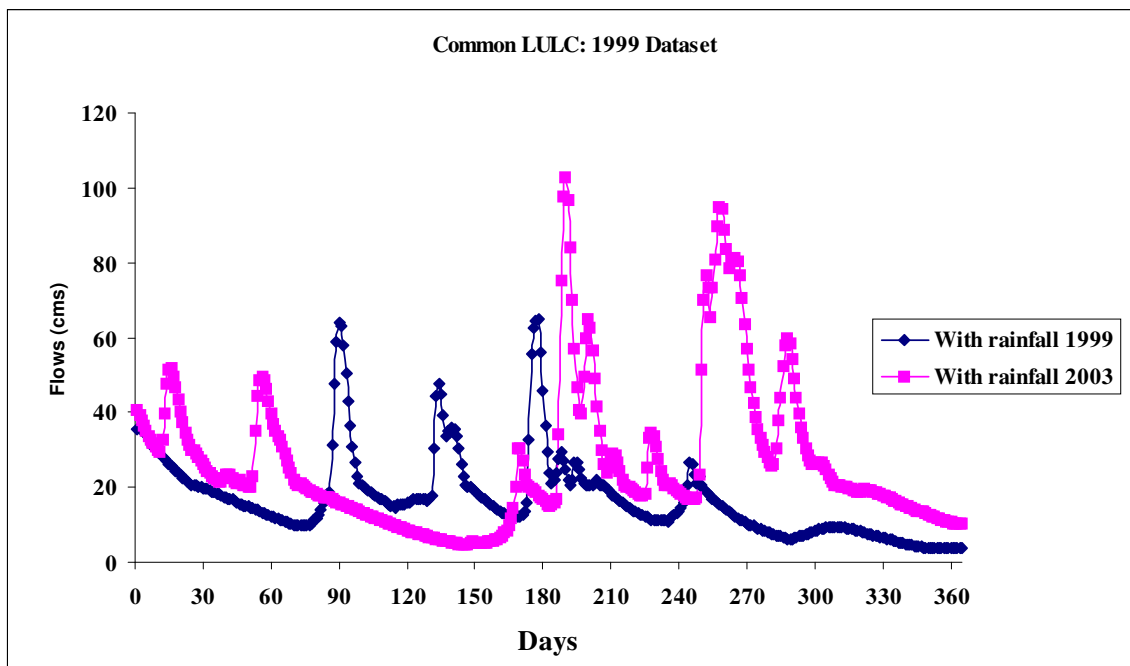


Figure V-13: Simulation results with a common 1999 LULC dataset and original hydroclimatic data for the year 1999 and 2003. Average daily flow (top) and average monthly flow (bottom) for both the years.

5.5 Conclusions

The present investigation suggested LULC change in the San Antonio River Basin can affect freshwater inflows to estuary. It can alter the hydrograph, by shifting the peak flows for a particular rainfall pattern. Peak flows usually increased with increase in impervious surfaces. Although studies suggested LULC change is a local phenomena, and can affect local processes; results based on simulation suggested that increase in impervious surface can also affect low flows such as baseflow. The results from this study suggested LULC change can also affect in larger scale, such as watershed/basin scale. Wavelet analysis suggested that changes in LULC can bring changes in scale and frequencies of freshwater inflows. Analysis suggested location of low frequencies changed due to LULC change. This study confirmed that rainfall pattern has a potential influence on the pattern of delivery of freshwater to the estuaries.

CHAPTER VI

CONCLUSIONS AND FUTURE WORK

The objective of this research was to assess the impact of land cover land use change on environmental flows to estuary in San Antonio River watershed. Time series analysis was conducted on various seasonal flows obtained from number of gauging stations located in the watershed; more importantly the last gauging station in the river. Wavelet analysis was conducted on seasonal flows to assess the presence of dominant frequencies and location of such frequencies. In order to quantify the impact of land cover land use change, HSPF model calibration was conducted using genetic algorithms. Land cover land use data sets for the years 1987, 1999, and 2003 were used for assessing its impact on environmental flows to estuary.

Time series analysis suggested that a greater number of trends in seasonal hydrologic variables in the watershed are observed than are expected to occur by chance. Analysis of bootstrapping results suggested about half of the hydrologic variables were significant at global. Results suggested most of the hydrologic variables for winter season showed significant trend. Results indicated presence of Station USGS 8188500 in most of the variable that is significant at global; particularly the winter flows. All the trends for this station were noted positive. Analysis suggested runoff has increased in this river basin. Although, this study suggested there is an increasing trend (particularly winter) in freshwater inflows, it is important to know if this increase is affecting salinity in the

estuary. Further investigation in freshwater inflow areas should consider the possibility of extra dilution in estuary.

Wavelet analysis suggested presence of dominant frequencies in 10-15 years scale in some of the hydrologic variables, with a decadal cycle. Dominant frequencies were also observed in 17-23 years of scale with repeatability in 20-30 years. Time series construction studies suggested presence of multi-scale temporal variability in the data. It is therefore important to understand various ecological processes that are dominant in this scale and quantify possible linkages among them. Quantifying various ecological processes dominant in this scale will help in designing water management strategies.

Calibration for the year 2003 was performed by Genetic algorithm coupled HSPF model. Genetic algorithm was successfully implemented in this study. Although, GA is computationally demanding, it is better than manual calibration. Parameters values had physical representation and were well within the ranges as suggested in literature.

LANDSAT imageries for the year 1987, 1999, and 2003 were used to quantify the impact of land use land cover change impact on environmental flows to estuary. Land use information was introduced to HSPF. Modeling studies suggested, although land use land cover change has a local impact, it can also impact in basin scale. With increase in impervious surface, peak flows increased over the years. Urbanization also impacted storage as suggested by wavelet analysis because impervious surfaces reduced

infiltration that is important for storage. This study also analyzed additional importance of precipitation variability. On average about 50% of variability in freshwater inflows could be attributed to variation in precipitation, and approximately 10% of variation in freshwater inflows could be attributed to land use and land cover change.

Future research will explore flows to all the estuaries in the U.S. Bootstrapping will be conducted on all the stations. The results will suggest if there is an increasing or decreasing trend in flows to the estuaries. Also, further investigations will suggest how these trends are related to climate or anthropogenic activities. Anthropogenic activities such as land use land cover change will be monitored by LANDSAT series data.

Similarly, wavelet analysis will be conducted on all the flows obtained from gauging station present in the coastal areas. Separation of geographical region will be based on similar signatures that will be obtained from wavelet analysis. This will help to regionalize estuarine flows, which will help in management of these systems.

GA calibration technique will be used in several watersheds differing by size, geography, physiographic etc. to test the robustness of this method, and to test its physical representation. This will be tested in several watersheds that have already been modeled. Further research is also needed to couple GA-HSPF-PEST, to increase the accuracy of the model.

Ultimately, this research will further be strengthened by coupling watershed scale model like HSPF with estuarine model like EFDC. This will help in understanding the impact of watershed management, water resources planning etc. on estuarine systems.

REFERENCES

- Acevedo, W., Foresman, T. W., Buchanan, J. T., 1996. Origins and philosophy of building a temporal database to examine human transformation processes. Proceedings. ASPRS/ACSM Annual Convention and Exhibition, Baltimore, MD, April 22-24, 1996.
- Adams, J. B., Bate, G. C., Harrison, T. D., Huizinga, P., Taljaard, S., Niekerk, L. V., Plumstead, E. E., Whitfield, A. K., Wooldridge, T. H., 2002. A method to assess the freshwater inflow requirements of estuaries and application to the Mtata Estuary, South Africa. *Estuaries* 25, 1382-1393.
- Alber, M., Flory, J., 2002. The Effects of Changing Freshwater Inflows to Estuaries: A Georgia Perspective. Georgia Coastal Research Council, Athens, GA.
- Allen, C., Gogineni, S., Wohletz, B., Jezek, K., Chuah, T., 1997. Airborne radio echo sounding of outlet glaciers in Greenland. *International Journal of Remote Sensing* 18, 3103-3107.
- Alongi, D. M., 1998. Coastal Ecosystem Processes. CRC Press, Boca Raton, FL.
- Anctil, F., Coulibaly, P., 2004. Wavelet analysis of the inter-annual variability in southern Quebec streamflow. *Journal of Climate* 17, 163-173.
- Archer, S. R., Boutton, T. W., Hibbard, K., 2001. Trees in grasslands: Biogeochemical consequences of woody plant expansion. In: *Global Biogeochemical Cycles in the Climate System*, E-D Schulze, SP Harrison, M Heimann, EA Holland, J Lloyd, IC Prentice, D Schimel, (Eds). Academic Press, San Diego, pp. 115-137.
- Arnold, J. G., Allen, P. M., 1999. Automated method for estimating baseflow and groundwater recharge from stream flow records. *Journal of the American Water Resources Association* 35, 411-424.
- Arnold, J. G., Allen, P. M., Muttiah, R., Bernhardt, G., 1995. Automated baseflow separation and recession analysis techniques. *Groundwater* 33, 411-424.
- Asner, G. P., Archer, S., Hughes, R. F., Ansleys, R. J., Wessman, C. A., 2003. Net changes in regional woody vegetation cover and carbon storage in Texas dry lands, 1937-1999. *Global Change Biology* 9, 316-335.
- Bayazit, M., Aksoy, H., 2001. Using wavelets for data generation. *Journal of Applied Statistics* 28, 157-166.

- Bhaduri, B., Minner, M., Tatalovich, S., Harbor, J., 2001. Long-term hydrologic impact of urbanization: A tale of two models. *Journal of Water Resources Planning and Management* 127, 13-19.
- Bicknell, B. R., Imhoff, J. C., Kittle, J., Donigian A. S., Johansen, R. C., 1996. Hydrological Simulation Program-FORTRAN, User's Manual for Release 11, U. S. Environmental Protection Agency, Environmental Research Laboratory, Athens, GA.
- Bicknell, B.R., Imhoff, J. C., Kittle, J. L., Donigian, Jr, A. S., Johanson, R. C., 1997. Hydrological Simulation. Program--Fortran: User's Manual for Version 11: U.S. Environmental Protection Agency, National Exposure Research. Laboratory, Athens, GA., EPA/600/R-97/080, 755 p.
- Bloschl, G., Ardoin-Bardin, S., Bonell, M., Dorninger, M., Goodrich, D., Gutknecht, D., Matamoros, D., Merz, B., Shand, P., Szolgay, J., 2007. At what scales do climate variability and land cover change impact flooding and low flows. *Hydrological Processes* 21, 1241-1247.
- Bradshaw, G. A., McIntosh, B. A., 1994. Detecting climate-induced patterns using wavelet analysis. *Environmental Pollution* 83, 135-142.
- Brivio, P. A., Colombo, R., Maggi, M., 2002. Integration of remote sensing data and GIS for accurate mapping of flooded areas. *International Journal of Remote Sensing* 23, 429-441.
- Brun, S. E., Band, L. E., 2000. Simulating runoff behaviour in an urbanizing watershed. *Computer, Environment, and Urban Systems* 24, 5-22.
- Burn, D. H., Elnur, M. A. H., 2002. Detection of hydrologic trends and variability. *Journal of Hydrology* 255, 107-122.
- Cahill, A. T. 2002. Determination of changes in streamflow variance by means of a wavelet-based test. *Water Resources Research*. 38, article number 1065.
- Caissie, D., El-Jabi N., 2003. Instream flow assessment: from holistic approaches to habitat modelling. *Canadian Water Resources Journal* 28, 173-184.
- Carrol, D. L., 1997. FORTRAN genetic algorithm (GA) driver. <http://cuaerospace.com/carroll/ga.html>, accessed on 12/25/2006. Department of Aeronautical and Astronautical Engineering. University of Illinois, Urbana.
- Chaubey, I., Sahoo, D., Haggard, B. E., Matlock, M. D., Costello, T. A., 2007. Nutrient retention, nutrient limitation, and sediment-nutrient interactions in a pasture-dominated stream. *Transactions of the ASABE* 50, 35-44.

- Cheng, S. J., Wang, R. Y., 2002. An approach for evaluating the hydrological effects of urbanization and its application. *Hydrological Processes* 16, 1403-1418.
- Conner, J. R., James, L., 1996. Environmental and natural resources: Trends and implications. Texas Agricultural and Natural Resources Summit on Environmental and Natural Resource Policy for the 21st Century. Texas A&M University, College Station, Texas.
- Cooperrider, A., Boyd, R. J., Stuart, H. R., 1986. Inventory and Monitoring of Wildlife Habitat. U.S. Dept. of the Interior, Bureau of Land Management: Washington, DC.
- Copeland, J.H., Pielke, R.A., Kittel, T.G., 1996. Potential climate impacts of vegetation changes: a regional modeling study. *Journal of Geophysical Research* 101, 7409-7412.
- Costa, H. M, Botta, A., Cardille, J. A., 2003. Effects of large-scale changes in land cover on the discharge of the Tocantins River, Southeastern Amazonia. *Journal of Hydrology* 283, 206-217.
- Coulibaly, P., Burn, D. H., 2005a. Spatial and temporal variability of Canadian seasonal streamflows. *American Meteorological Society* 18, 191-210.
- Coulibaly, P., Burn, D. H., 2005b. Spatial and temporal variability of Canadian seasonal streamflows. *Journal of Climate* 18, 191-209.
- Cummins, K. L. 2000. The temporal mapping of riparian vegetation at Leon Creek in Bexar County, Texas from 1987 to 1999. MS Thesis, Texas A&M University, College Station.
- Daubechies, I., 1992. Ten Lectures on Wavelets. Society for Industrial and Applied Mathematics: Philadelphia.
- Donnay, J. P., Barnsley, M.J., Longley, P. A., 2001. Remote Sensing and Urban Analysis. London and New York.
- Douglas, E. M., Vogel, R. M., Kroll, C. N., 2000. Trends in floods and low flows in the United States: Impact of spatial correlation. *Journal of Hydrology* 240, 90-105.
- Dow, C. L., DeWalle, D. R., 2000. Trends in evaporation and Bowen ratio on urbanizing watersheds in eastern United States. *Water Resources Research* 36, 1835-1843.
- Duan, Q., Sorooshian, S., Gupta, V. K., 1992. Effective and efficient global optimization for conceptual rainfall-runoff models. *Water Resources and Research*. 28, 1015-1031.

Duda, R. O., Hart, P. E., Stork, D. G., 2001. *Pattern Classification*. John Wiley & Sons, New York.

Eckhardt, K., 2005. How to construct recursive digital filters for baseflow separation. *Hydrological Processes* 19, 507-515.

Eckhardt, K., Arnold, J. G., 2001. Automatic calibration of distributed catchment model. *Journal of Hydrology* 251, 103-109.

Engelmann, C. J. K., Ward, A. D., Christy, A. D., Bair, E. S., 2002. Application of the BASINS database and NPSM model on a small Ohio watershed. *Journal of the American Water Resources Association* 38, 289-300.

Farge, M., 1992. Wavelet transformations and their applications to turbulence. *Annual Reviews of Fluid Mechanics* 24, 395-457.

Flanagan, M., Civco, D. L., 2001. Subpixel impervious surface mapping. *Proceedings of 2001 ASPRS*, St Louis, MO.

Goldberg, D. E., 1989. *Genetic Algorithms in Search, Optimization, and Machine Learning*. Reading, MA, Addison-Wesley.

Haan, C. T. 2002. *Statistical Methods in Hydrology*. Second Edition. Iowa State Press, Ames, IA.

Heimlich, R. E., Anderson, W. D., 2001. Development at the urban fringe and beyond. *Agricultural Economic Report no.803* (p.88). Washington D. C: U.S.D.A, Economic Research Service.

Holland, J. H., 1975. *Adoption in Natural and Artificial Systems*. Ann Arbor, University of Michigan.

Hurrell, J. W., 1995. Decadal trends in the North Atlantic Oscillation: Regional temperature and precipitation. *Science* 269, 676-679.

Im, S., Brannan, K. M., Mostaghimi, S., 2004. Simulating hydrologic and water quality impacts in an urbanizing watershed. *Journal of the American Water Resources Association*. 39, 1465-1479.

Ines, A. V. M., Honda, K., 2005. On quantifying agricultural and water management practices from low spatial resolution RS data using genetic algorithms: A numerical study for mixed-pixel environment. *Advances in Water Resources* 28, 856-870.

Ines, V. M. A., Droogers, P., 2002. Inverse modeling in estimating soil hydraulic functions: a genetic algorithm approach. *Hydrology and Earth System Sciences* 6, 49-65.

Jensen, J. R., 2005. *Introductory digital image processing: A remote sensing perspective*. 3rd edition, Prentice Hall, Upper Saddle River, NJ.

Kendall, M. G., 1975. *Rank Correlation Methods*. Charles Griffin, London.

Kennish, M. J., 2000. *Estuary Restoration and Maintenance: The National Estuary Program*. CRC Press, Boca Raton, FL.

Kennish, M. J., 2001. *Practical Handbook of Marine Science*, 3rd ed. CRC Press, Boca Raton, FL.

Kreuter, U. P., Harris, H. G., Matlock, M. D., Lacey, R. E., 2001. Estimated change in ecosystem service values in San Antonio area. *Ecological Economics* 39, 333-346.

Kumar, P., Foufoula-Georgiou, E., 1997. Wavelet analysis for geophysical applications. *Reviews of Geophysics* 35, 385-412.

Labat, D., Ronchail, J., Callede, J., Guyot, J. L., 2004. Wavelet analysis of Amazon hydrological regime variability. *Geophysical Research Letters* 31, 1-4.

Laroche, A. M., Gallichand, J., Lagace, R., Pesant, A., 1996. Simulating atrazine transport with HSPF in an agricultural watershed. *Journal of Environmental Engineering* 122, 622-630.

Legates, D. R., McCabe Jr., G. J., 1999. Evaluating the use of "goodness-of-fit" measure in hydrologic and hydroclimatic model validation. *Water Resources Research* 35, 233-241.

Leggese, D., Vallet Coulomb, C., Gasse, F., 2003. Hydrological response of a catchment to climate and land use changes in tropical Africa: South Central Ethiopia. *Journal of Hydrology* 275, 67-85.

Lettenmaier, D. P., Wood, E. F., Wallis, J. R., 1994. Hydro-climatological trends in the continental United States. *Journal of Climate* 7, 586-607.

Lim, K. J., Engel, B. A., Tang, Z., Choi, J., Muthukrishnan, S., Tripathy, D., 2005. Web GIS-based hydrograph analysis tool, WHAT. *Journal of the American Water Resources Association* 41, 1407-1416.

Lins, H. F., 1997. Regional streamflow regimes and hydroclimatology of the United States. *Water Resources Research*. 33, 1655-1667.

- Lins, H. F., Michaels, P. J., 1994. Increasing U. S. streamflow linked to greenhouse forcings. *EOS Transactions American Geophysical Union* 75, 281-285.
- Lins, H.F., Slack, J.R., 1999. Streamflow trends in the United States. *Geophysical Research Letters* 26, 227-230.
- Liong, S. Y., Chan, W. T., ShreeRam, J., 1996. Peak flow forecasting with genetic algorithm and SWMM. *Journal of Hydraulic Engineering* 121, 613-617.
- Liu, P.C. 1994. Wavelet spectrum analysis and ocean wind waves. In: *Wavelets in Geophysics*. E. Foufoula-Georgiou and P. Kumar, Eds., Academic Press: New York, pp. 151-166.
- Longley, W. L. 1994. Freshwater inflows to Texas bays and estuaries: ecological relationships and methods for determination of needs. Texas Water Development Board and Texas Parks and Wildlife Department. Austin, Texas.
- Lumb, A. M., McCammon, R. B., Kittle, J. L. 1994. Users manual for an Expert System (HSPEXP) for calibration on the Hydrological Simulation Program-Fortran. Water Resources Investigations Report 94-4168, U. S. Geological Survey, Reston, VA.
- Lyne, V., Hollick, M., 1979. Stochastic time variable rainfall runoff modeling. Hydrology and water resources symposium, Berth, Australia. Proceedings, National Committee on Hydrology and Water Resources of the Institution of Engineers, Australia, 89-92.
- Mann, H. B., 1945. Non-parametric tests against trend. *Econometrica* 13, 245-259.
- Mau, D. P., Winter, T. C., 1997. Estimating groundwater recharge from streamflow hydrographs for a small mountain watershed in a temperate humid climate, New Hampshire, USA. *Groundwater* 35, 291-304.
- McCarl, B. A., Dillon, C. R., Keplinger, K. O., Williams, R. L., 1999. Limiting pumping from the Edwards Aquifer: An economic investigation of proposals, water markets, and spring flow guarantees. *Water Resources Research* 35, 1257-1268.
- Moore, I. D., Burch, G. J., Mackenzie, D. H., 1988. Topographic effects on the distribution of surface soil-water and the location of ephemeral gullies. *Transactions of the ASABE* 31, 1098-1107.
- Muleta, M. K., Nicklow, J. W., 2005. Sensitivity and uncertainty analysis coupled with automatic calibration for a distributed watershed model. *Journal of Hydrology* 306, 127-145.

- Nakken, M. 1999. Wavelet analysis of rainfall-runoff variability isolating climatic from anthropogenic patterns. *Environmental Modeling and Software* 14, 283-295.
- Nash, J. E., Sutcliffe, J. V., 1970. River flow forecasting through conceptual models, Part 1: a discussion of principles. *Journal of Hydrology* 10, 282-290.
- Nathan, R. J., McMahon, T. A., 1990. Evaluation of automated techniques for baseflow and recession analysis. *Water Resources Research* 26, 1465-1473.
- National Climate Data Center (NCDC), 2006. Rainfall Data. <http://ncdc.noaa.gov>. Accessed on 11/30/2006.
- Nicklow, J. W., 2000. Discrete-time optimal control for water resources engineering and management. *Water International* 25, 89-95.
- Nivin, S., Perez, A., 2006. San Antonio, Texas Economic indicators and demographics. Economic development department, City of San Antonio. <http://www.satai-network.com/>. Accessed on 09/20/2006.
- NRC, 1995. Earth observation from space: History, Promise and Reality, National Academy of Sciences, Committee of Earth Studies, Space Sciences Board, Commission on Physical Sciences, Mathematics, and Applications.
- NRC. 2000. Ecological Indicators of the Nation. Washington D. C. National Academy Press.
- NRC. 2005. The Science of Instream Flows: A Review of Texas Instream Flow Program. National Academy Press, Washington D. C.
- Paul, S., Haan, P. K., Matlock, M. D., Mukhtar, S., Pillai, S. D., 2004. Analysis of the HSPF water quality parameter uncertainty in predicting peak in-stream fecal coliform concentration. *Transaction of the ASABE* 47, 69-78.
- Peschel, J. M., 2004. Quantifying land cover in a semi-arid region of Texas. M. S Thesis, Texas A&M University, College Station.
- Peterson, B.J., Holmes, R.M., McClelland, J.W., Vorosmarth, C.J., Lammers, R.B., Shiklomanov, A.I., Shiklomanov, I.A., Rahmstor, S., 2002. Increasing river discharge to the Arctic Ocean. *Science* 298, 2171-2173.
- Pielke Sr., Walko, R. A., Steyaert, L. T., Vidale, P. L, Chase, T. N., 1999. The influence of anthropogenic landscape changes on weather in south Florida. *Monthly Weather Review* 127, 1663-1673.

- Pierson, W. L., Bishop, K., Senden, D. V., Horton P. R., Adamantidis, C. A., 2002. Environmental water requirements to maintain estuarine processes. Environmental flows initiative technical report, report number 3. Commonwealth of Australia, Canberra.
- Poff, N. L., Allan, J. D., Bain, M. B., Karr, J. R., Prestegard, K. L., Richter, B. D., Sparks, R. E., Stromberg, J. C., 1997. The natural flow regime. *Bioscience* 47, 769-784.
- Reeves, C. R., 1993. Genetic Algorithms. Modern Heuristic Techniques for Combinatorial Problems, C. R. Reeves (ed.). Halsted Press, John Wiley and Sons, New York.
- Saco, P., and Kumar, P., 2000. Coherent modes in multiscale variability of streamflow over the United States. *Water Resources Research*. 36: 1049-1067.
- Sahoo, D., Smith, P. 2007. Hydrologic trend detection in a rapidly urbanizing semi-arid coastal river basin. *The Journal of Hydrology* (submitted).
- Sahoo, D., Smith, P., 2007. Characterization of freshwater inflows to a Gulf Coast estuary and stream flows at various gauging stations in a rapidly urbanizing semi-arid watershed using wavelet analysis. *Estuaries, Coastal and Shelf Sciences* (submitted).
- Sahoo, D., Smith, P., Ines, A. 2007. Parameter estimation for calibration of a hydrologic model using evolutionary algorithm and inverse modeling. Presented in ASABE 2007 Annual Conference, Minneapolis, MN.
- Sala O. E, Paruelo, J. M., 1997. Ecosystem Services in Grasslands. *Ecosystem Services*. Island Press, Washington, D. C.
- San Antonio River Authority (SARA). 2003. Regional Watershed Modeling Master plan for the San Antonio River Basin. <http://www.sara-tx.org/>. Accessed on 12/10/2005.
- San Antonio River Authority. Water Resources Regional Planning. <http://www.sara-tx.org/>. Accessed on 09/10/2006.
- San Antonio Water Systems. About Edwards Aquifer. <http://www.saws.org/>. Accessed on 09/10/2006.
- Santhi, C., Arnold, J. G., Williams, J. R., Dugas W. A., Srinivasan, R., Hauck L. M., 2001. Validation of the swat model on a large river basin with point and nonpoint sources. *Journal of the American Water Resources Association* 37, 1169-1188.
- Senarath, S. U. S., Ogden, F. L., Downer, C. W., Sharif, H. O., 2000. On the calibration and verification of two-dimensional, distributed, hortonian, continuous watershed models. *Water Resources Research*. 36, 1495-1510.

Smith, A. J., Goetz, S. J., Prince, S. D., 2003. Subpixel estimates of impervious surface cover from Landsat thematic mapper imagery. *Remote Sensing of Environment*. 87, 22-30.

Smith, L. C., Turcotte, D. L., Isacks, B. L., 1998. Stream flow characterization and feature detection using discrete wavelet transform. *Hydrological Processes*. 12: 233-249.

Sorooshian, S., Gupta, V. K., 1995. Model Calibration, in *Computer Models of Watershed Hydrology*, edited by V. P. Singh. Water Resources Publication, Highlands Ranch, CO.

SPSS, Inc, SPSS 14.0, 2007. SPSS, Inc., Chicago, IL 60606.

Srivastava, P., Hamlett, J. M., Robillard, P. D., Day, R. L., 2002. Watershed optimization of best management practices using AnnAGNPS and a genetic algorithm. *Water Resources Research*. 38, 1-14.

Stewart, J. T., Janssen, R., and Herwijnen, M. V., 2004. A genetic algorithm approach to multiobjective land use planning. *Computers and Operations Research*. 31:2293-2313.

Stohlgren, T., Chase, T., Pielke, R., Kittel, T., Baron, J. 1998. Evidences that local land use practices influence regional climate, vegetation and stream flow patterns in adjacent natural areas. *Global Change Biology* 4, 495-504.

Tanaka, S., Sugimura, T., 2001. A new frontier of remote sensing from IKONOS images. *International Journal of Remote Sensing* 22, 1-5.

Texas Park and Wildlife Department. 1998. Freshwater inflow recommendation for the Guadalupe Estuary of Texas. Coastal Studies Technical Report No. 98-1.

Texas Parks and Wildlife Department, Coastal Studies Program., 1998. Freshwater inflow recommendation for the Guadalupe Estuary of Texas. Austin, TX.

Texas State Data Center. <http://txsdc.utsa.edu/>. Census Demographic Profile. Accessed on 03/06/2005.

Texas Water Development Board, Environmental Section., 1998. Appendix of Freshwater inflow recommendation for Guadalupe Estuary of Texas, Austin, TX.

Texas Water Development Board., 1994. Freshwater inflows to Texas bays and estuaries: ecological relationships and methods for determination of needs. ed. W.L. Longley. Texas Water development Board and Texas Parkas and Wildlife department, Austin, TX.

Tharme, R. E. 2003. A global perspective on environmental flow assessment: emerging trends in the development and application of environmental flow methodologies for rivers. *River Research and Applications* 19, 397-441.

Torrence, T., and Compo, G. P., 1998. A practical guide to wavelet analysis. *Bulletin of the American Meteorological Society* 79, 61-77.

TPWD: Texas Parks and Wildlife Department, Coastal Studies Program. 1998. Freshwater inflow recommendation for the Guadalupe Estuary of Texas. Austin, TX.

TWDB: Texas Water Development Board, Environmental Section. 1998. Appendix of Freshwater inflow recommendation for Guadalupe Estuary of Texas, Austin, TX.

TWDB: Texas Water Development Board. 1994. Freshwater inflows to Texas bays and estuaries: ecological relationships and methods for determination of needs. ed. W.L. Longley (ed.). Texas Water Development Board and Texas Parkas and Wildlife Department, Austin, TX.

U. S. Census Bureau, <http://www.census.gov/>. Accessed on 03/06/2005.

US EPA, 2000. BASINS Technical Note 6: Estimating hydrology and hydraulic parameters for HSPF. EPA-823-R00-012. U. S. Environmental Protection Agency, Office of Water, Washington, D. C.

US EPA, 2001. Better Assessment Science Integrating Point and Nonpoint Sources: User's Manual for Release 3.0. EPA/823/B-01/001. U. S. Environmental Protection Agency, Office of Water, Washington, D. C.

US EPA, 2001. Better Assessment Science Integrating Point and Nonpoint Sources: User's Manual for Release 3.0. EPA/823/B-01/001. U. S. Environmental Protection Agency, Office of Water, Washington, D. C.

USGS, 2006. Stream Flow Data. <http://waterdata.usgs.gov/nwis/rt>. Accessed on 11/25/2006.

Waylen, P., Poveda, G., 2002. El Nino-Southern Oscillation and aspects of western South American hydro-climatology. *Hydrological Processes* 16, 1247-1260.

Weglarczyk, S. 1998. The interdependence and applicability of some statistical quality measures for hydrological models. *Journal of Hydrology* 206, 98-103.

White, K. 1998. Remote sensing progress report. *Progress in Physical Geography* 22, 95-102.

- White, M. A., Schmidt, J. C., Topping, D. J., 2005. Application of wavelet analysis for monitoring the hydrologic effects of dam operation: Glean canyon dam and Colorado River at Lees Ferry, Arizona. *River Research and Application* 21, 551-565.
- Wicklein, S. M., Schiffer, D. M., 2002. Simulation of runoff and water quality for 1990 and 2008 land use conditions in the Reedy Creek Watershed, East-Central Florida. U.S Geological Survey Water-Resources Investigations Report 02-4018, Tallahassee, FL.
- Yue, S., Pilon, P., Phinney, B., Cavadis, G., 2001. Patterns of trends in Canadian streamflow. *Proceedings of 58th Eastern Snow Conference*, Ottawa, Ontario, Canada.
- Yue, S., Wang, C. Y., 2002. Regional streamflow trend detection with consideration of both temporal and spatial correlation. *International Journal of Climatology* 22, 933-946.
- Zhang, X., Harvey, K. D., Hogg, W. D., Yuzyk, T. R., 2001. Trends in Canadian streamflow. *Water Resources Research* 37, 987-998.
- Zhang, X., Vincent, L. A., Hogg, W. D., Niitsoo, A., 2000. Temperature and precipitation trends in Canada during 20th century. *Atmosphere and Ocean* 38, 395-429.
- Zhang, Y. K., Schilling, K. E., 2006. Increasing streamflow and baseflow in Mississippi River since the 1940s: Effect of land use change. *Journal of Hydrology* 324, 412-442

VITA

Debabrata Sahoo, son of Sri Brundaban Sahoo and Smt. Kanakalata Sahoo, graduate from J. N. V. Zinc Nagar, Sundargarh. Sahoo pursued 12th grade in Govt. College Rourkela. After graduation he attended College of Agriculture and Technology, O.U.A.T Bhubaneswar to pursue his B.S. degree. After completing his B.S. in 2000, he attended the University of Arkansas, Fayetteville for his Masters degree. After completion of M.S. in 2004, he joined the Ph.D. program at Texas A&M University in the spring of 2004. He worked as a GRA/GTA in the Department of Biological and Agricultural Engineering. Debabrata received his Ph.D. in May 2008. His permanent address is D/61 Koel Nagar, Rourkela, Sundargarh, Orissa, India.